Electronic Supplementary Material (ESI) for RSC Advances.

Ganocochlearic Acid A, A Rearranged Hexanorlanostane Triterpenoid, and Cytotoxic Triterpenoids from the Fruiting Bodies of *Ganoderma cochlear*

Xing-Rong Peng,[a,b] Xia Wang,[a,b] Lin Zhou,[a,b] Bo Hou,[a,b] Zhi-Li Zuo,[a] Ming-Hua Qiu*[,a]

[a]State Key Laboratory of Phytochemistry and Plant Resources in West China, Kunming Institute of Botany, Chinese Academy of Sciences, Kunming 650201, People's Republic of China

[b]Graduate University of the Chinese Academy of Sciences, Beijing 100049, People's Republic China

*To whom correspondence should be addressed. Tel: +86-0871-5223327. Fax: +86-0871-5223325. E-mail: mhchiu@mail.kib.ac.cn

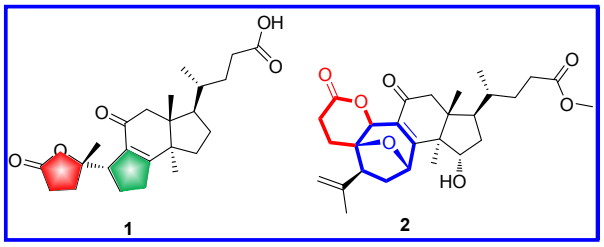

Contents of Supporting Information

Figure S1. ^{1}H NMR (600 MHz, C_5D_5N) spectrum of ganochlearic acid A (1).

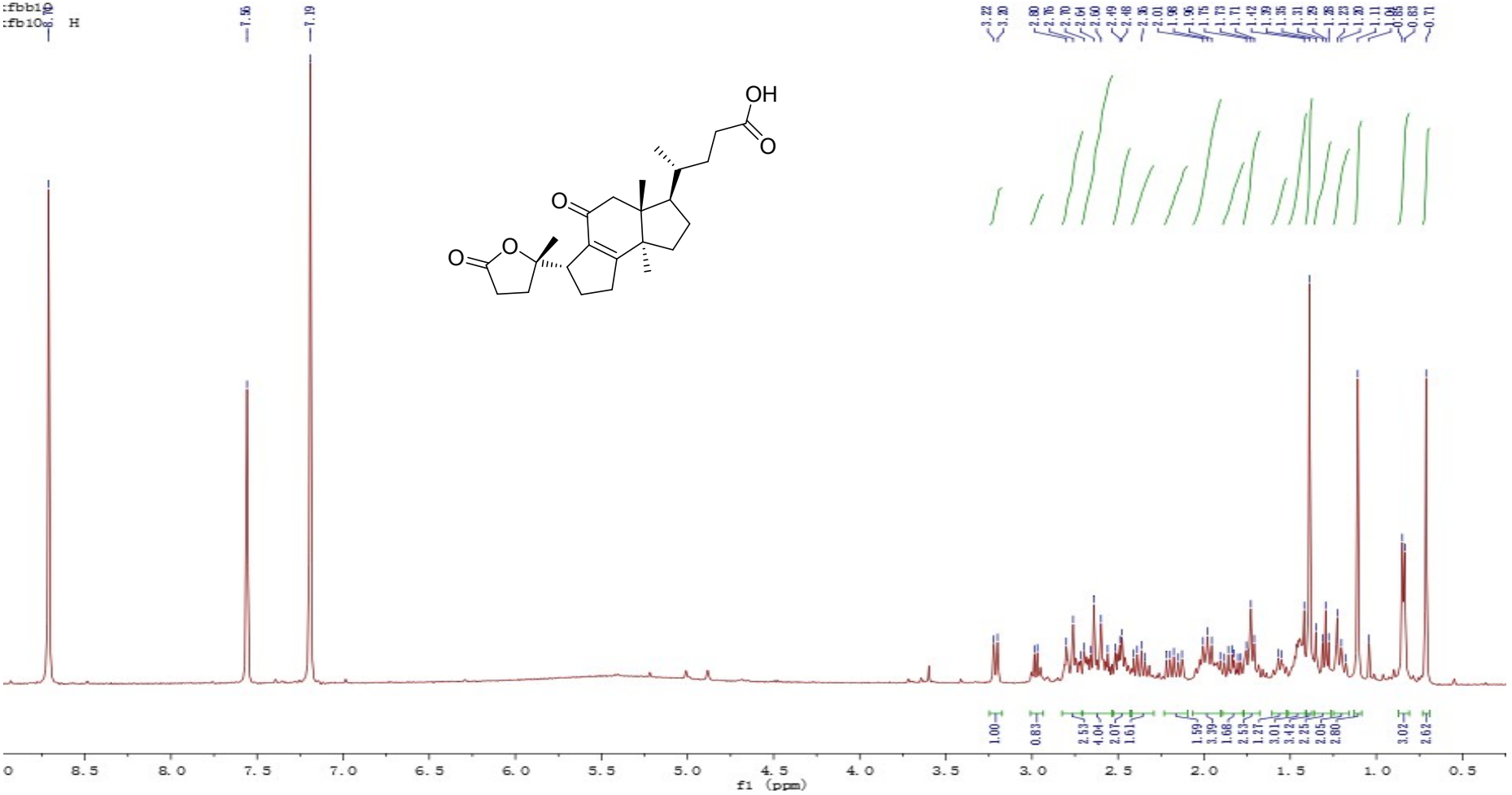

Figure S2. ^{13}C NMR spectrum (150 MHz, C_5D_5N) of ganochlearic acid A (1).

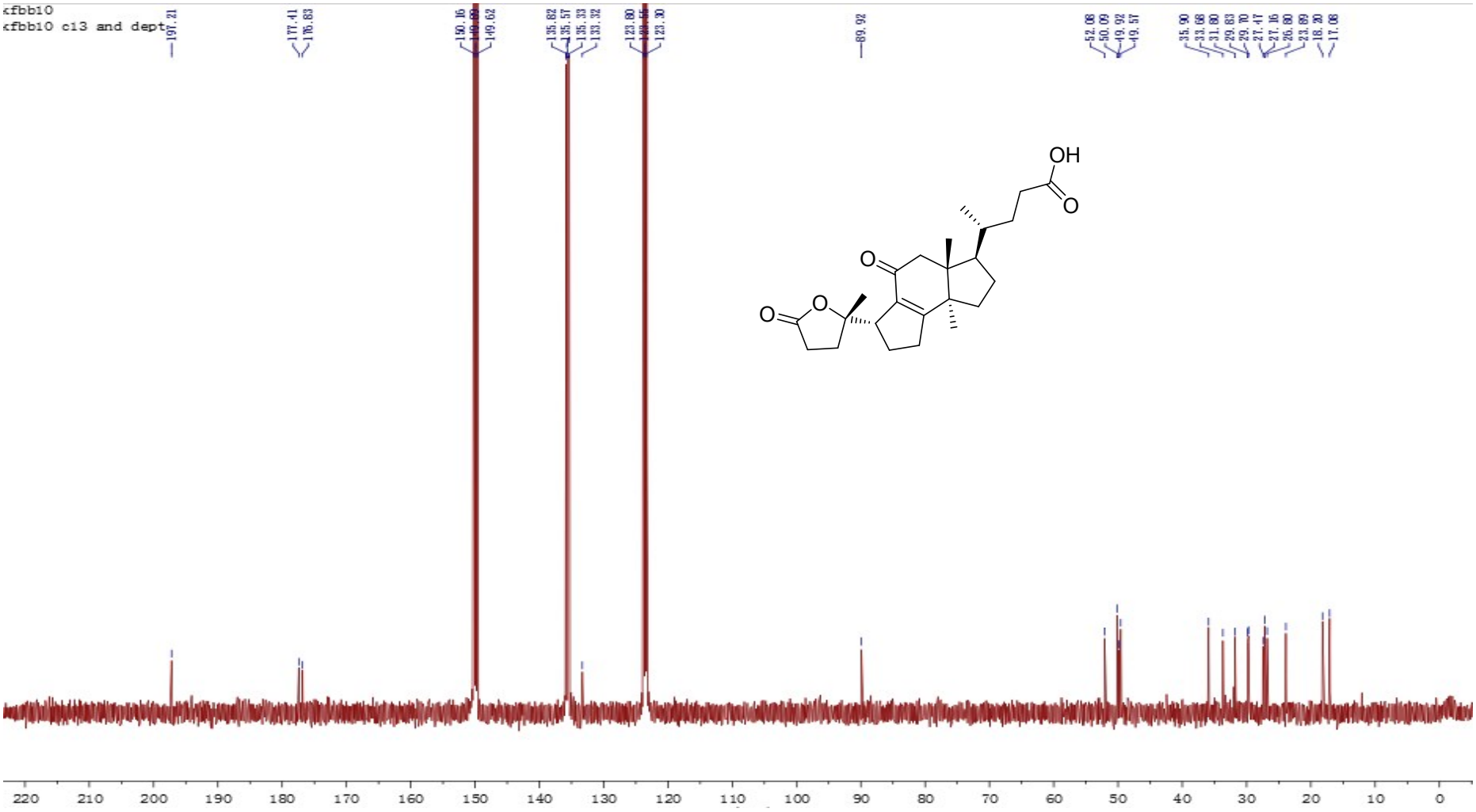

Figure S3. HSQC spectrum of ganochlearic acid A (1).

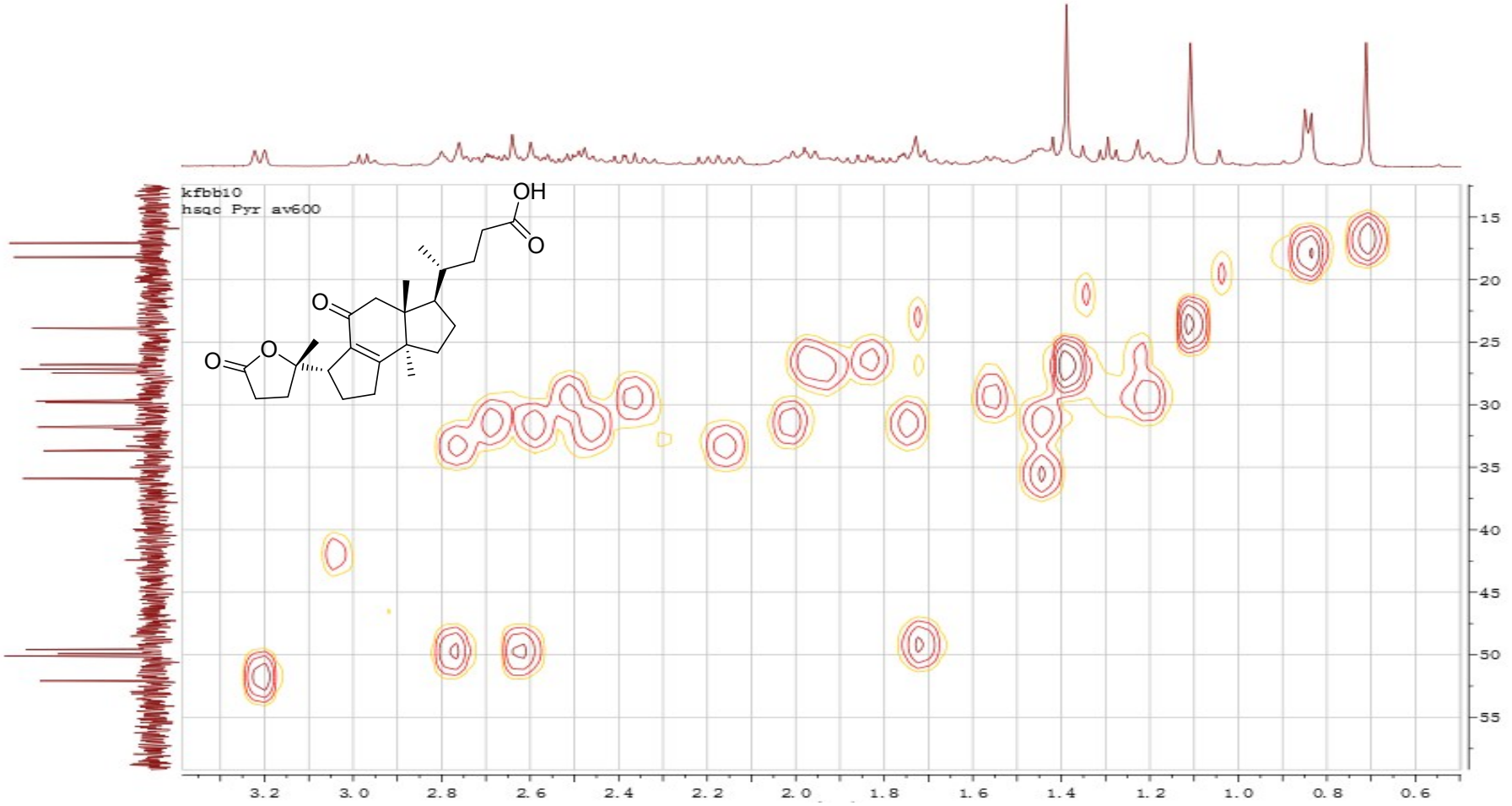

Figure S4. HMBC spectrum of ganochlearic acid A (1).

Figure S5. ^{1}H-^{1}H COSY spectrum of ganochlearic acid A (1).

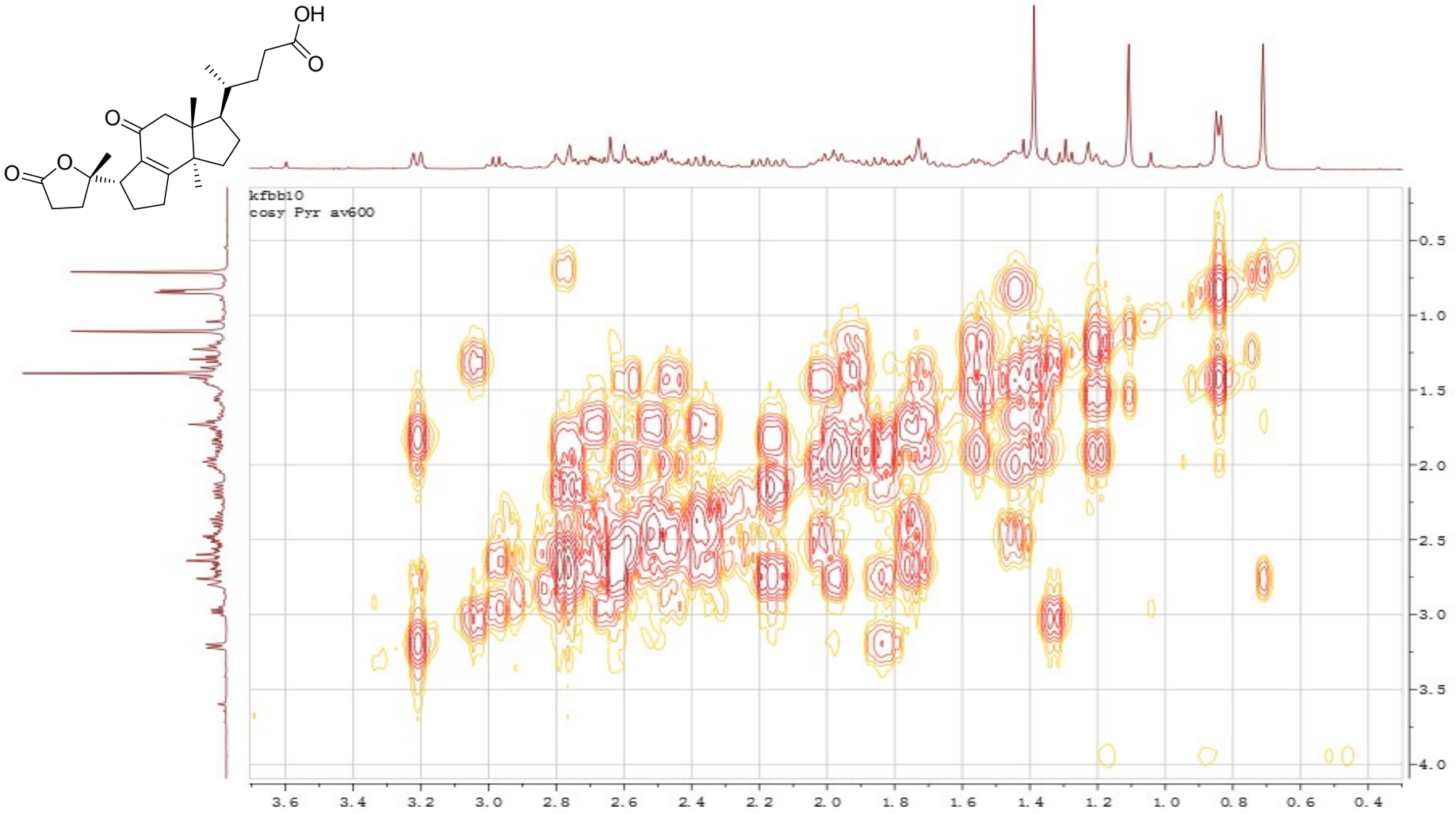

Figure S6. The ROESY spectrum of ganochlearic acid A (1).

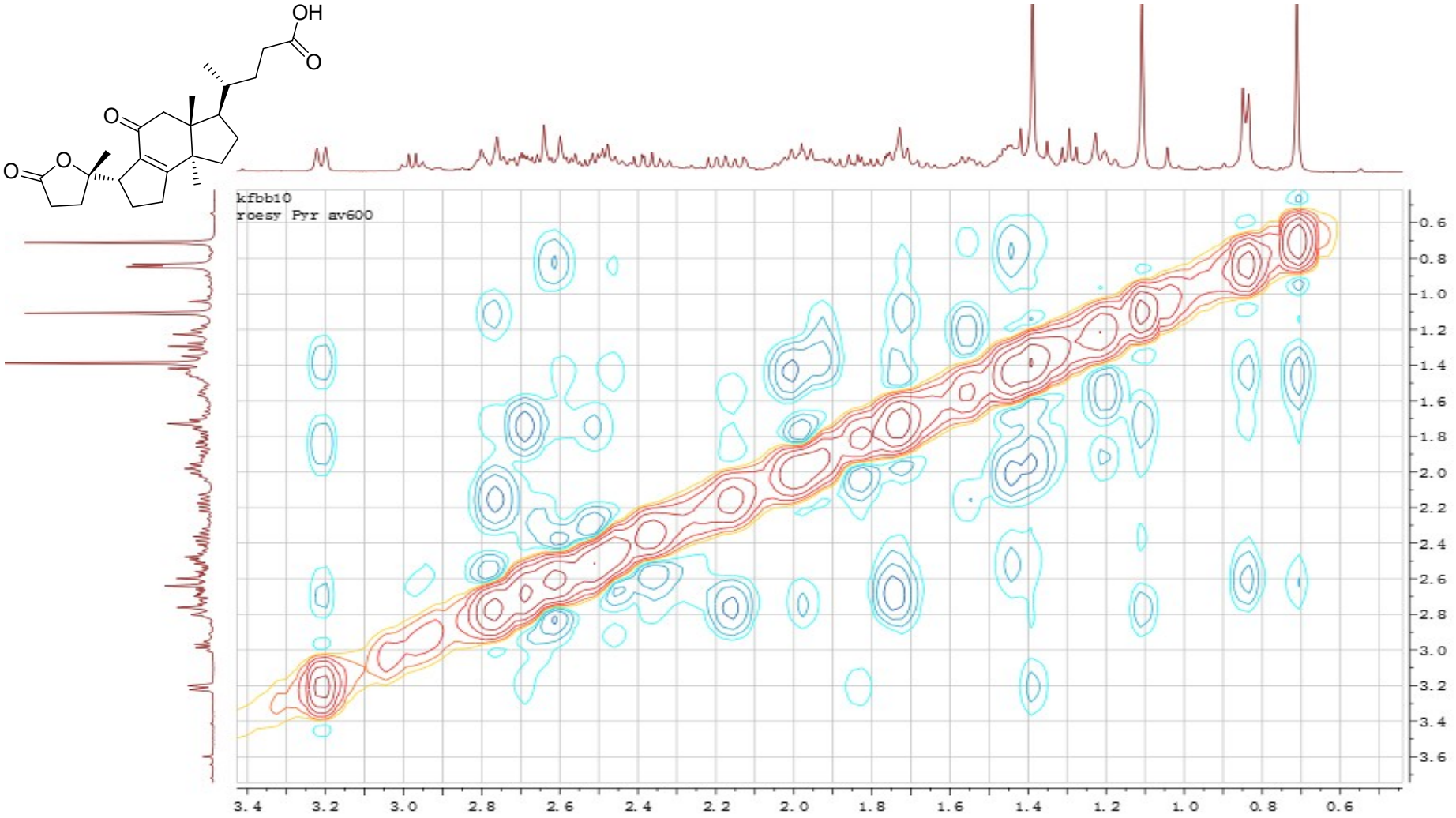

Figure S7. ^{1}H NMR (600 MHz, C_5D_5N) spectrum of cochlate C (2).

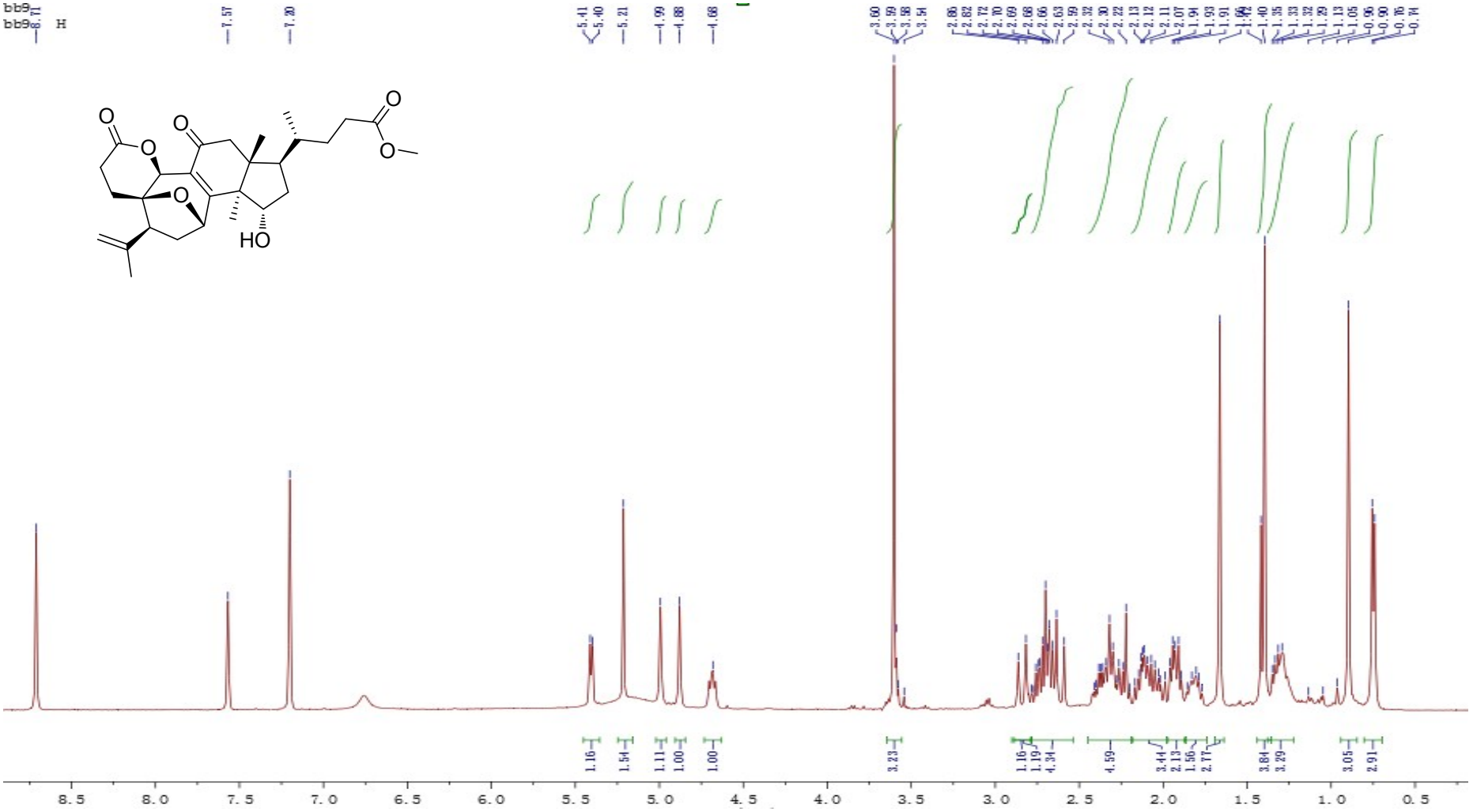

Figure S8. ^{13}C NMR (150 MHz, C_5D_5N) spectrum of cochlate C (2).

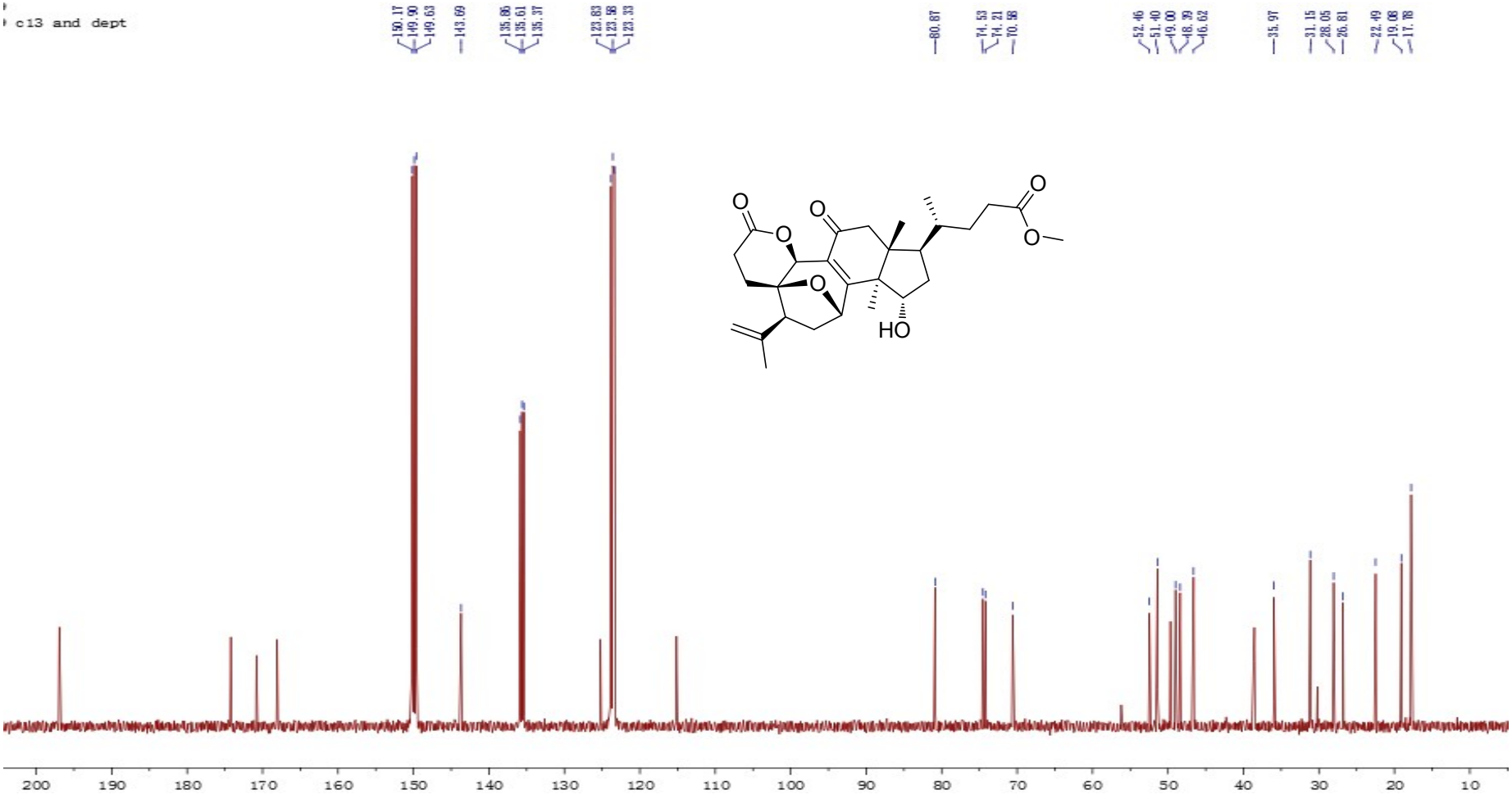

Figure S9. The HSQC spectrum of cochlate C (2).

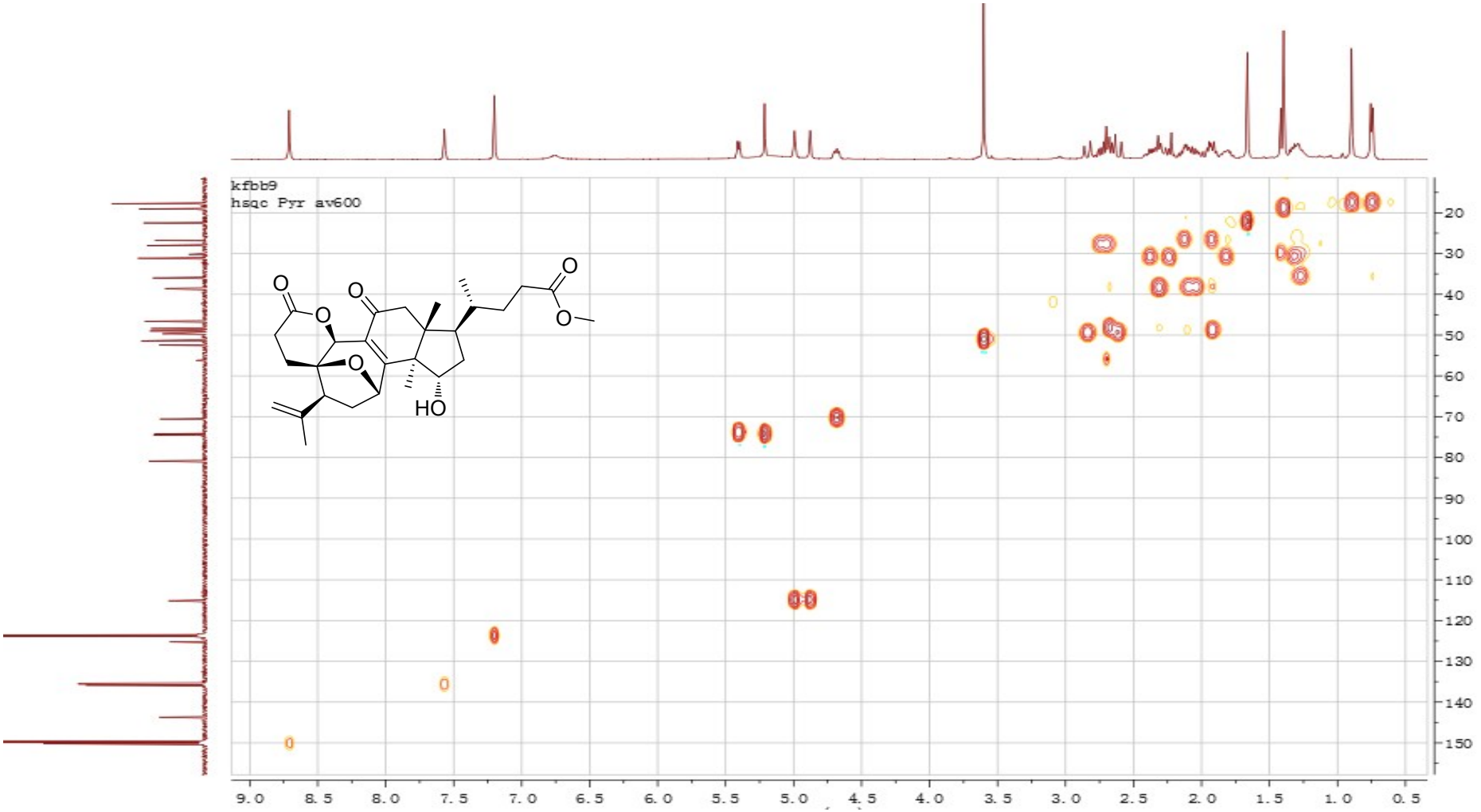

Figure S10. The HMBC spectrum of cochlate C (2).

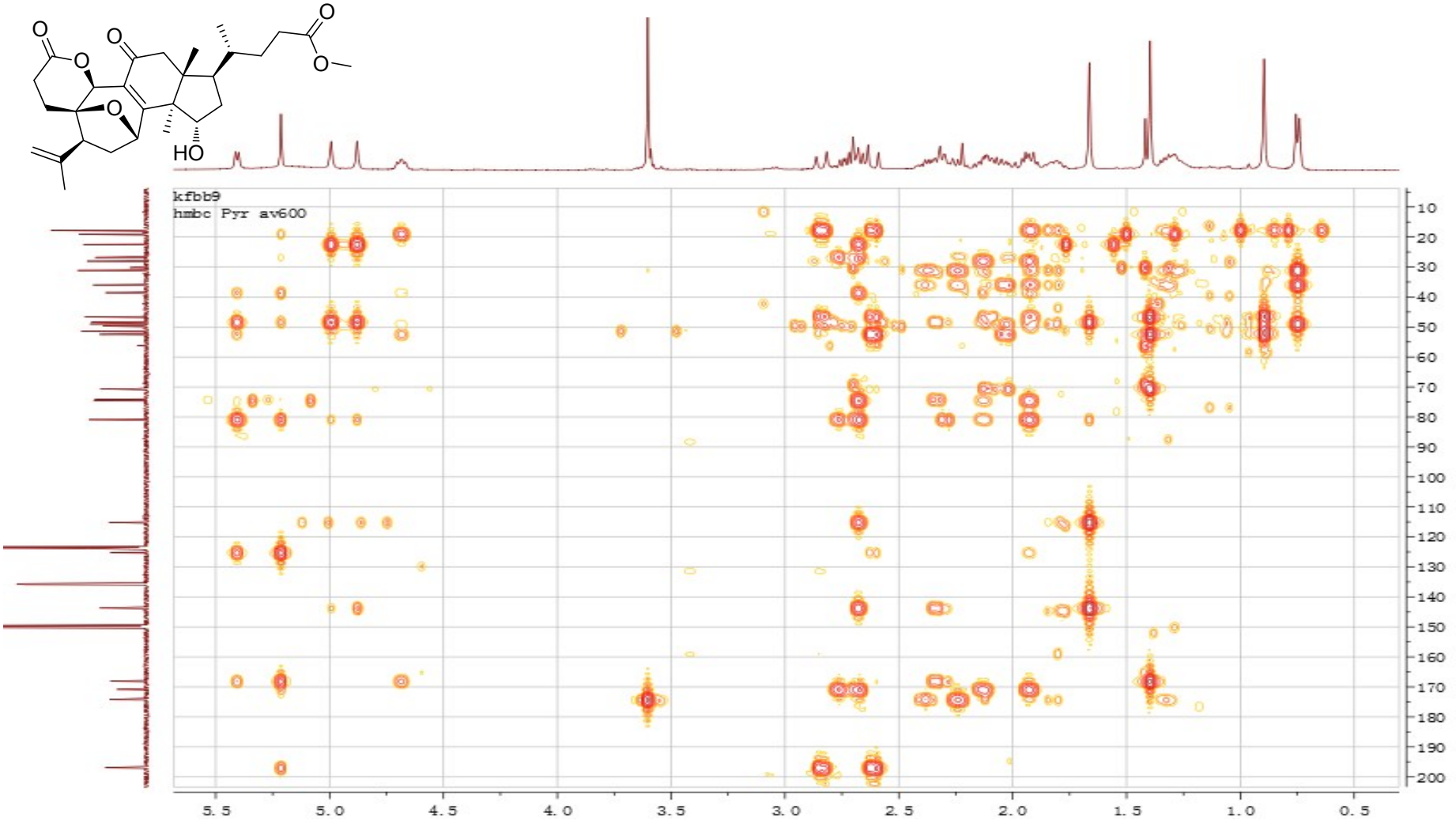

Figure S11. The ^{1}H-^{1}H COSY spectrum of cochlate C (2).

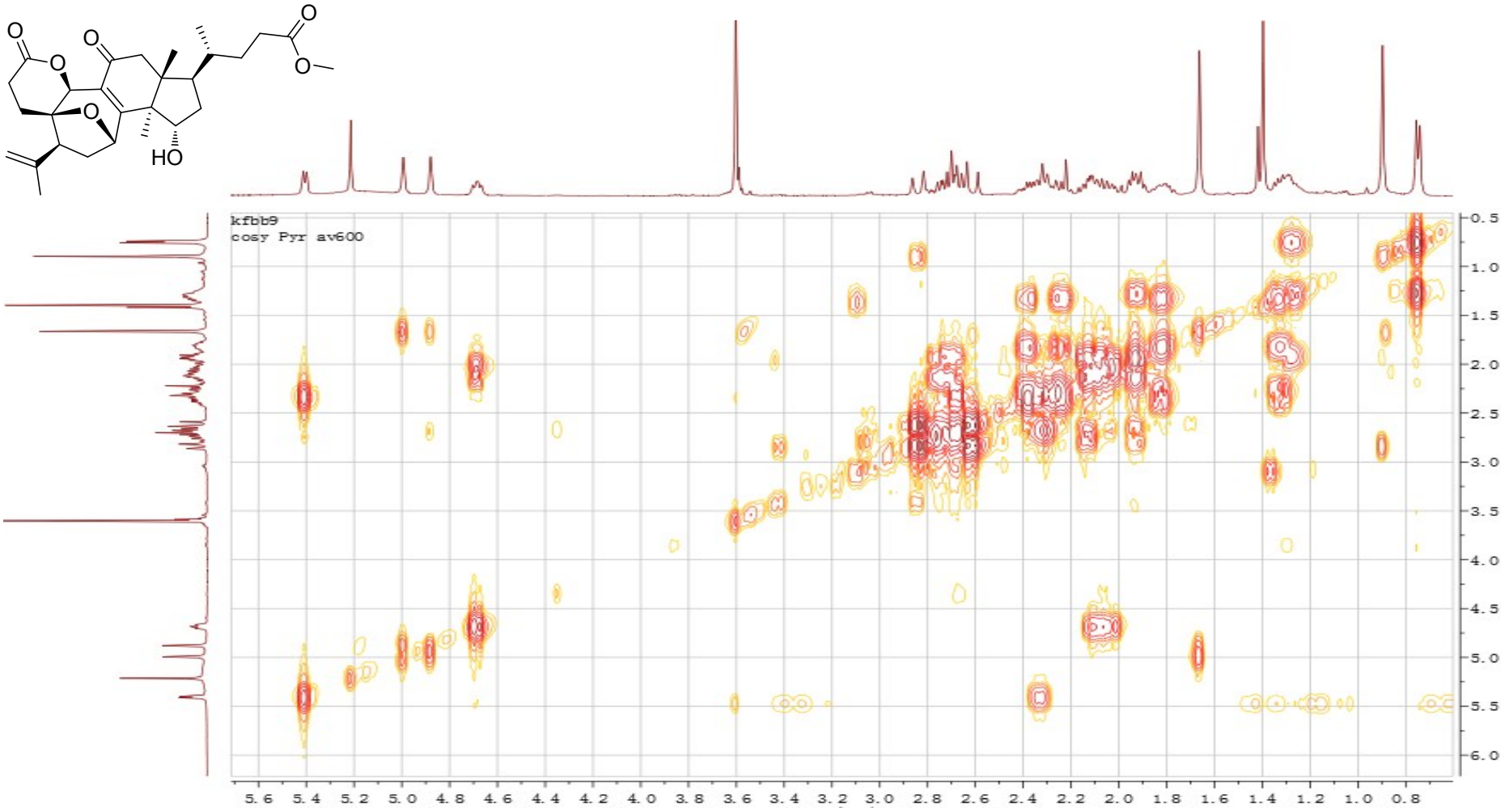

Figure S12. The ROESY spectrum of cochlate C (2).

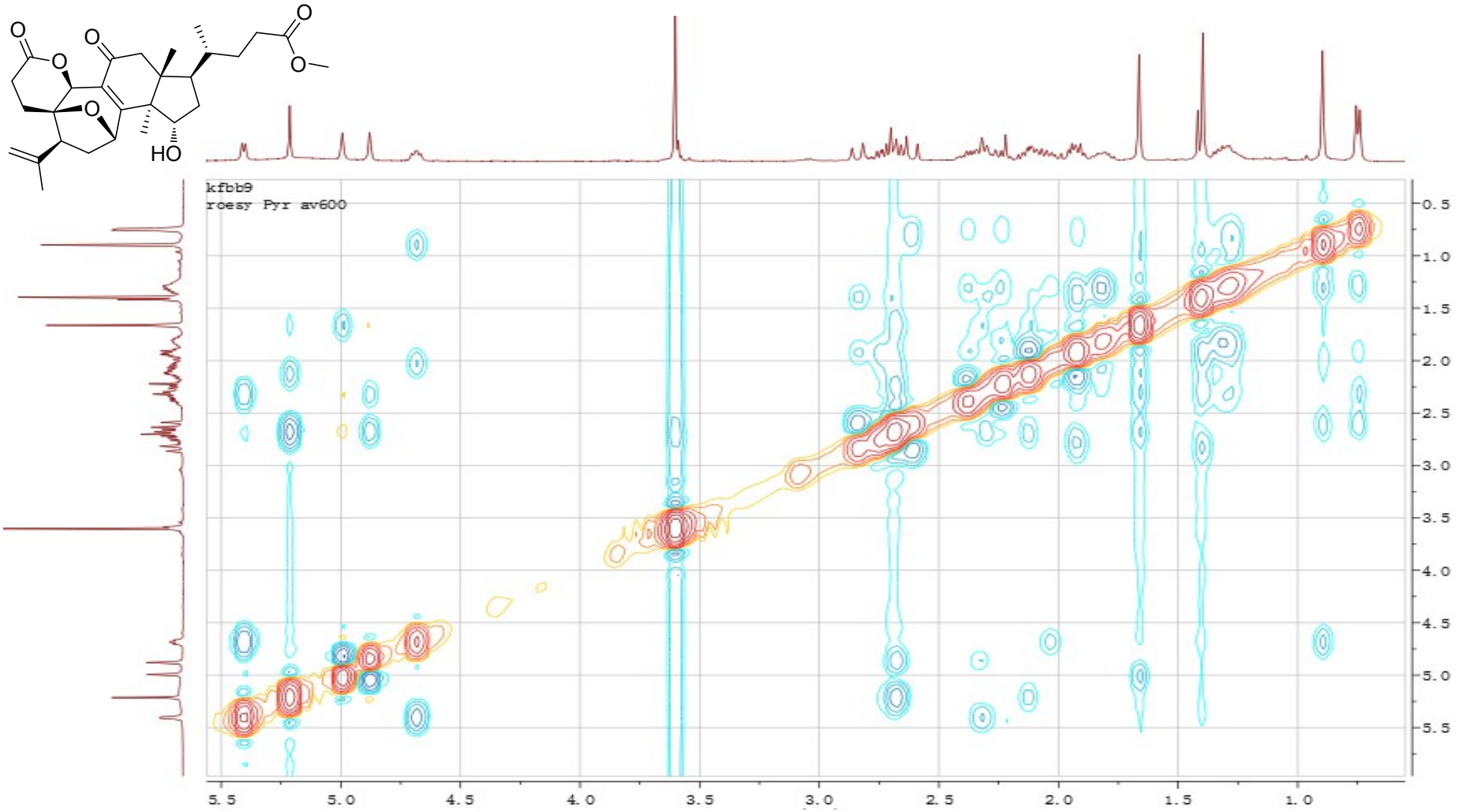

Figure S13. The ^{1}H NMR (500 MHz, C_5D_5N) spectrum of ganocochlate A (3).

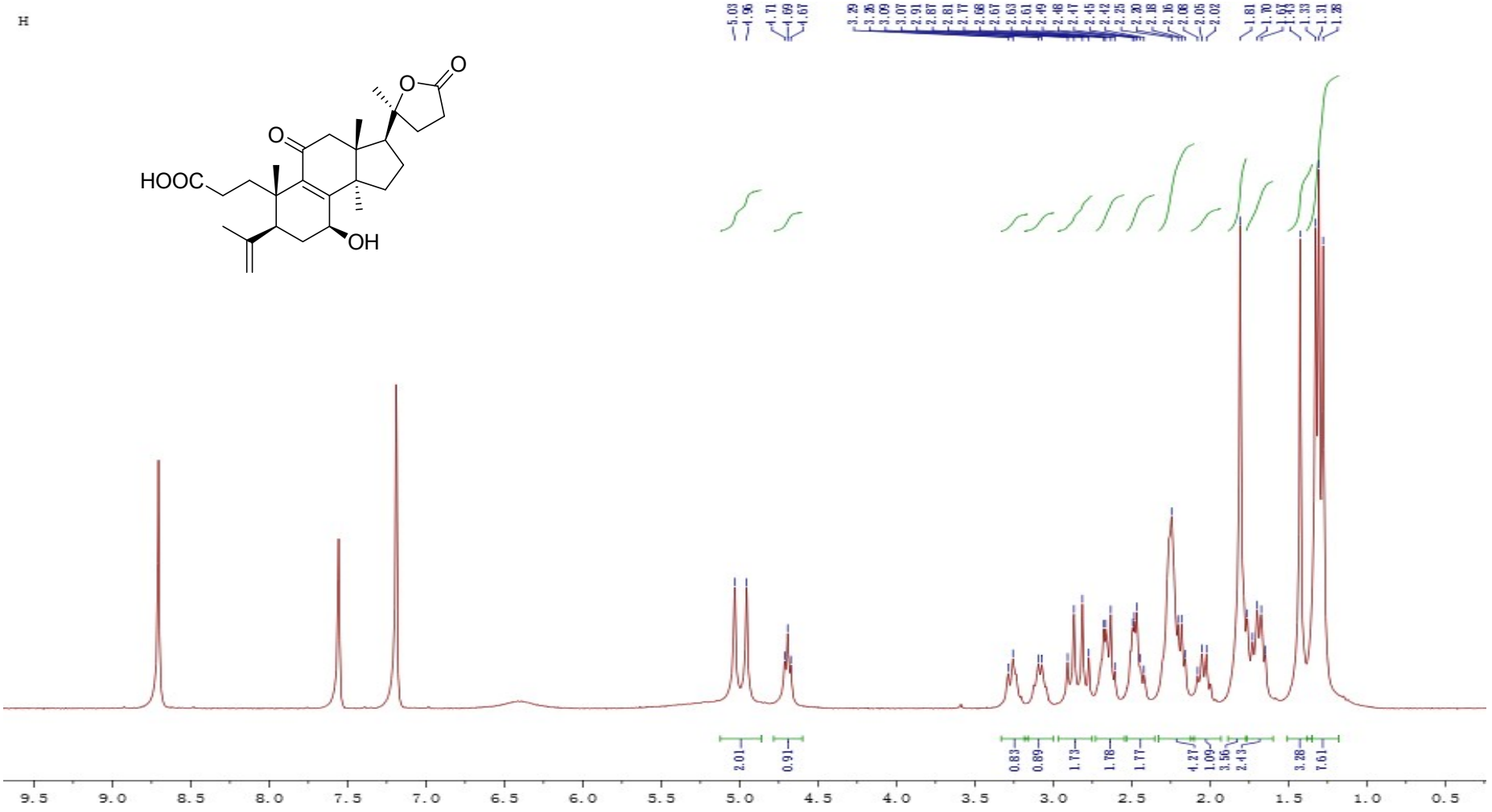

Figure S14. The ^{13}C NMR (125 MHz, C_5D_5N) spectrum of ganocochlate A (3).

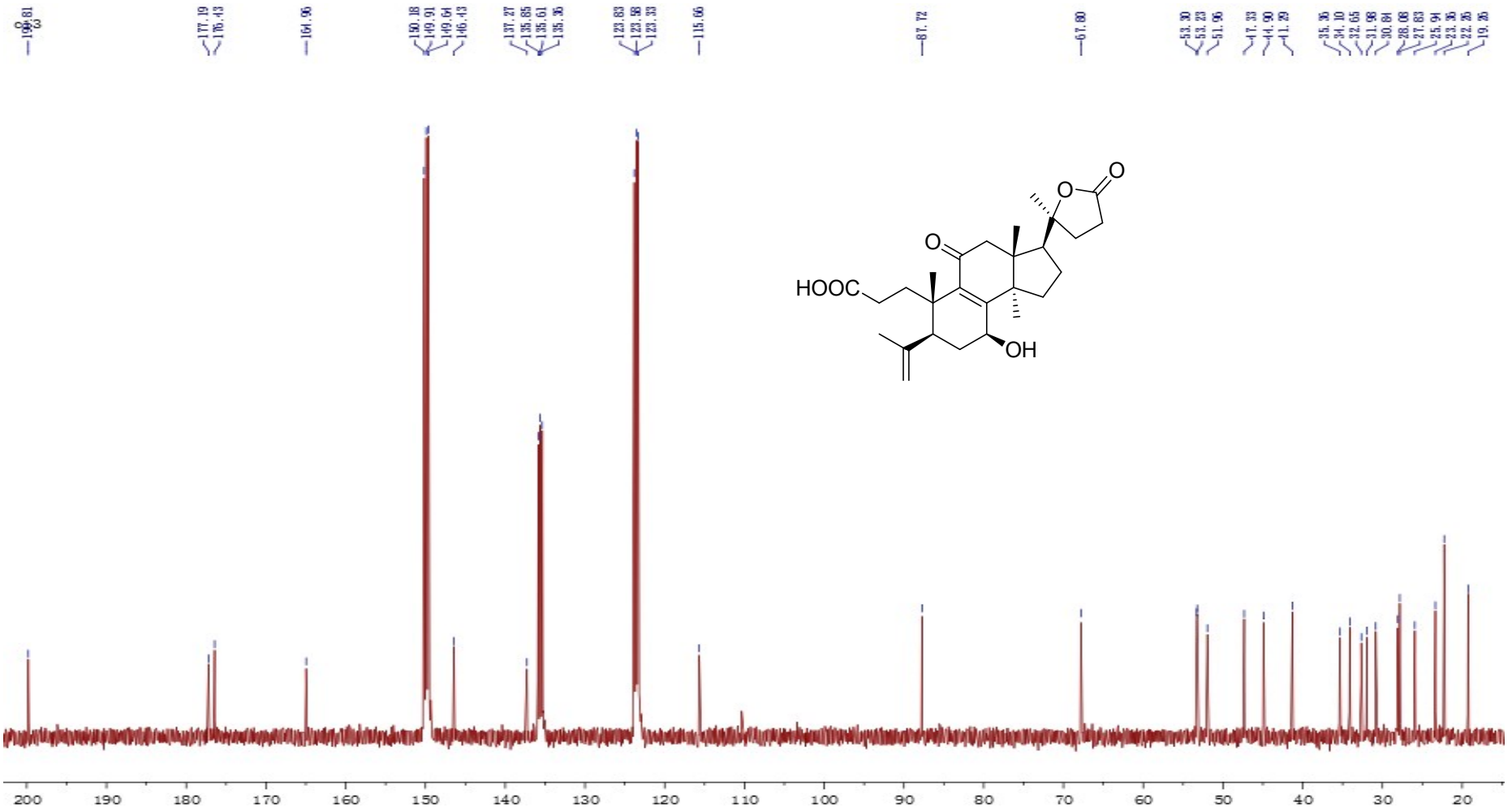

Figure S15. The HSQC spectrum of ganocochlate A (3).

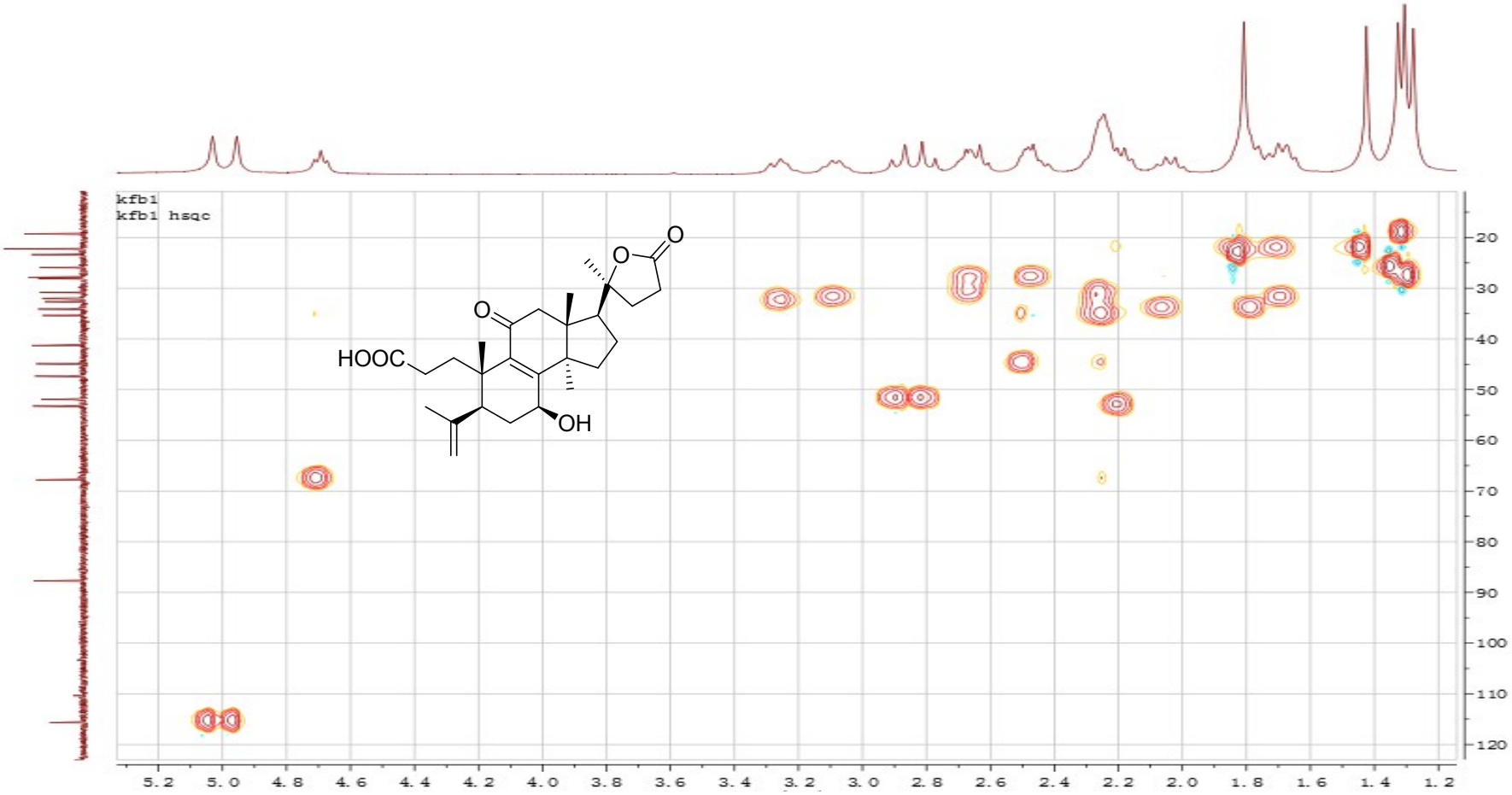

Figure S16. The HMBC spectrum of ganocochlate A (3).

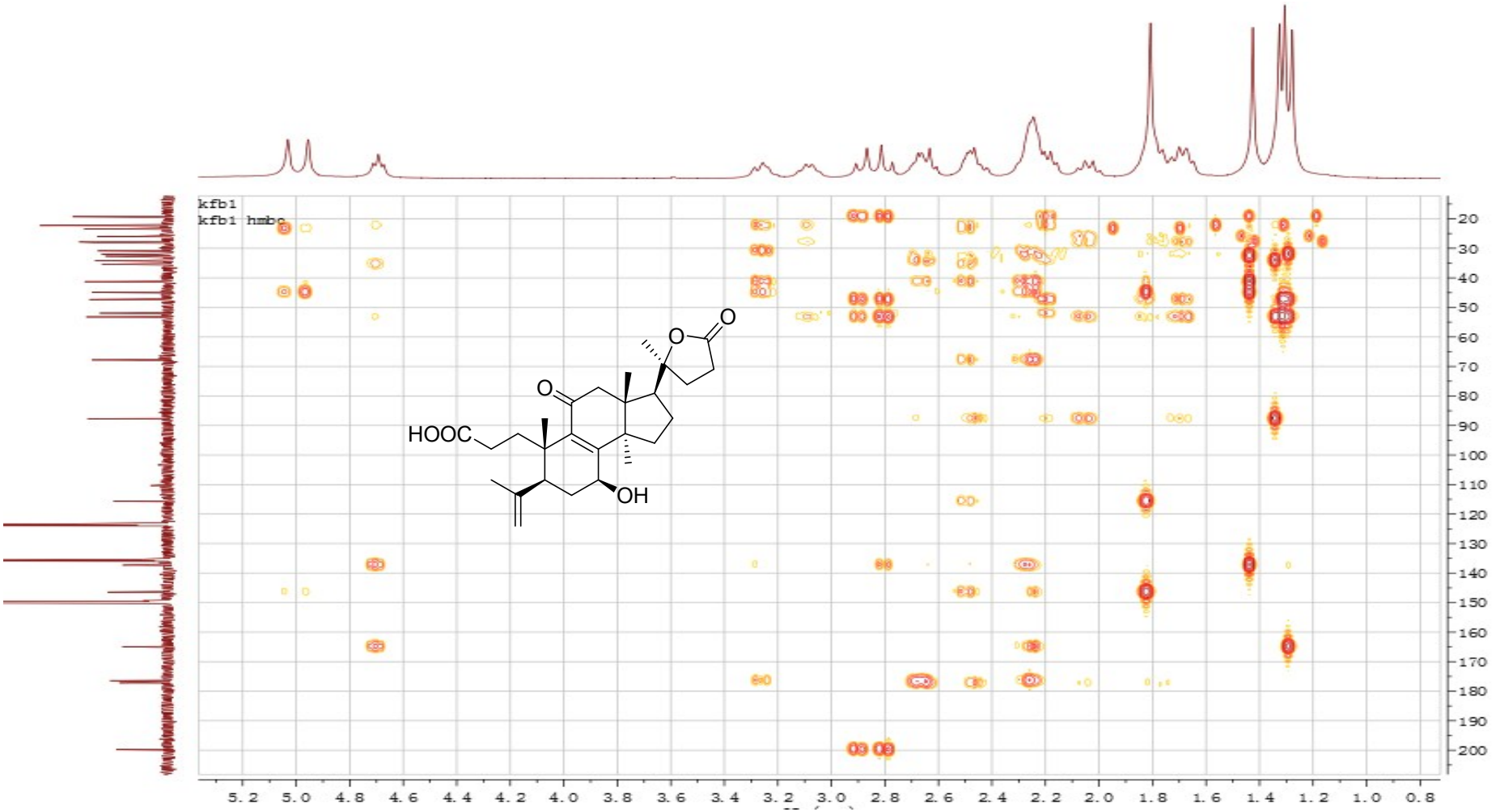

Figure S17. The ^{1}H-^{1}H COSY spectrum of ganocochlate A (3).

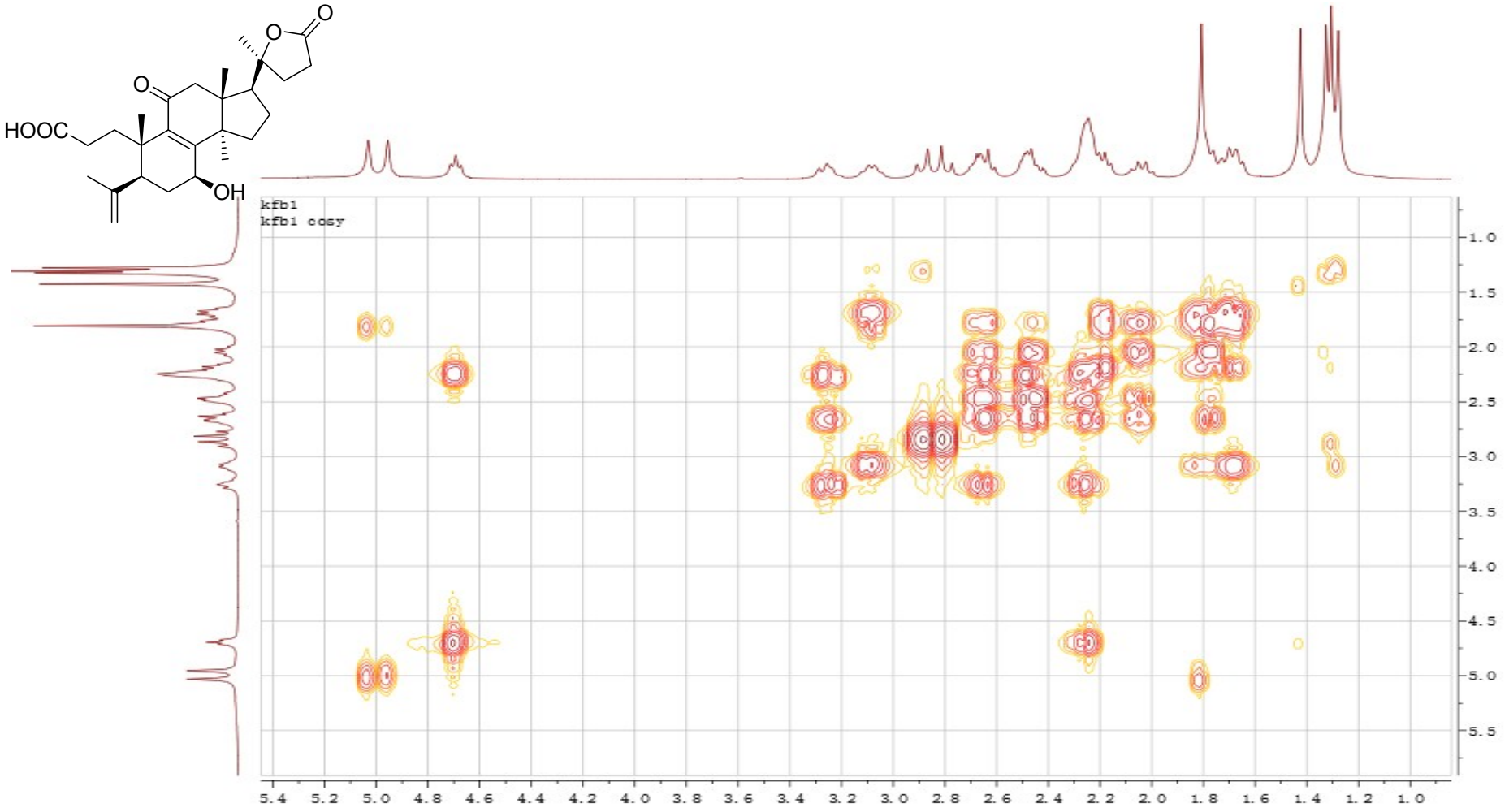

Figure S18. The ROESY spectrum of ganocochlate A (3).

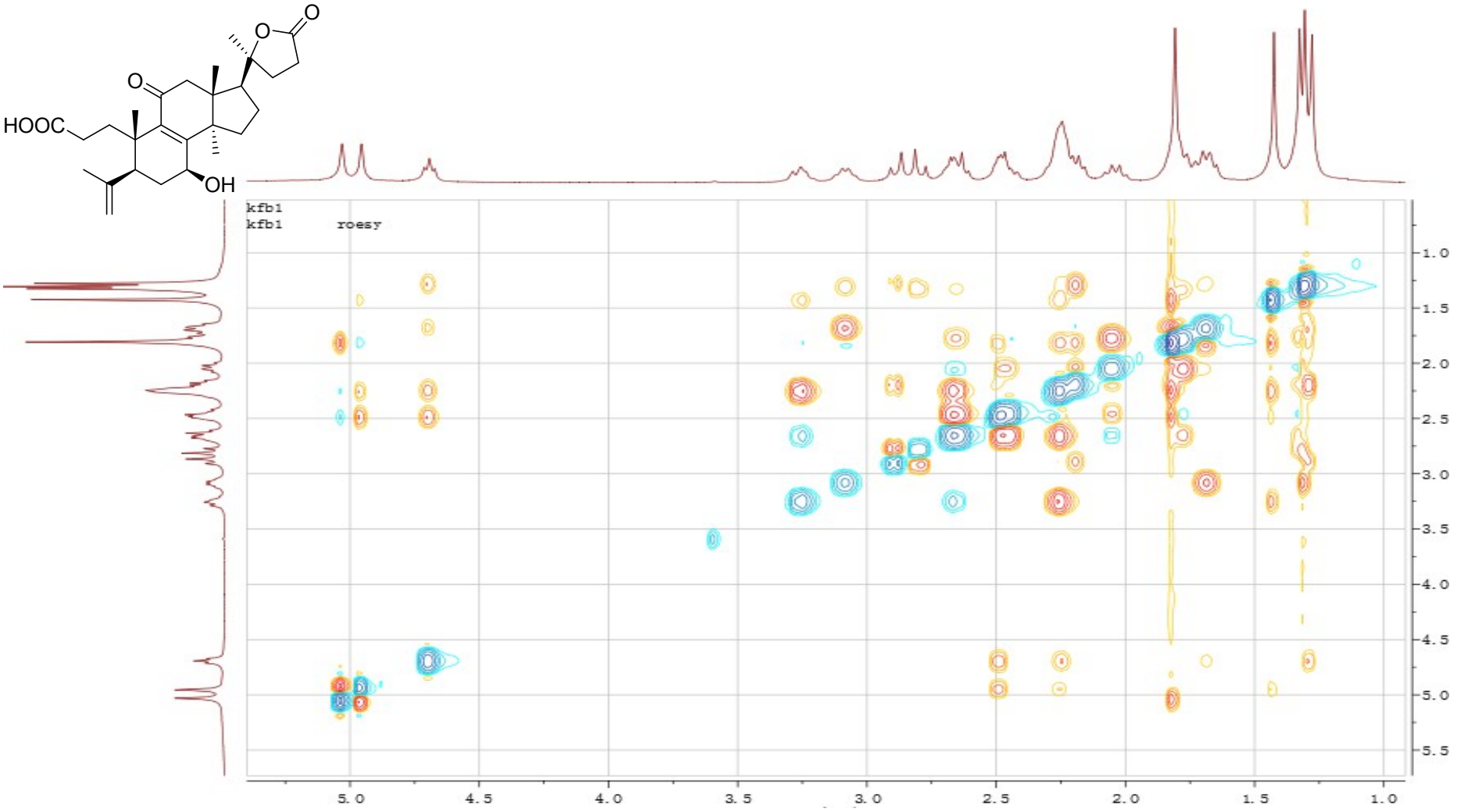

Figure S19. The ^{1}H NMR (600 MHz, $CDCl_3$) spectrum of ganodecochlearin D (4).

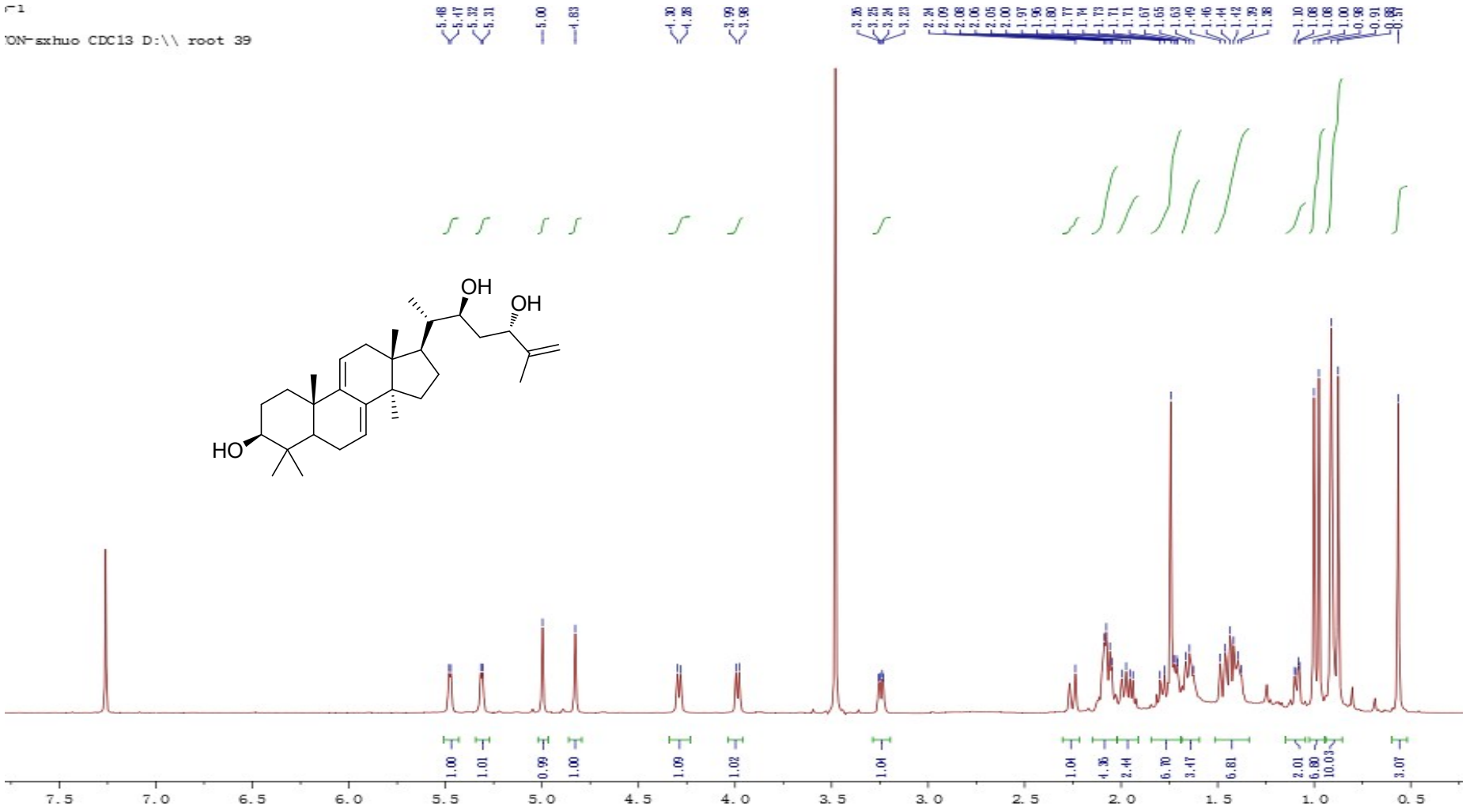

Figure S20. The ^{13}C NMR (150 MHz, $CDCl_3$) spectrum of ganodecochlearin D (4).

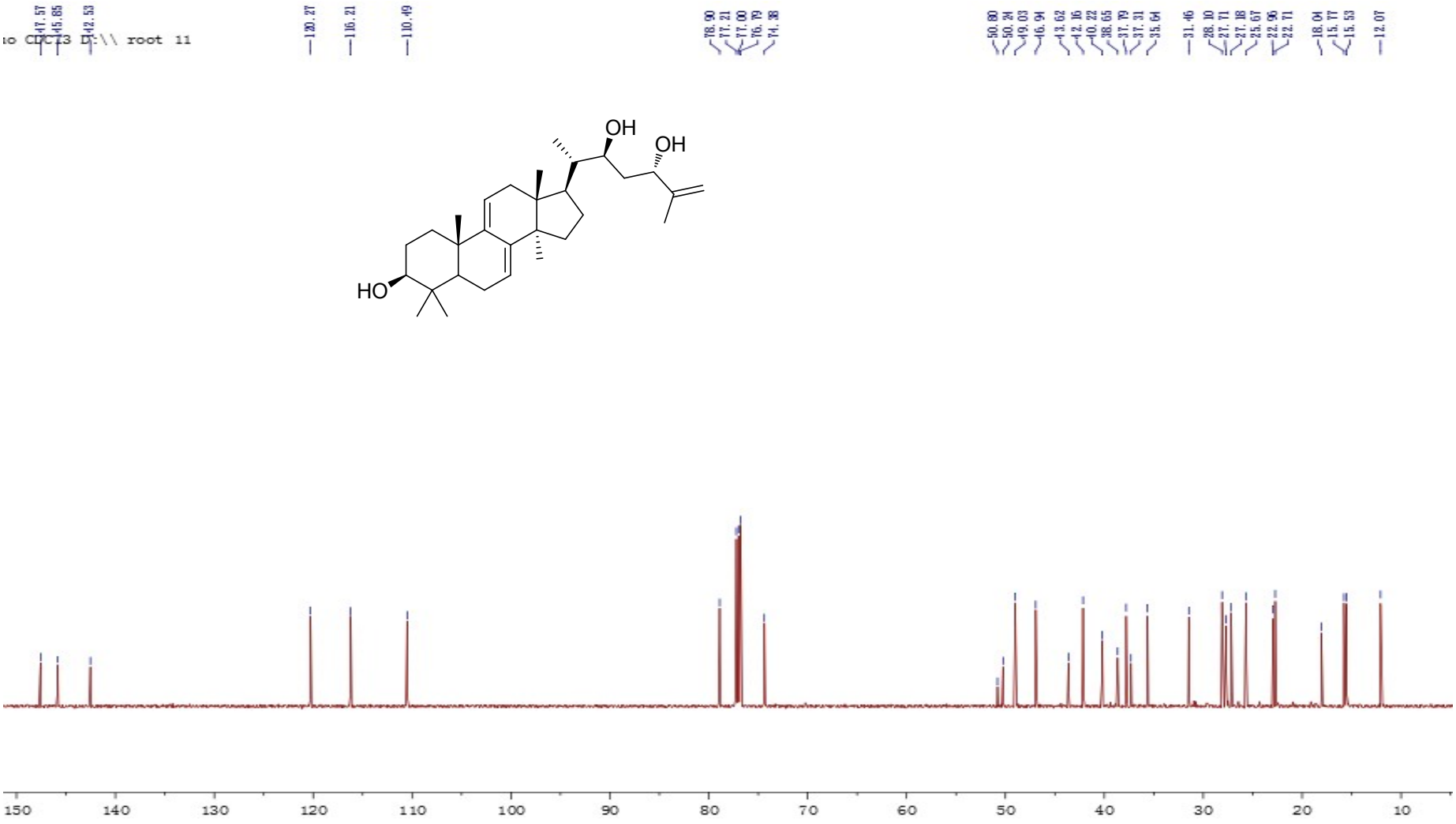

Figure S21. The HSQC spectrum of ganodecochlearin D (4).

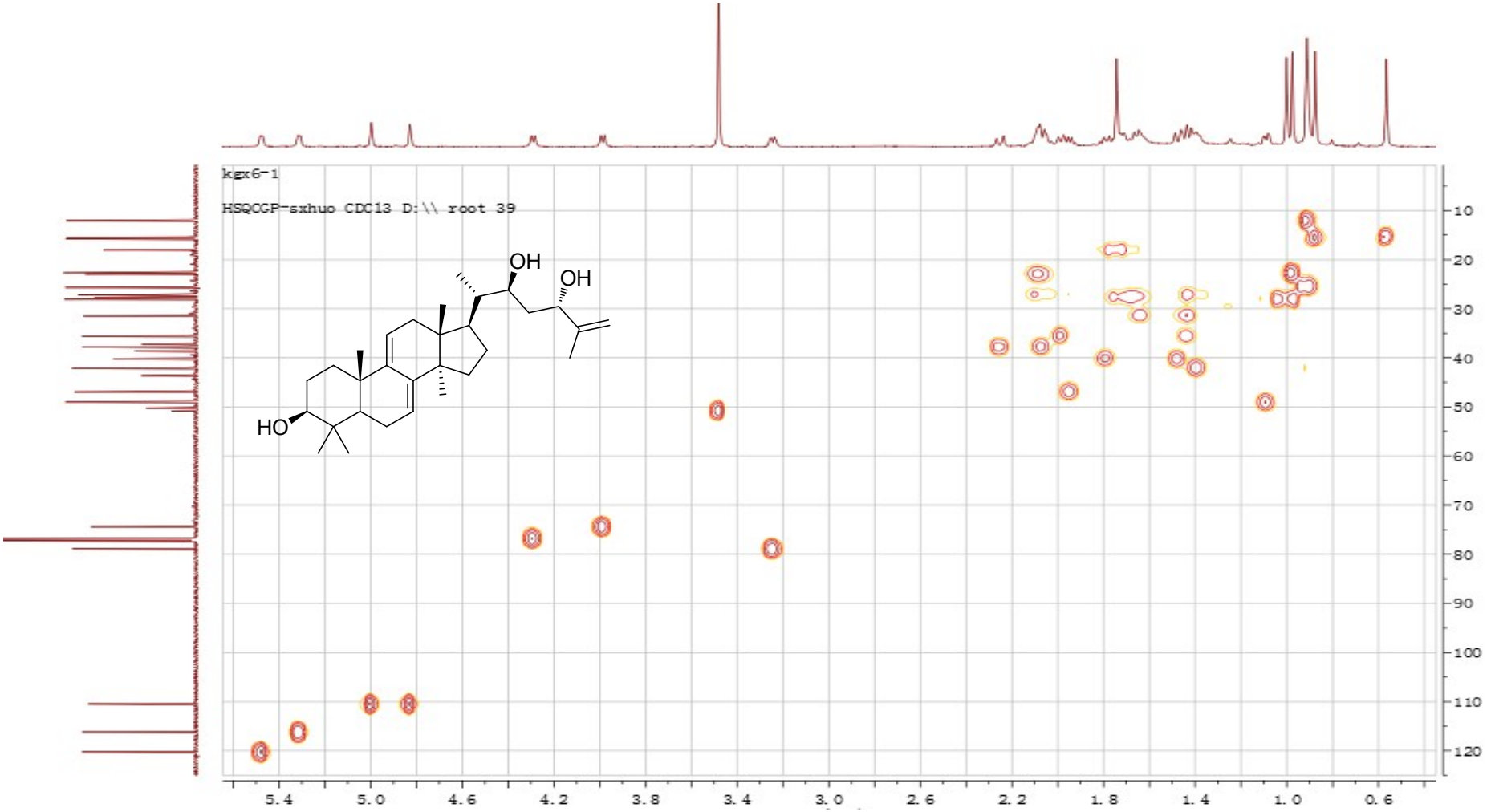

Figure S22. The HMBC spectrum of ganodecochlearin D (4).

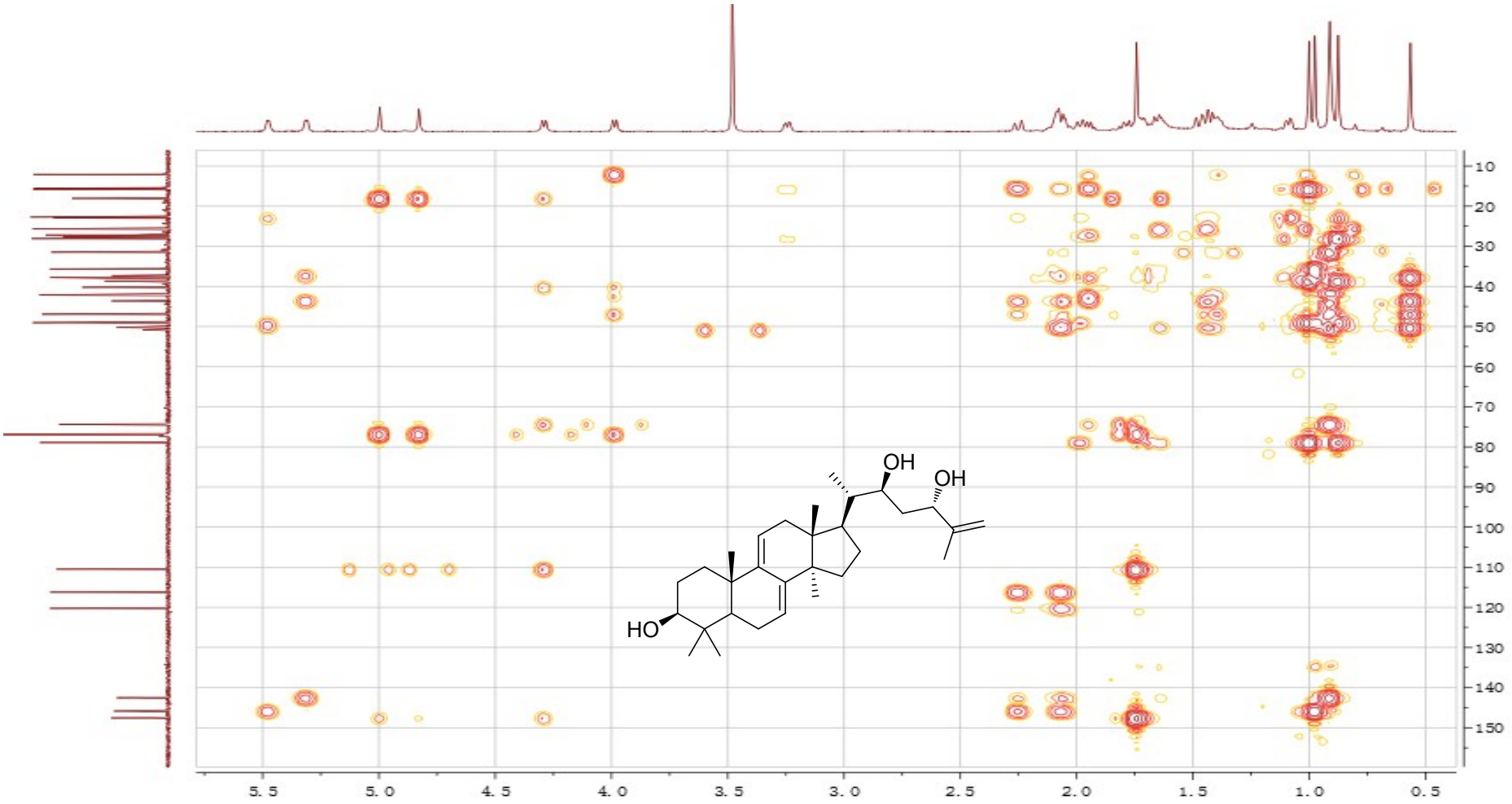

Figure S23. The ^{1}H-^{1}H COSY spectrum of ganodecochlearin D (4).

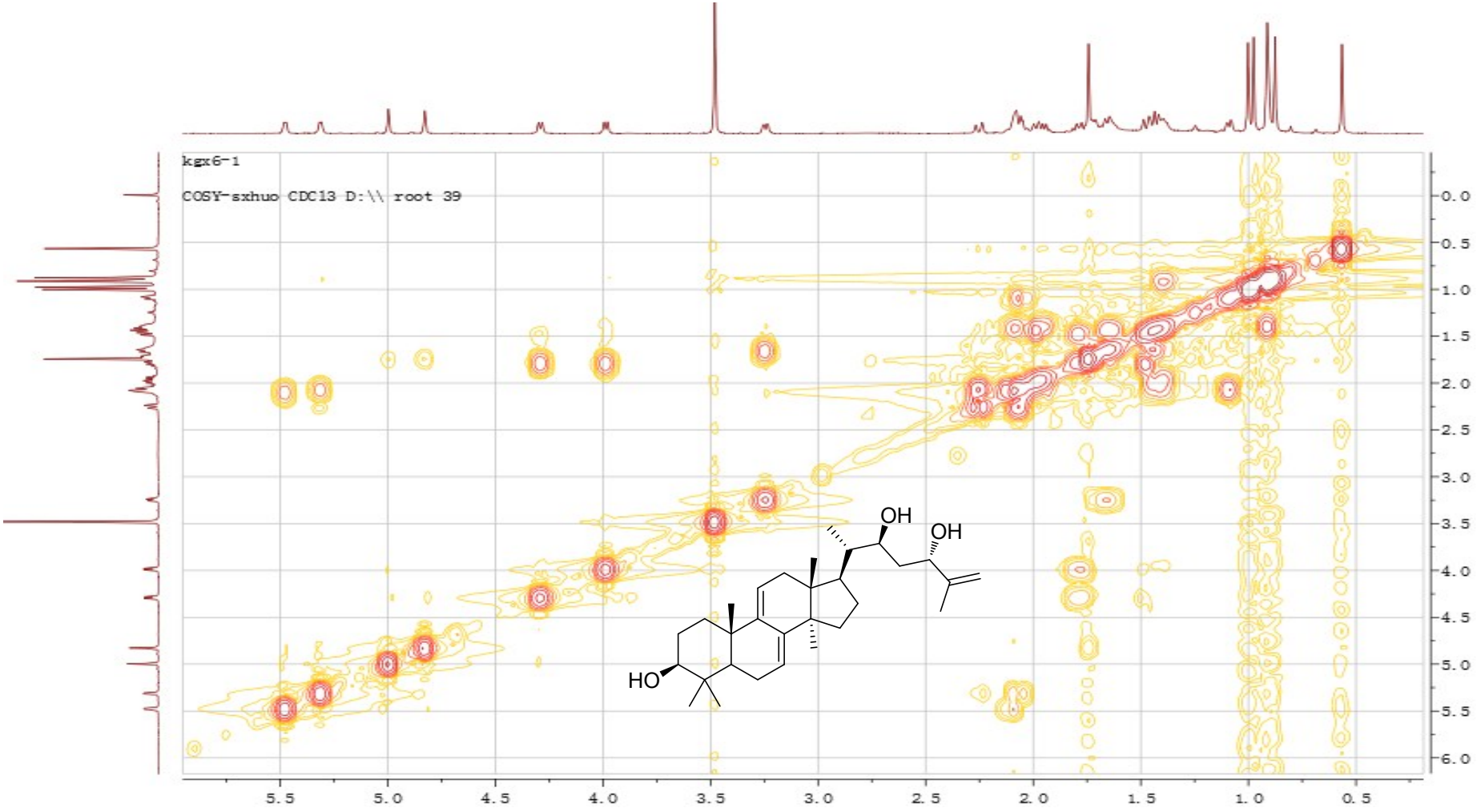

Figure S24. The ROESY spectrum of ganodecochlearin D (4).

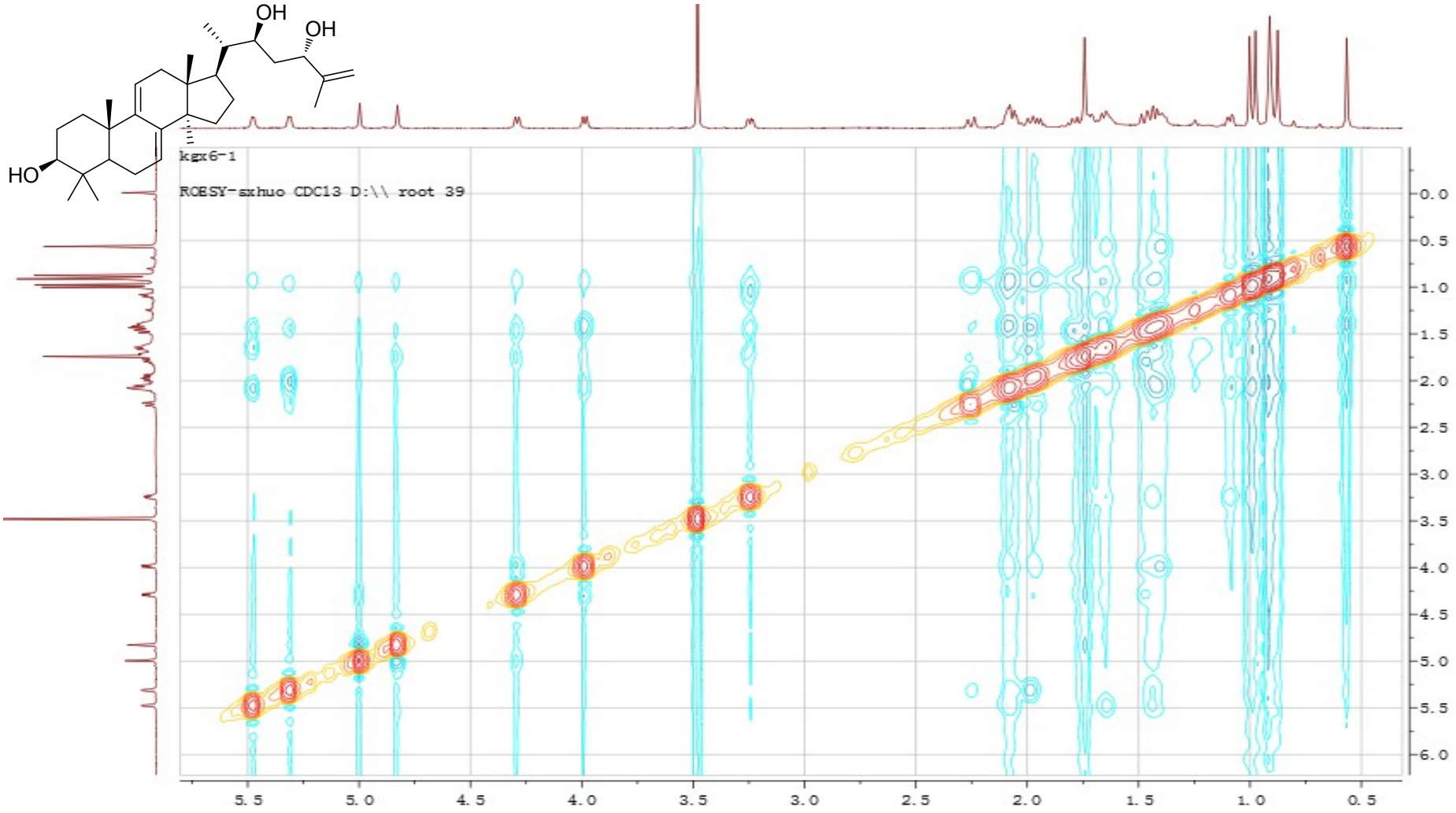

Figure S25. The ^{1}H NMR (600 MHz, C_5D_5N) spectrum of ganodercochlearin E (5).

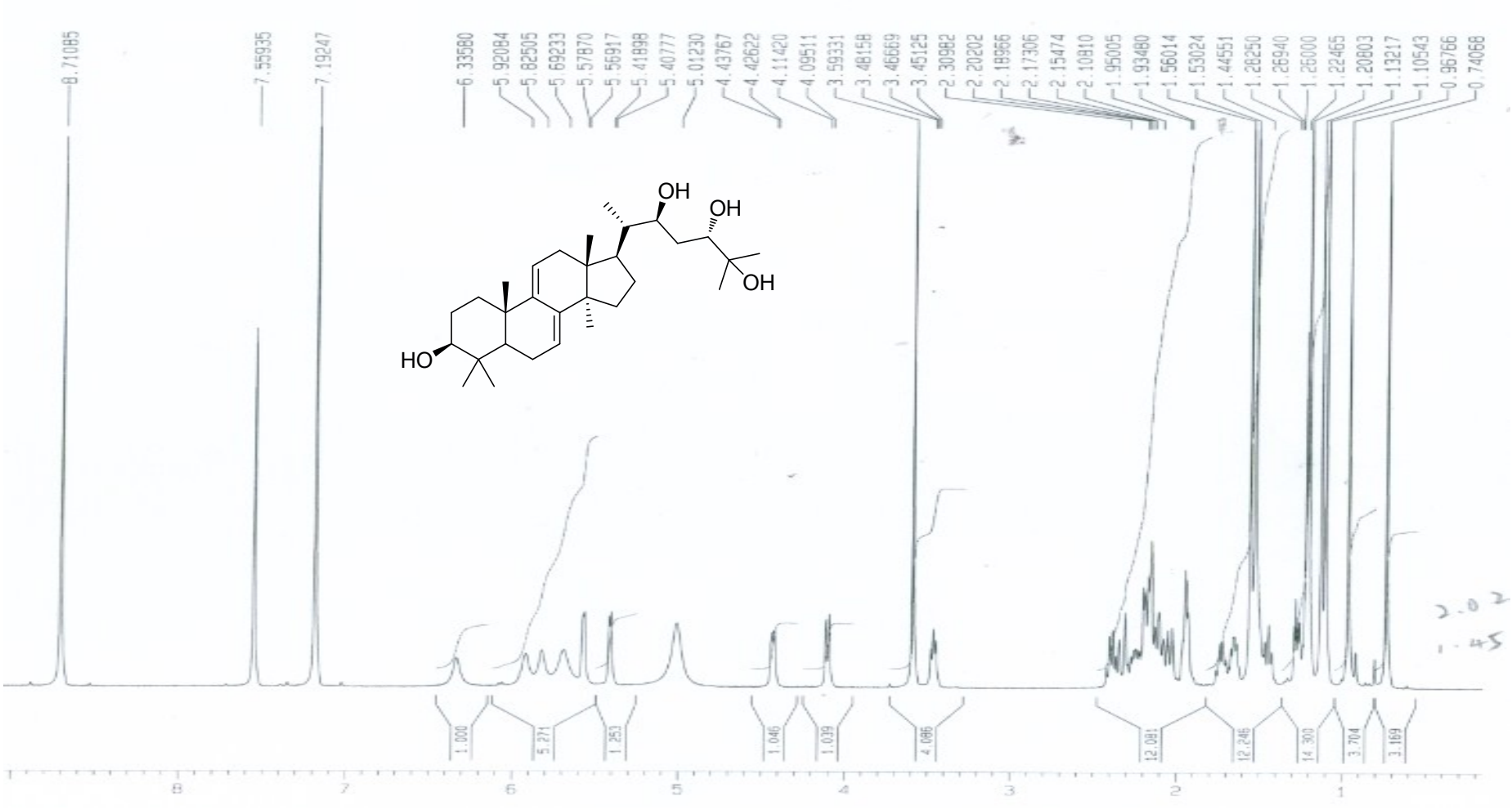

Figure S26. The ^{13}C NMR (150 MHz, , C_5D_5N) spectrum of ganodercochlearin E (5).

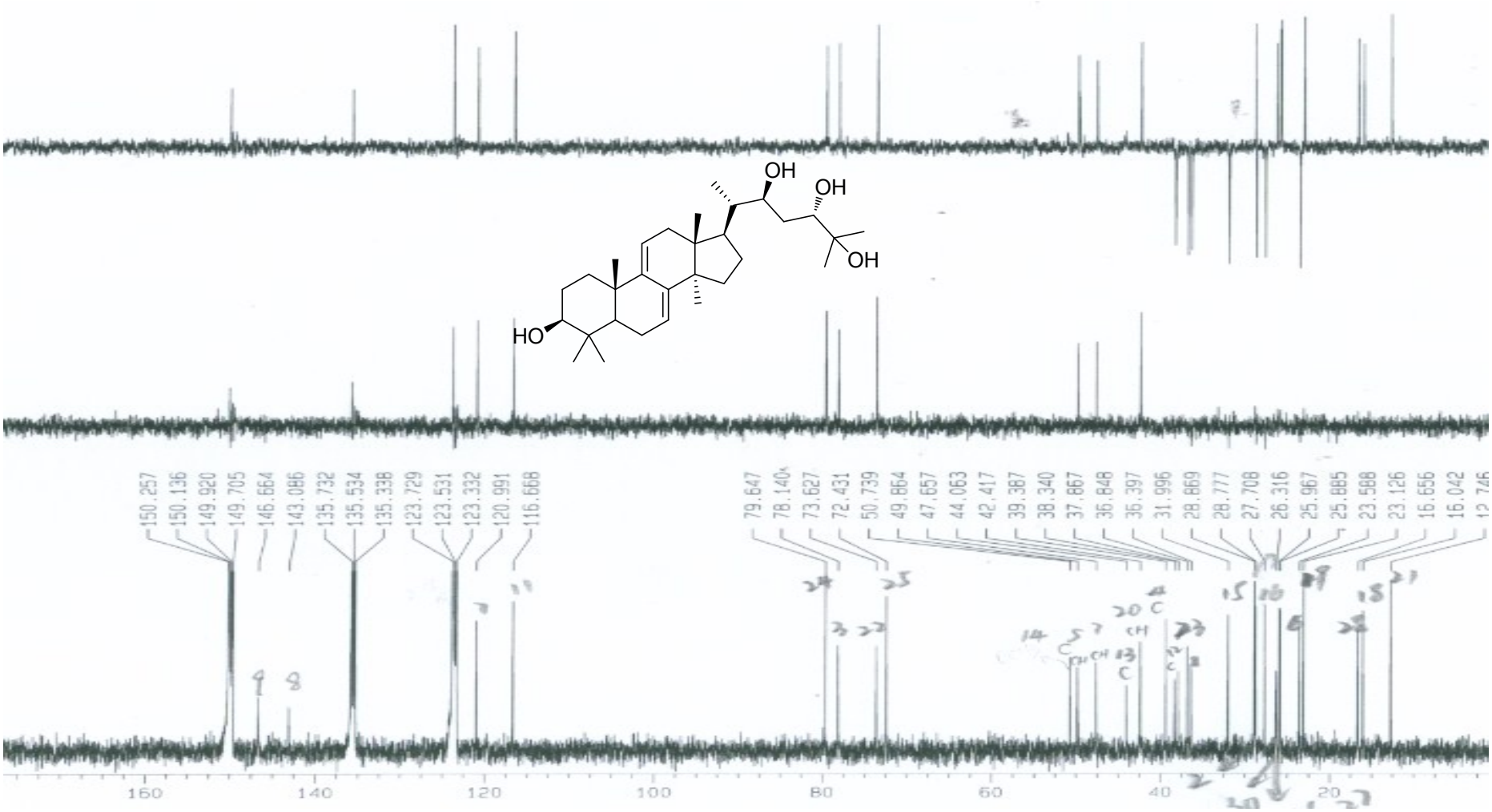

Figure S27. The HSQC spectrum of ganodercochlearin E (5).

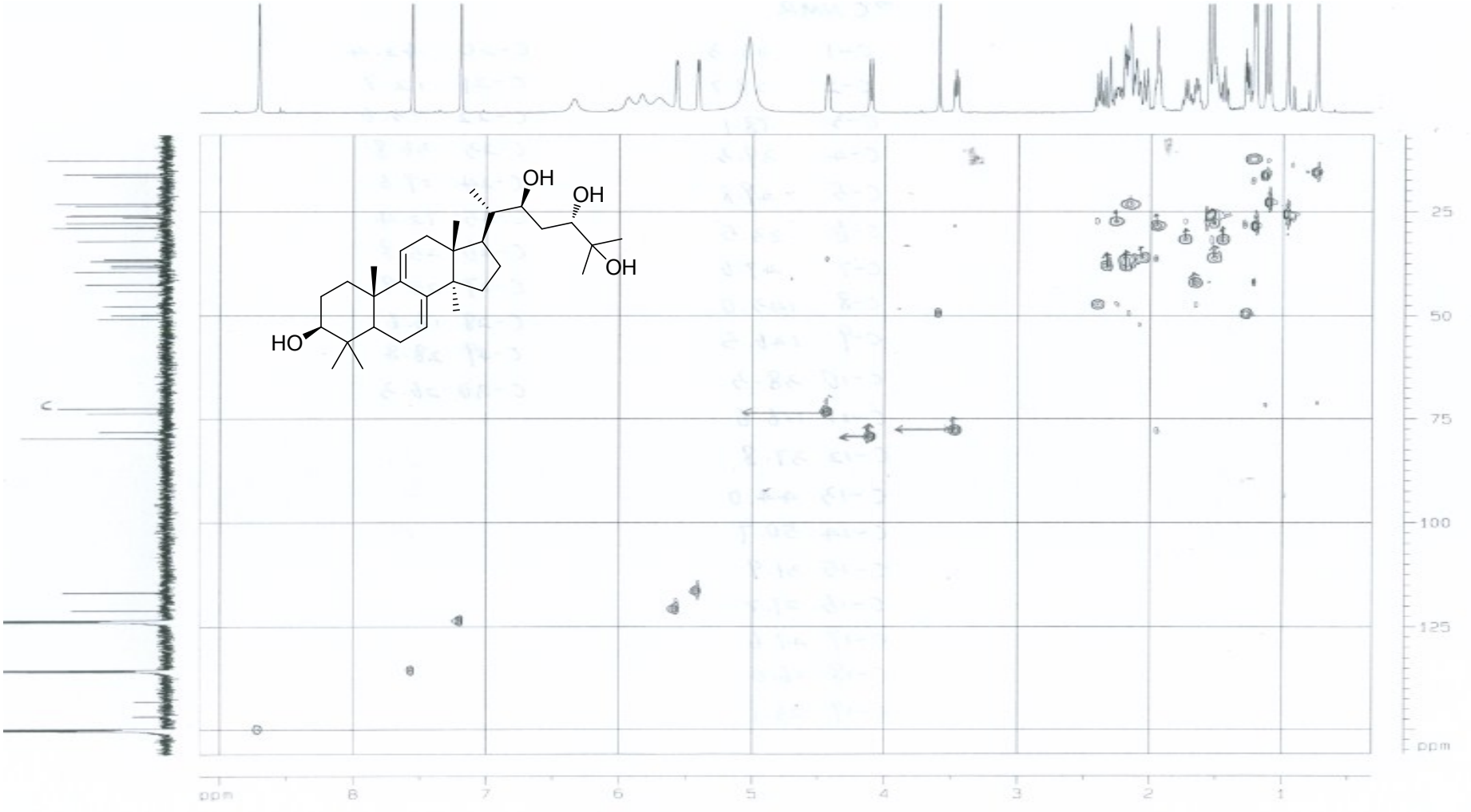

Figure S28. The HMBC spectrum of ganodercochlearin E (5).

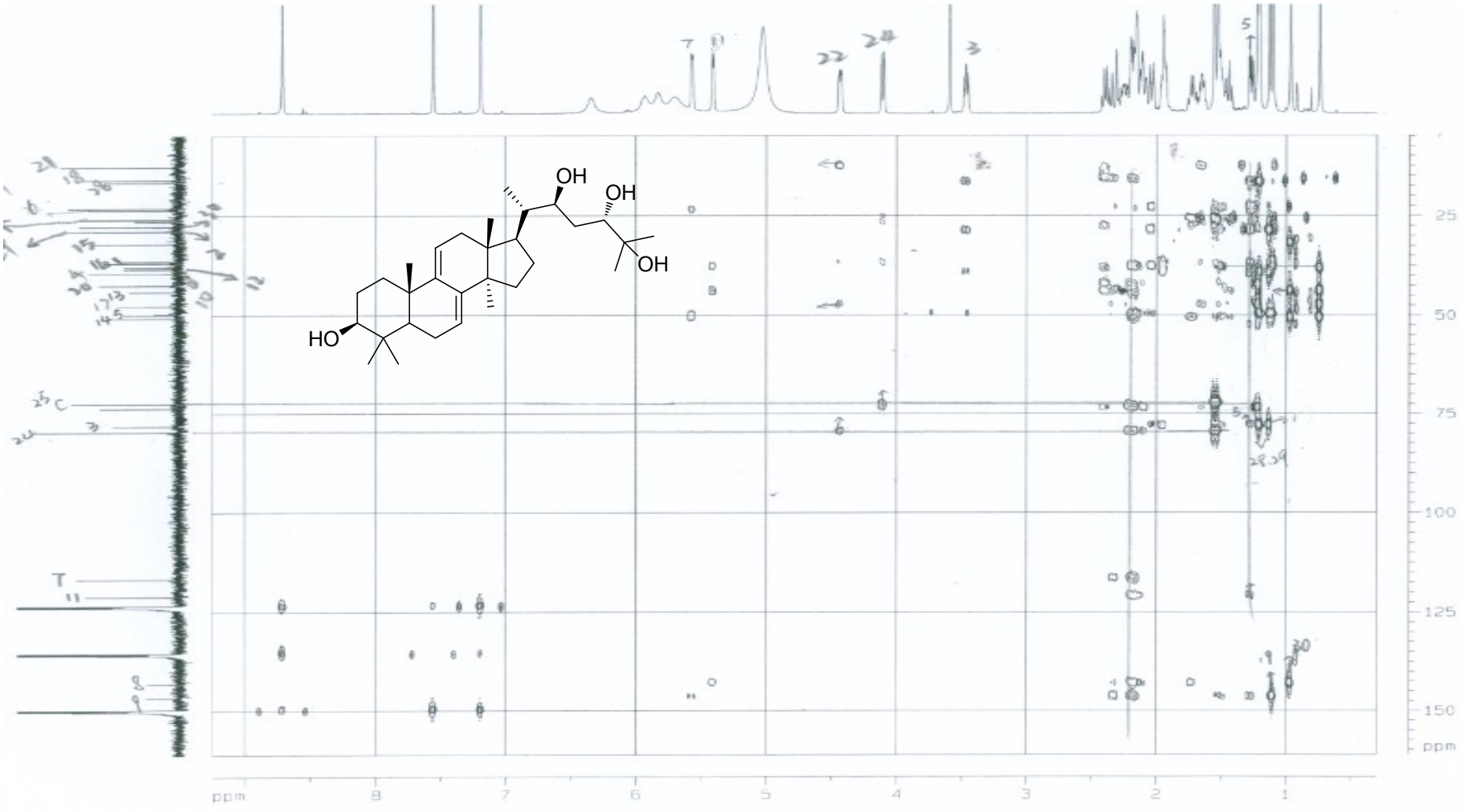

Figure S29. The ^{1}H-^{1}H COSY spectrum of ganodercochlearin E (5).

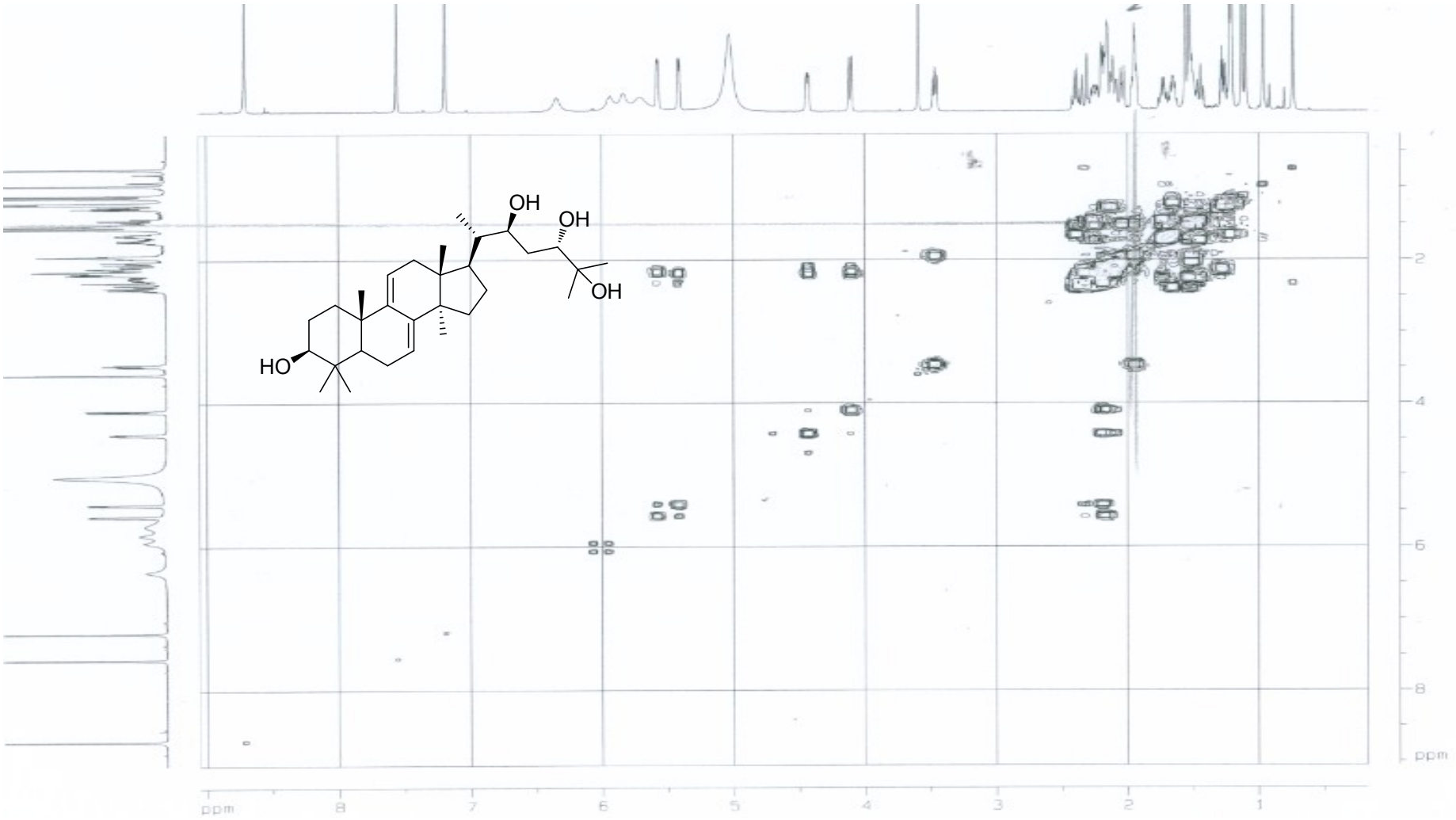

Figure S30. The ROESY spectrum of ganodercochlearin E (5).

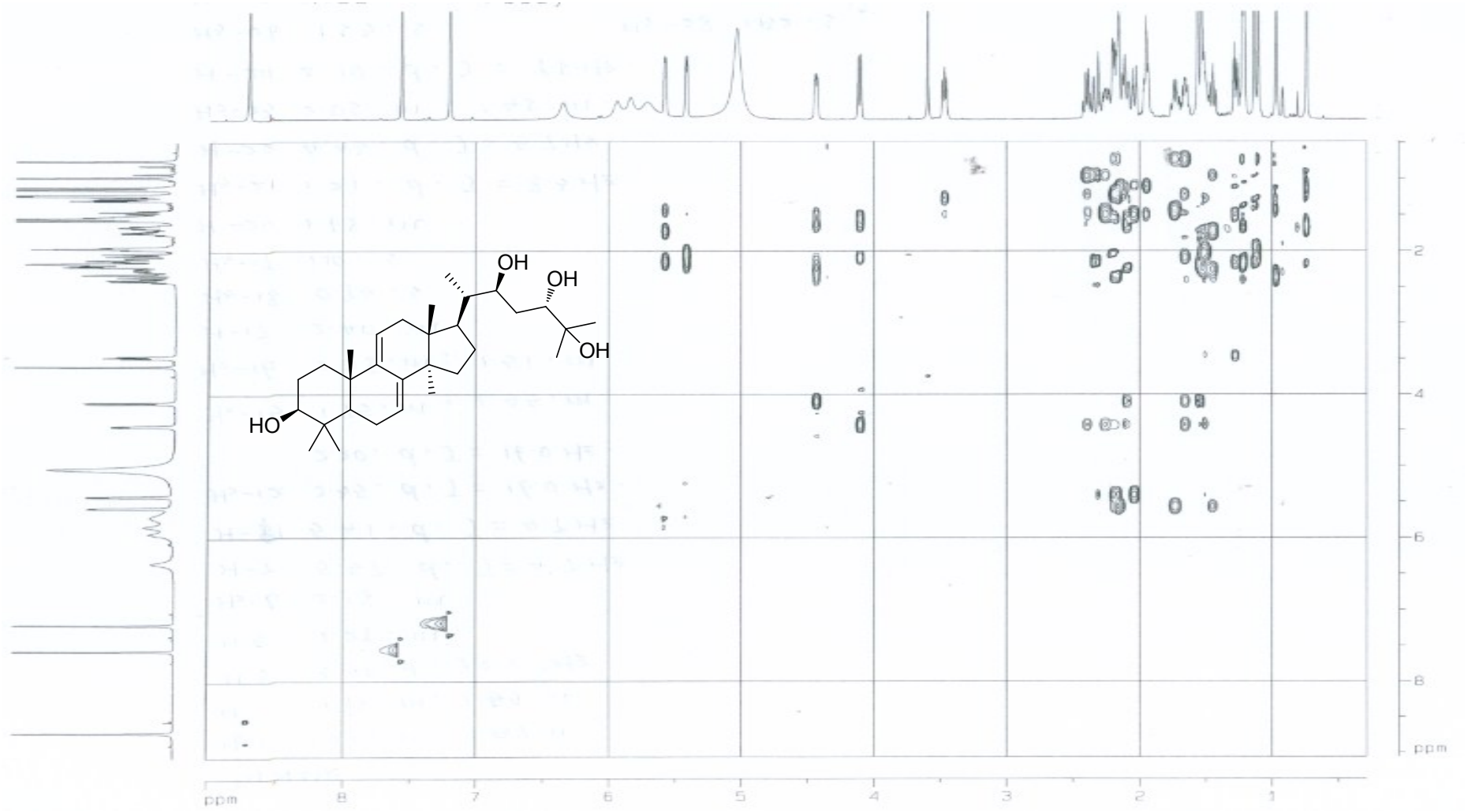

Figure S31. The ^{1}H NMR (600 MHz, $CDCl_3$) spectrum of cochlearic acid A (6).

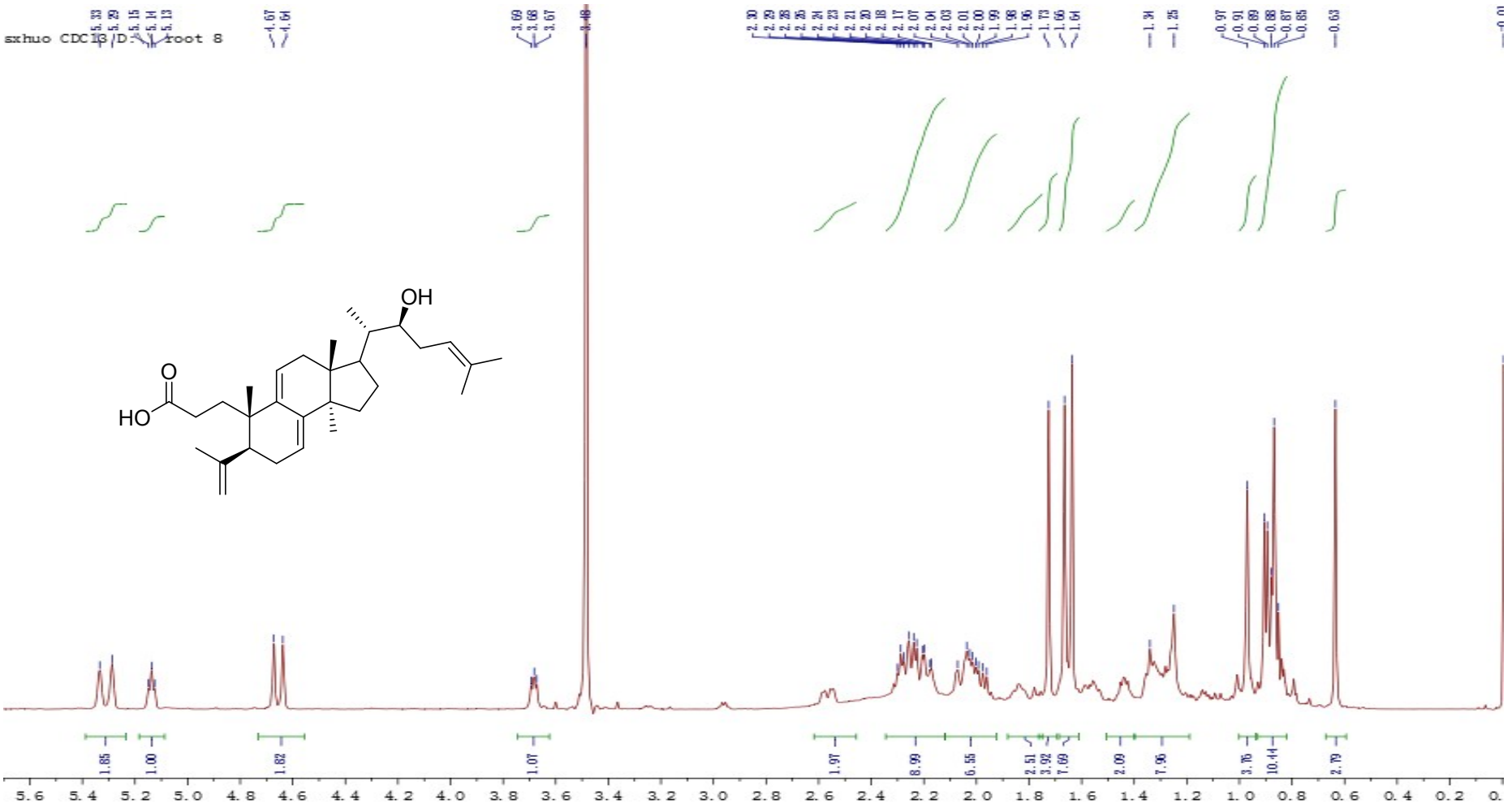

Figure S32. The ^{1}H NMR (150 MHz, $CDCl_3$) spectrum of cochlearic acid A (6).

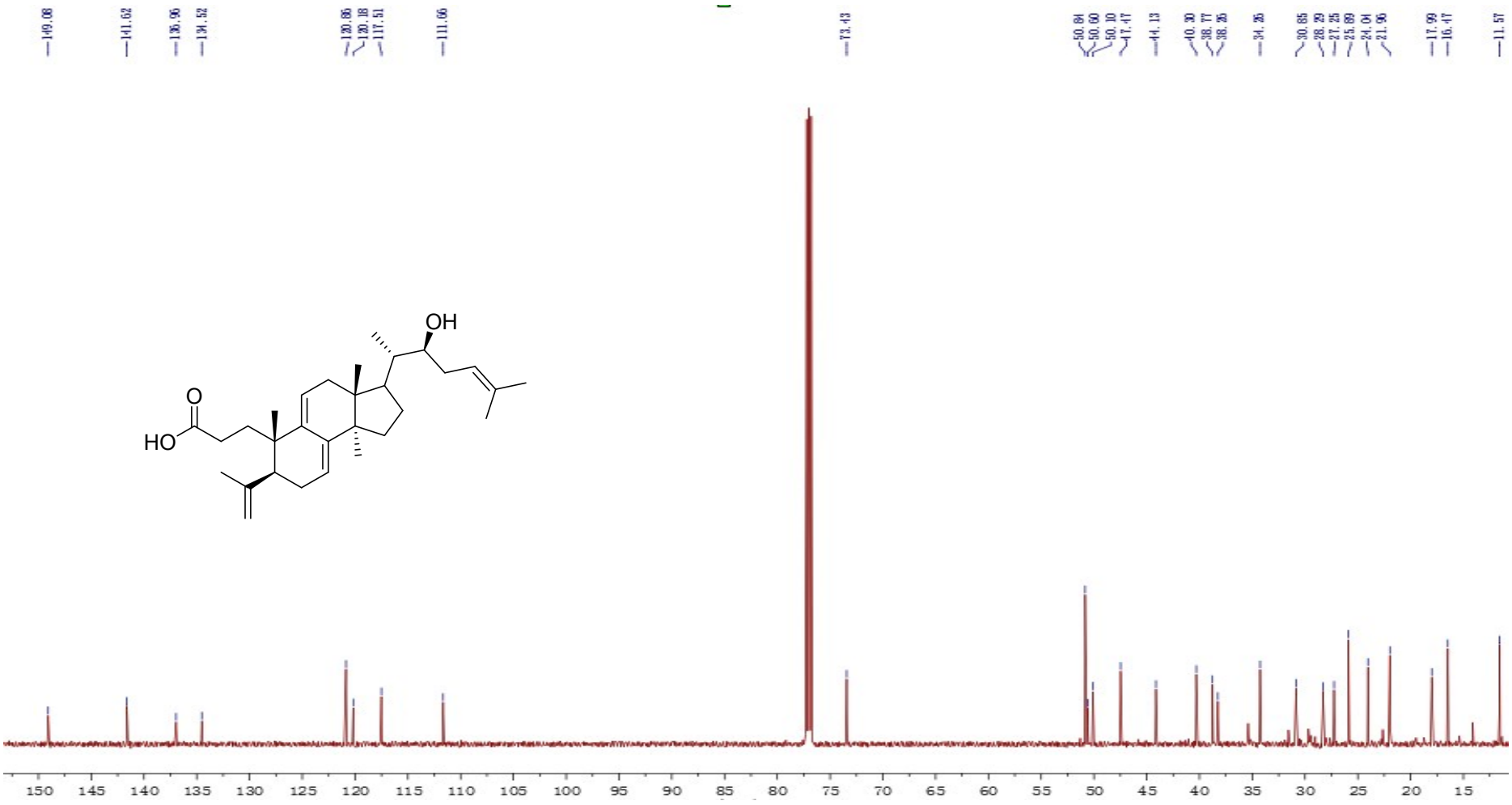

Figure S33. The HSQC spectrum of cochlearic acid A (6).

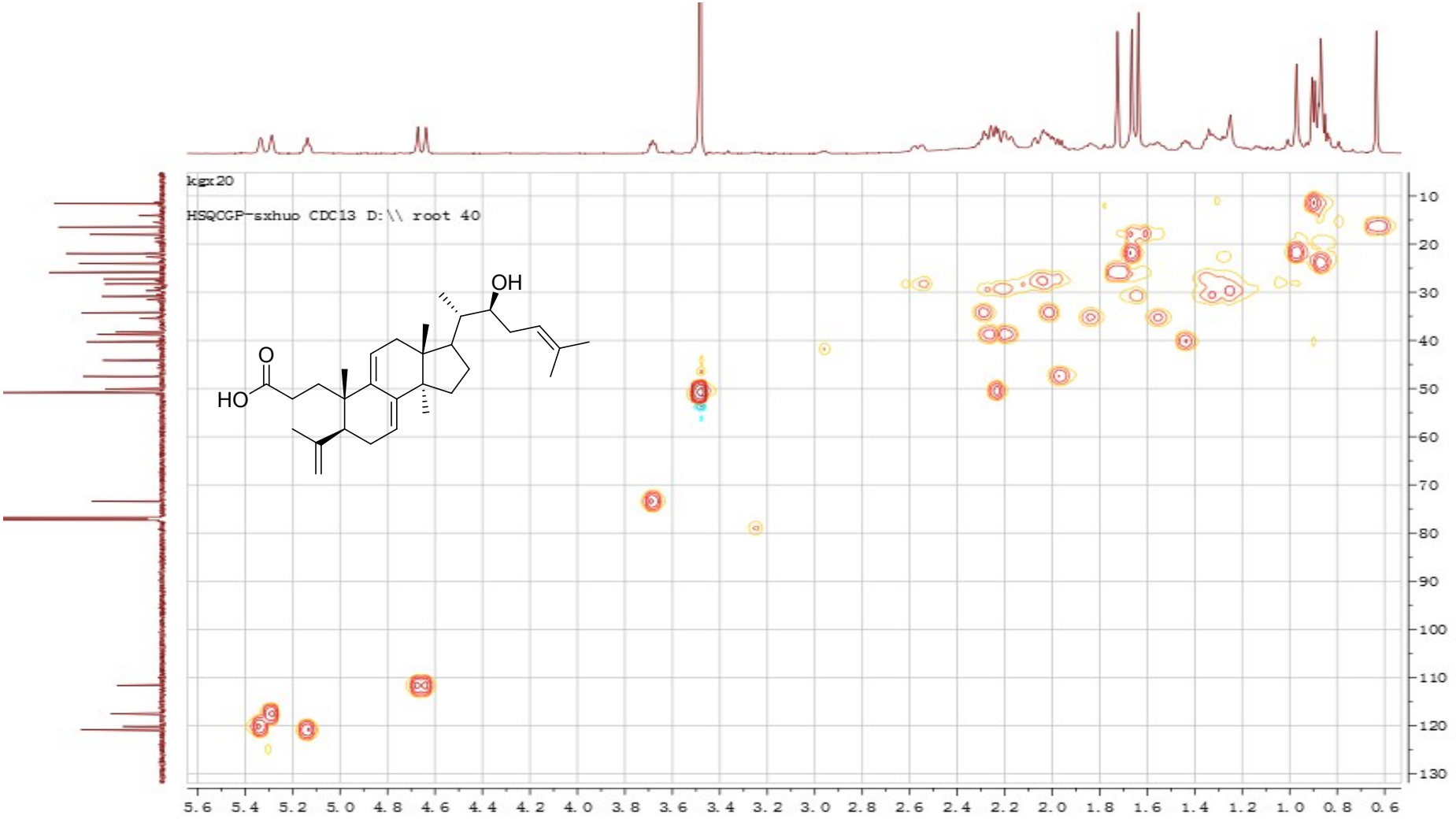

Figure S34. The HMBC spectrum of cochlearic acid A (6).

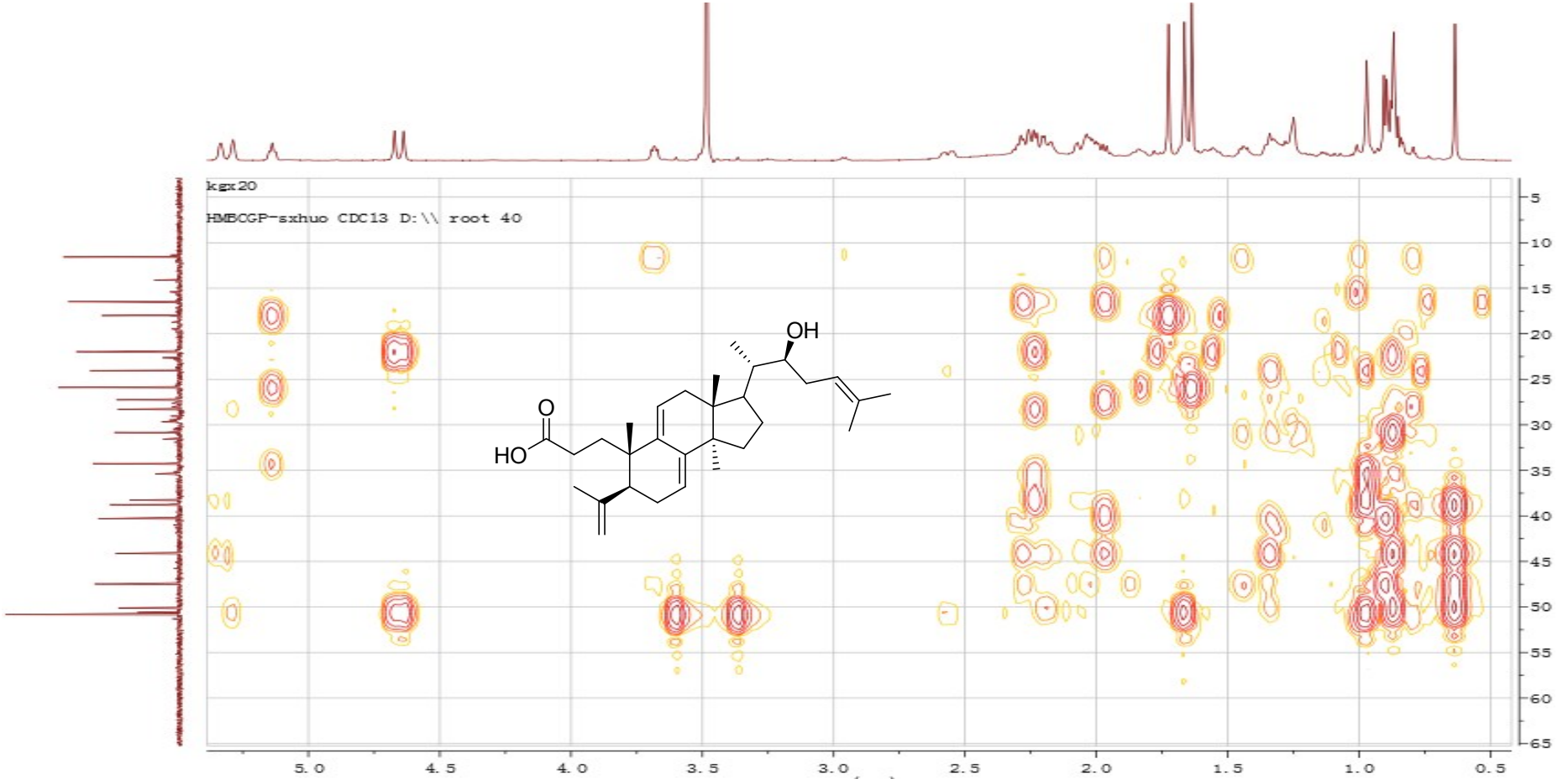

Figure S35. The ^{1}H-^{1}H COSY spectrum of cochlearic acid A (6).

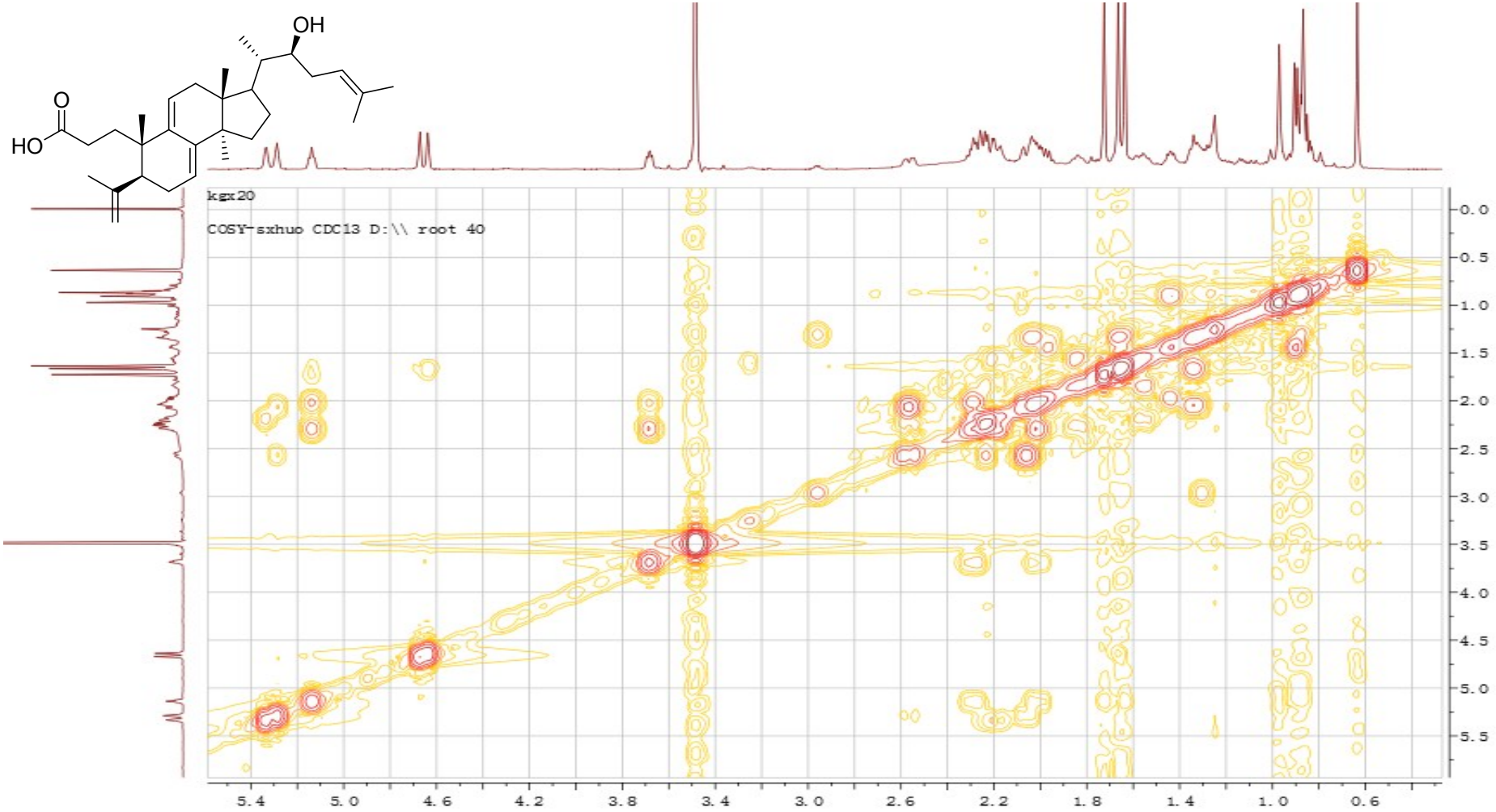

Figure S36. The ROESY spectrum of cochlearic acid A (6).

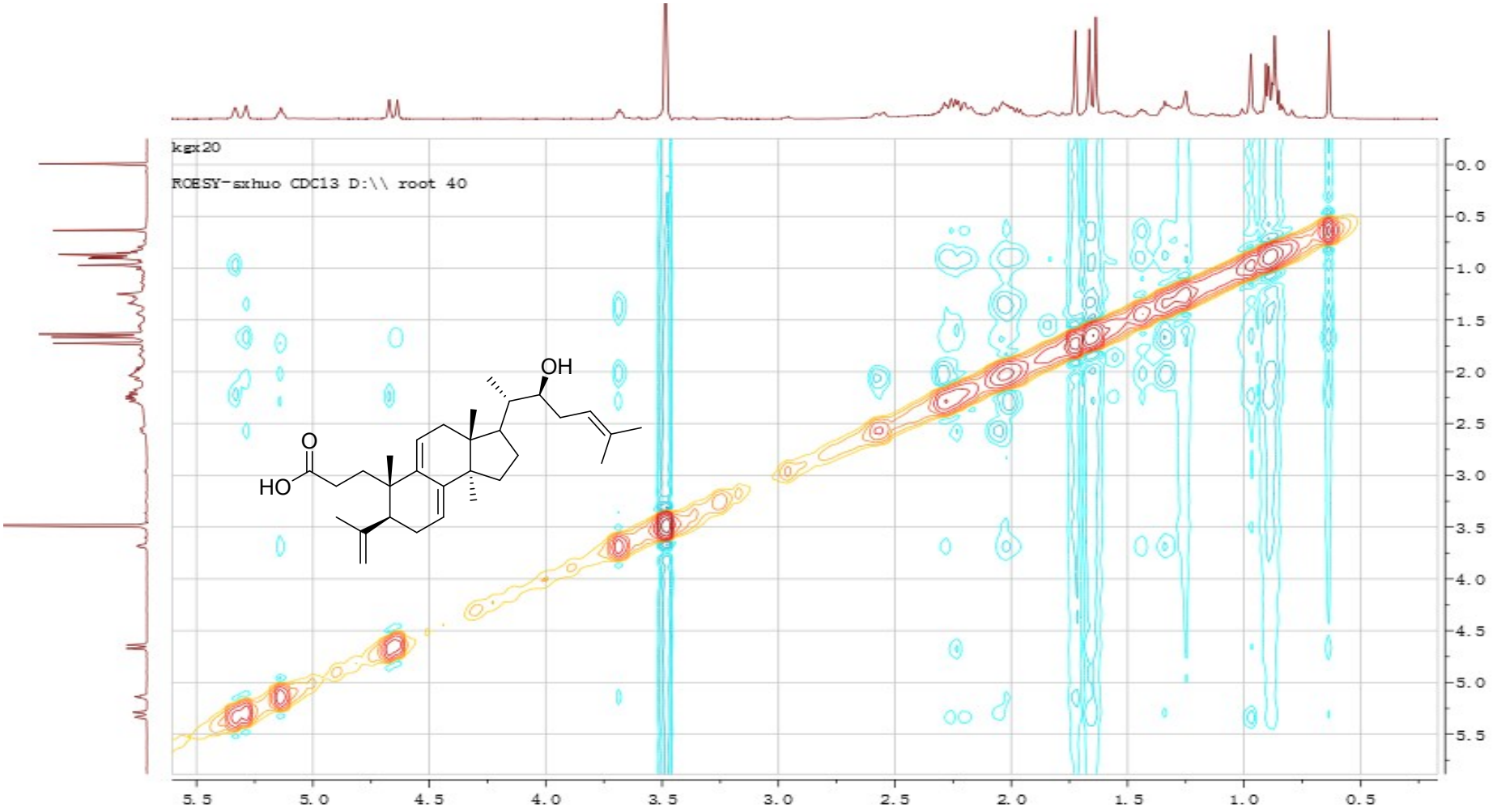

Figure S37. The ^{1}H NMR (600 MHz, C_5D_5N) spectrum of ganodercochlearin F (7).

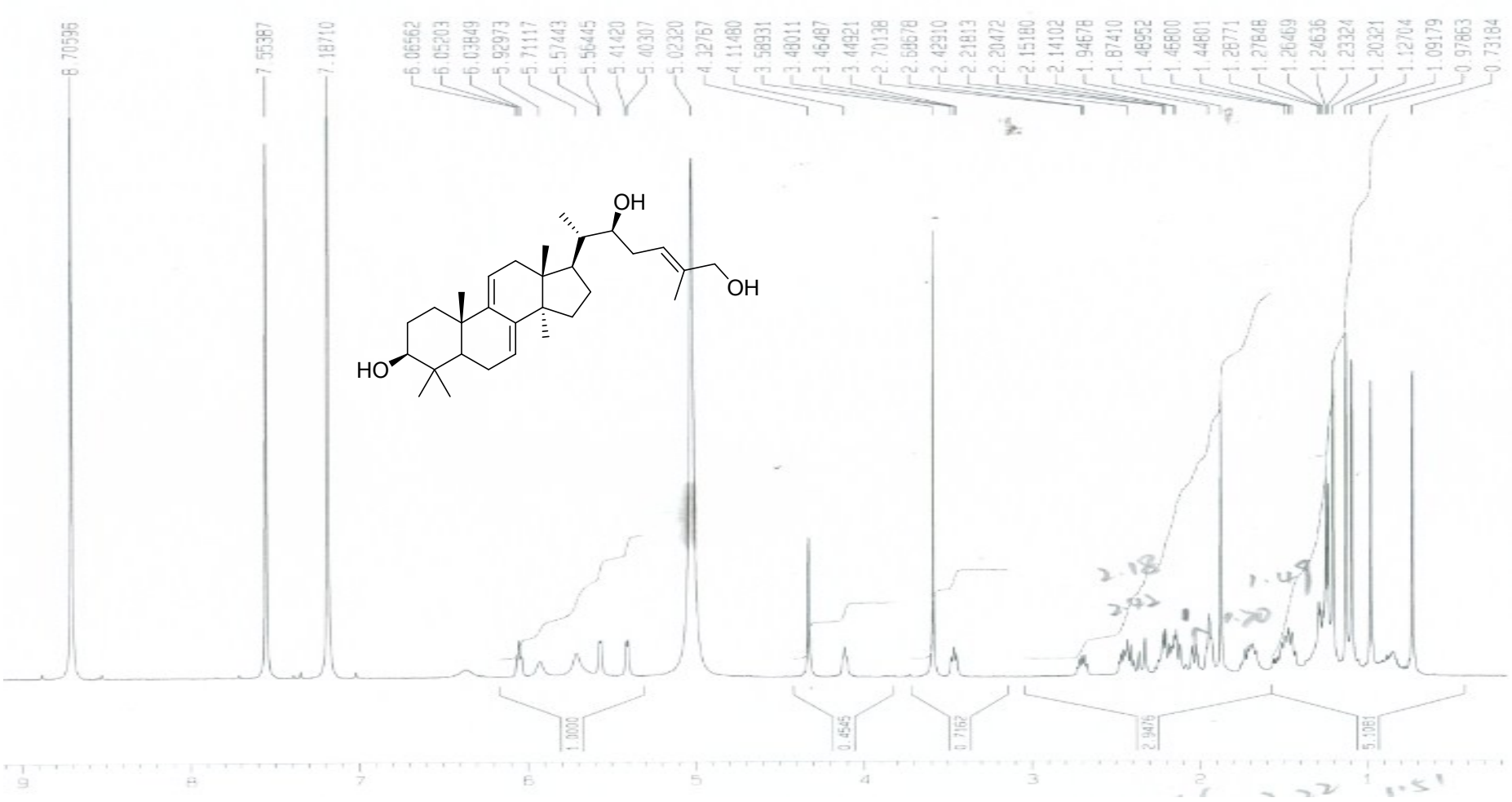

Figure S38. The ^{13}C NMR (150 MHz, , C_5D_5N) spectrum of ganodercochlearin F (7).

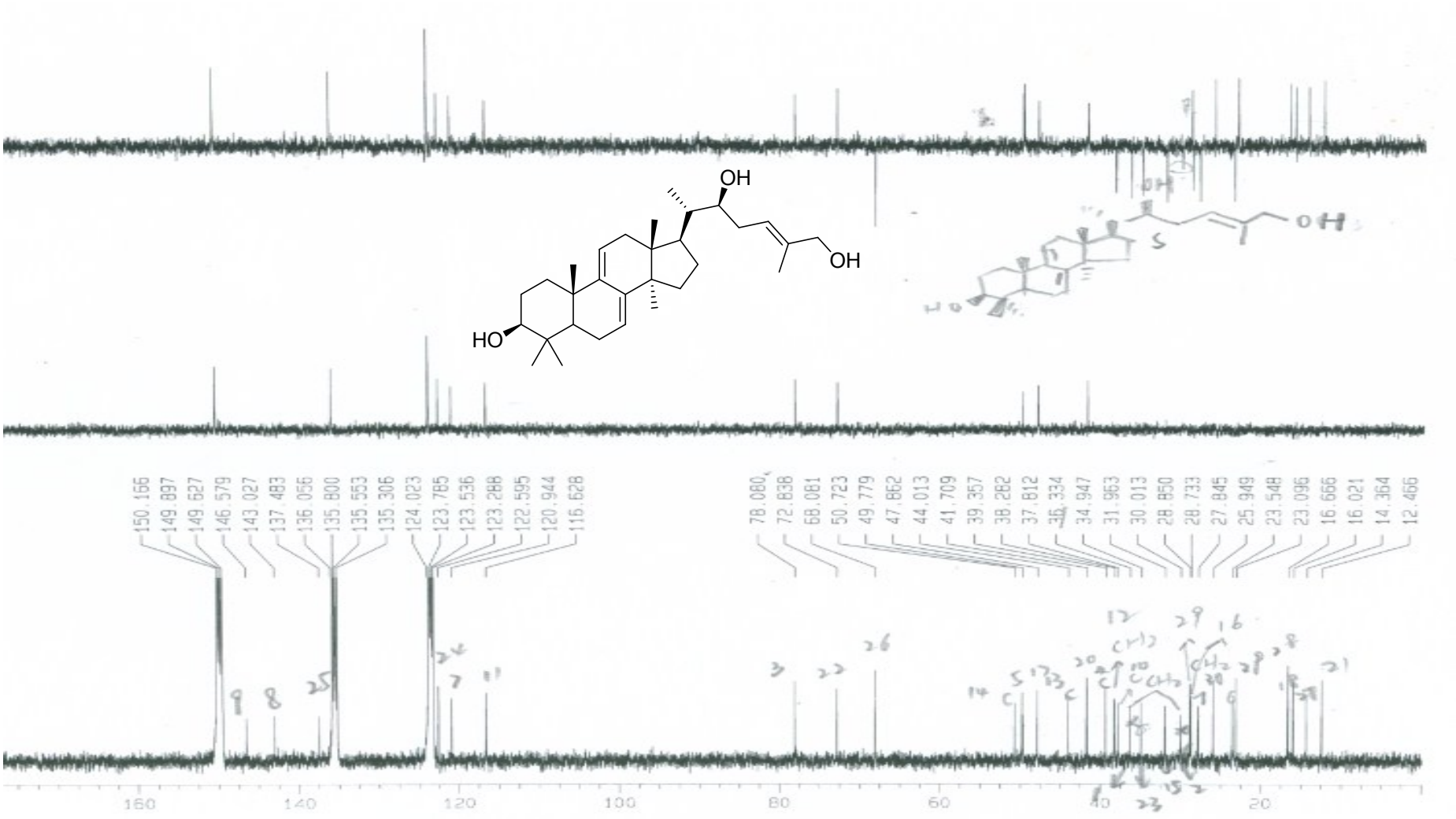

Figure S39. The HSQC spectrum of ganodercochlearin F (7).

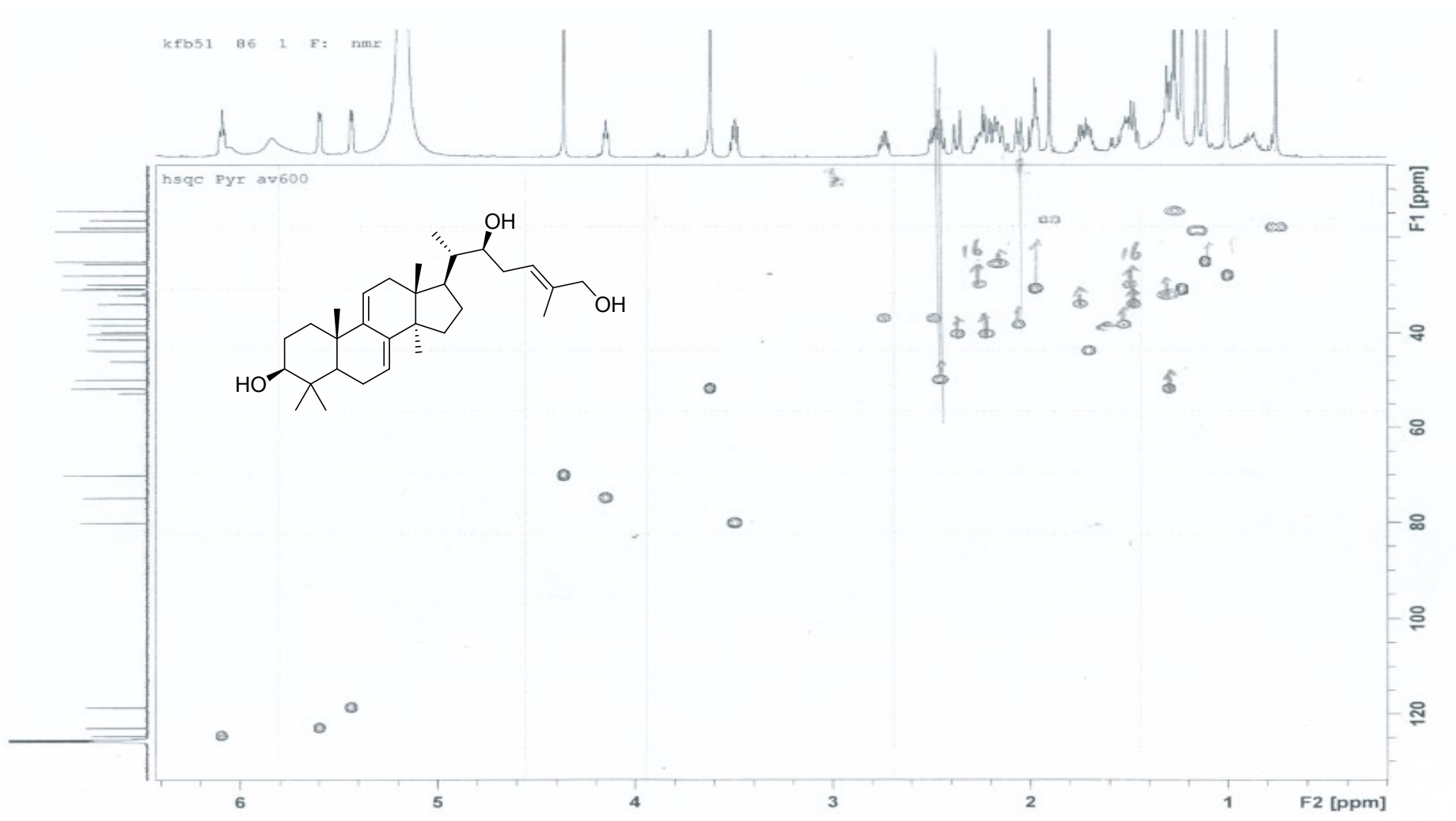

Figure S40. The HMBC spectrum of ganodercochlearin F (7).

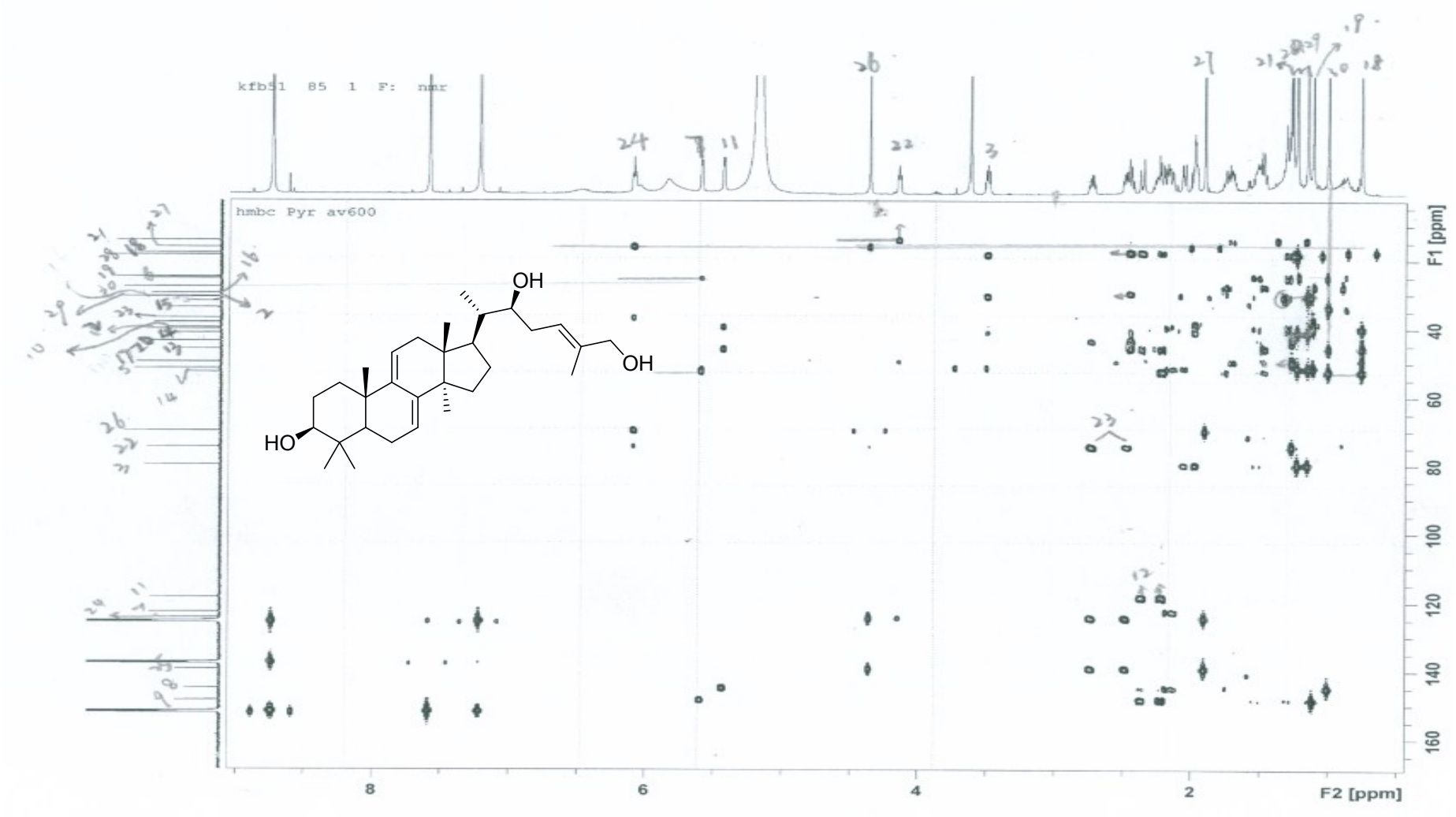

Figure S41. The ^{1}H-^{1}H COSY spectrum of ganodercochlearin F (7).

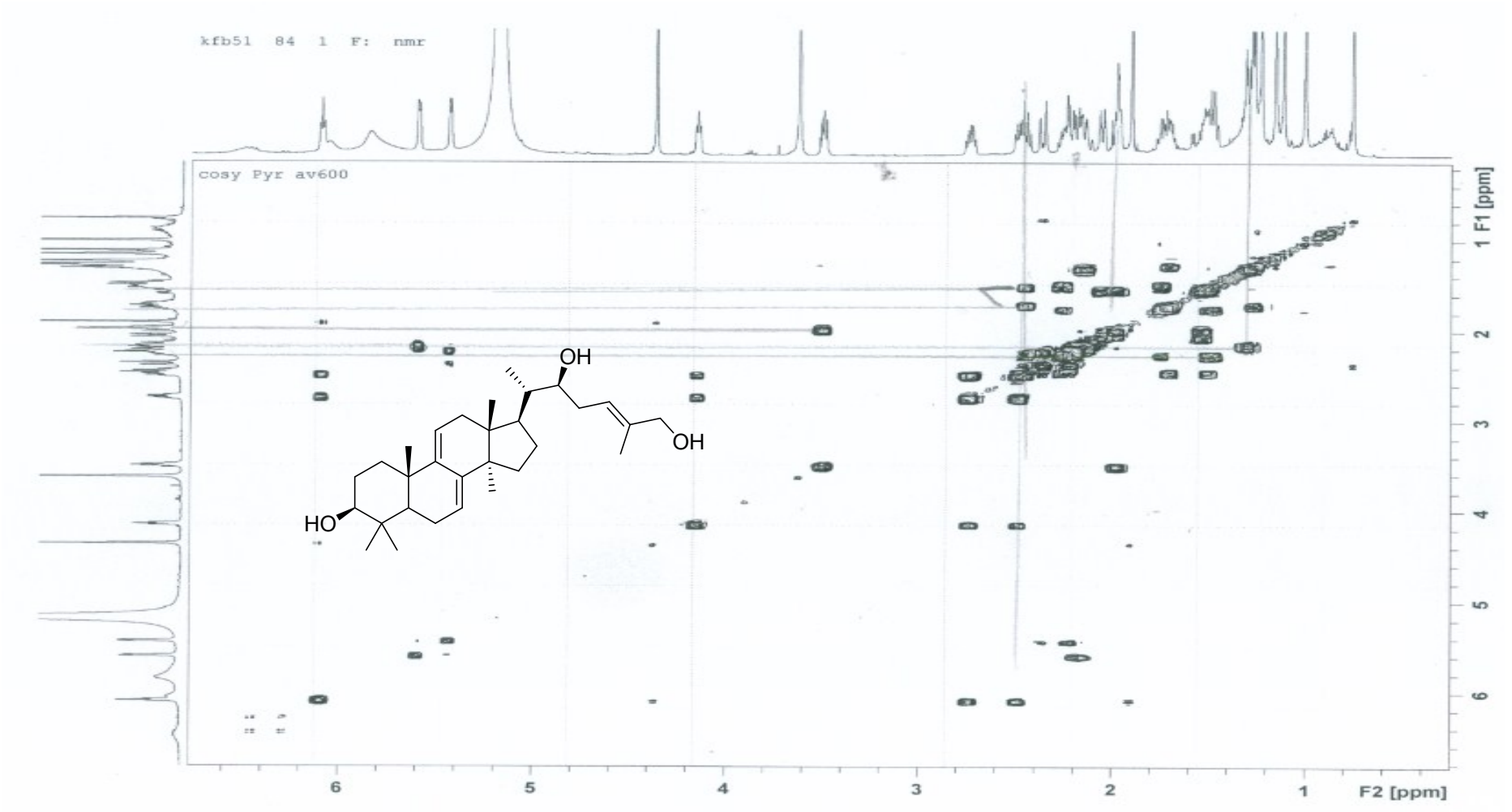

Figure S42. The ROESY spectrum of ganodercochlearin F (7).

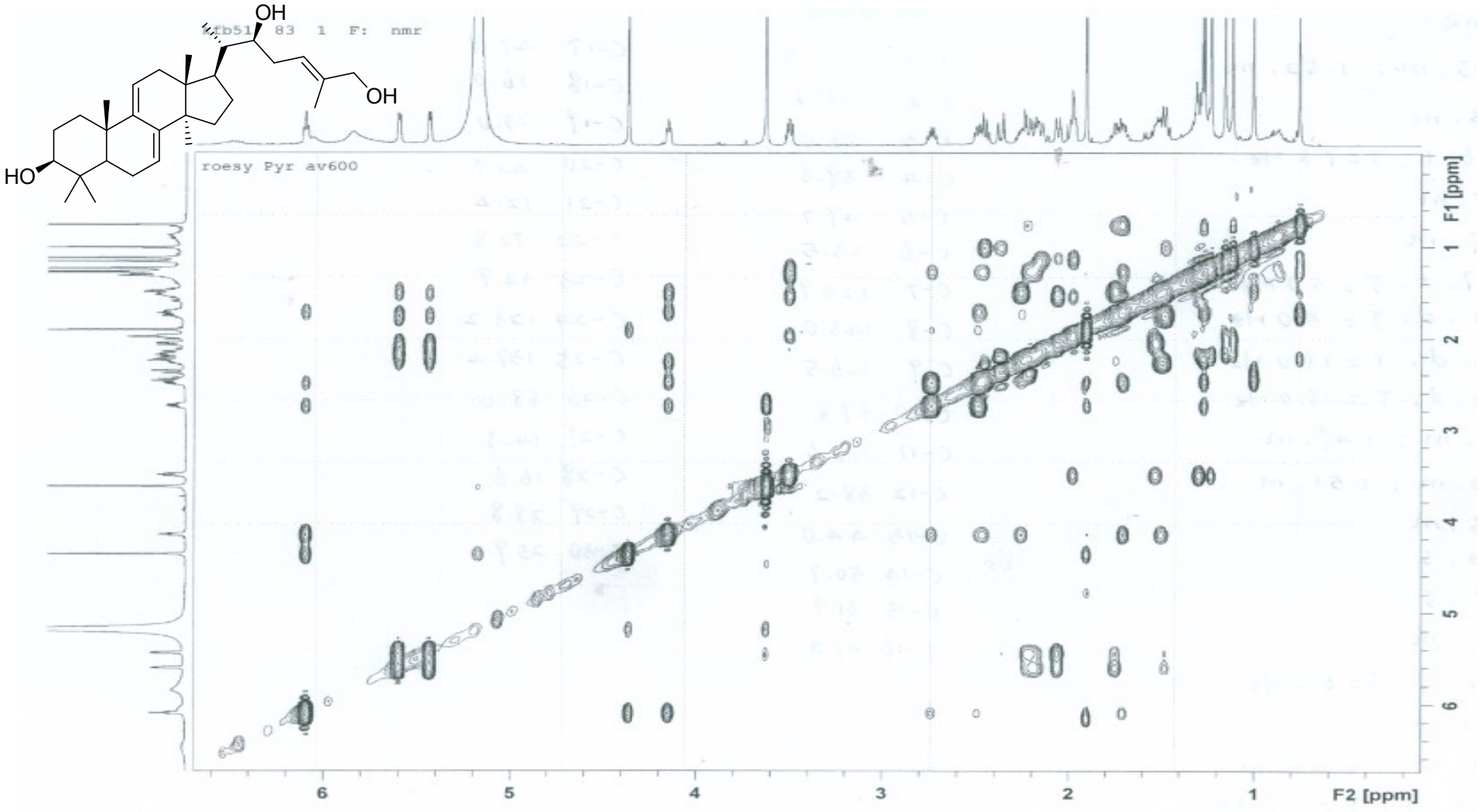

Figure S43. The ^{1}H NMR (600 MHz, $CDCl_3$) spectrum of ganodercochlearin G (8).

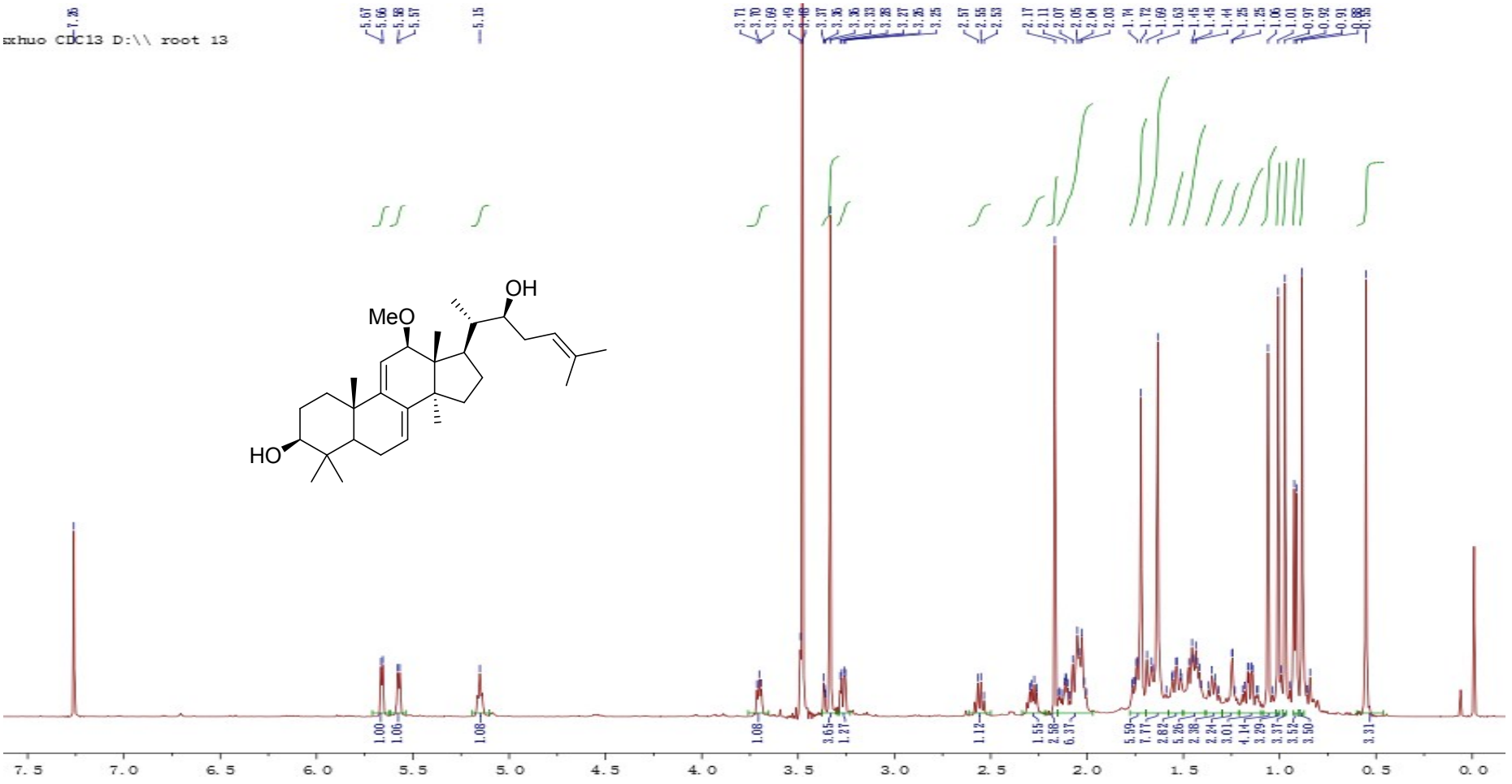

Figure S44. The ^{13}C NMR (150 MHz, $CDCl_3$) spectrum of ganodercochlearin G (8).

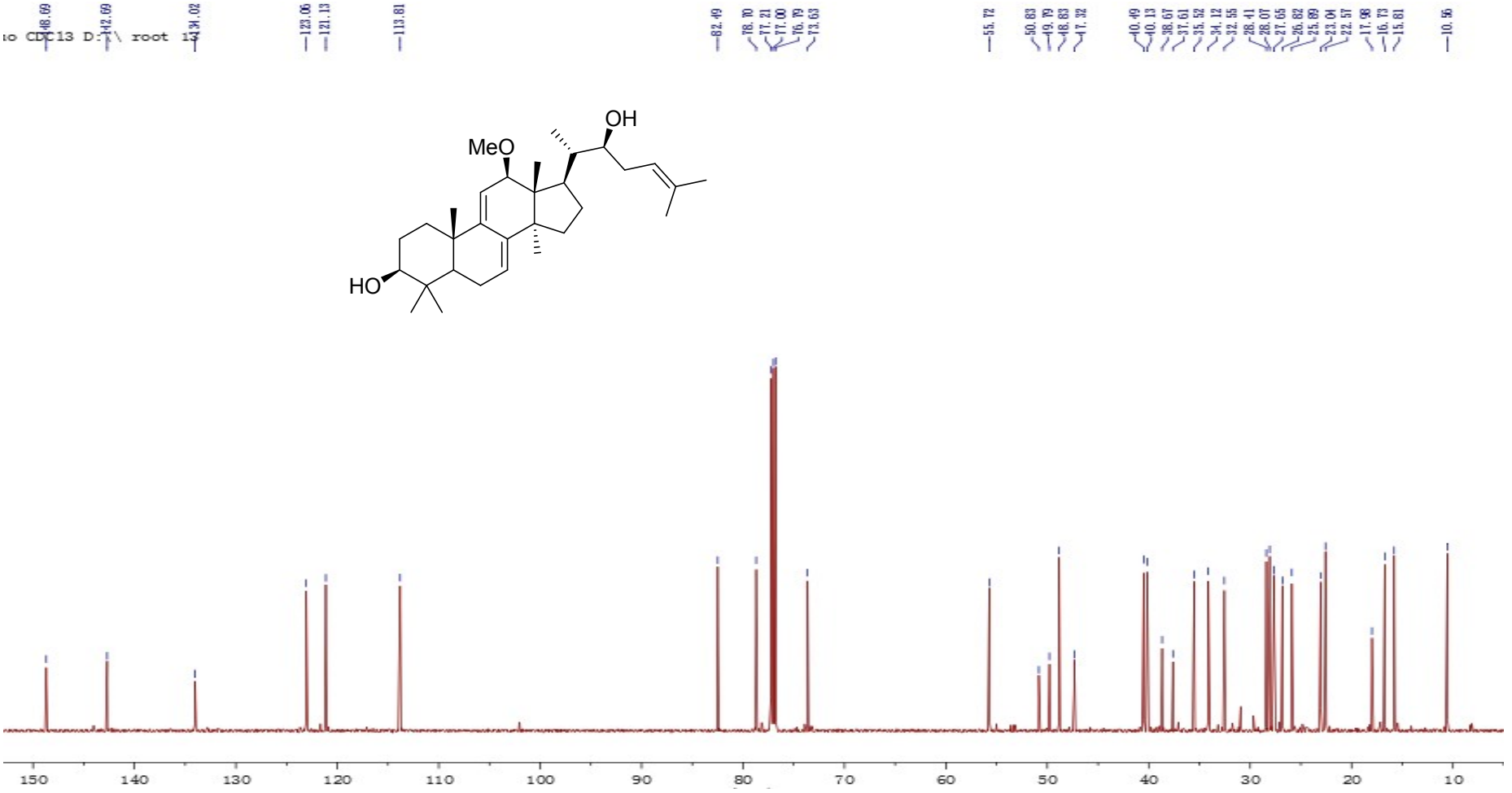

Figure S45. The HSQC spectrum of ganodercochlearin G (8).

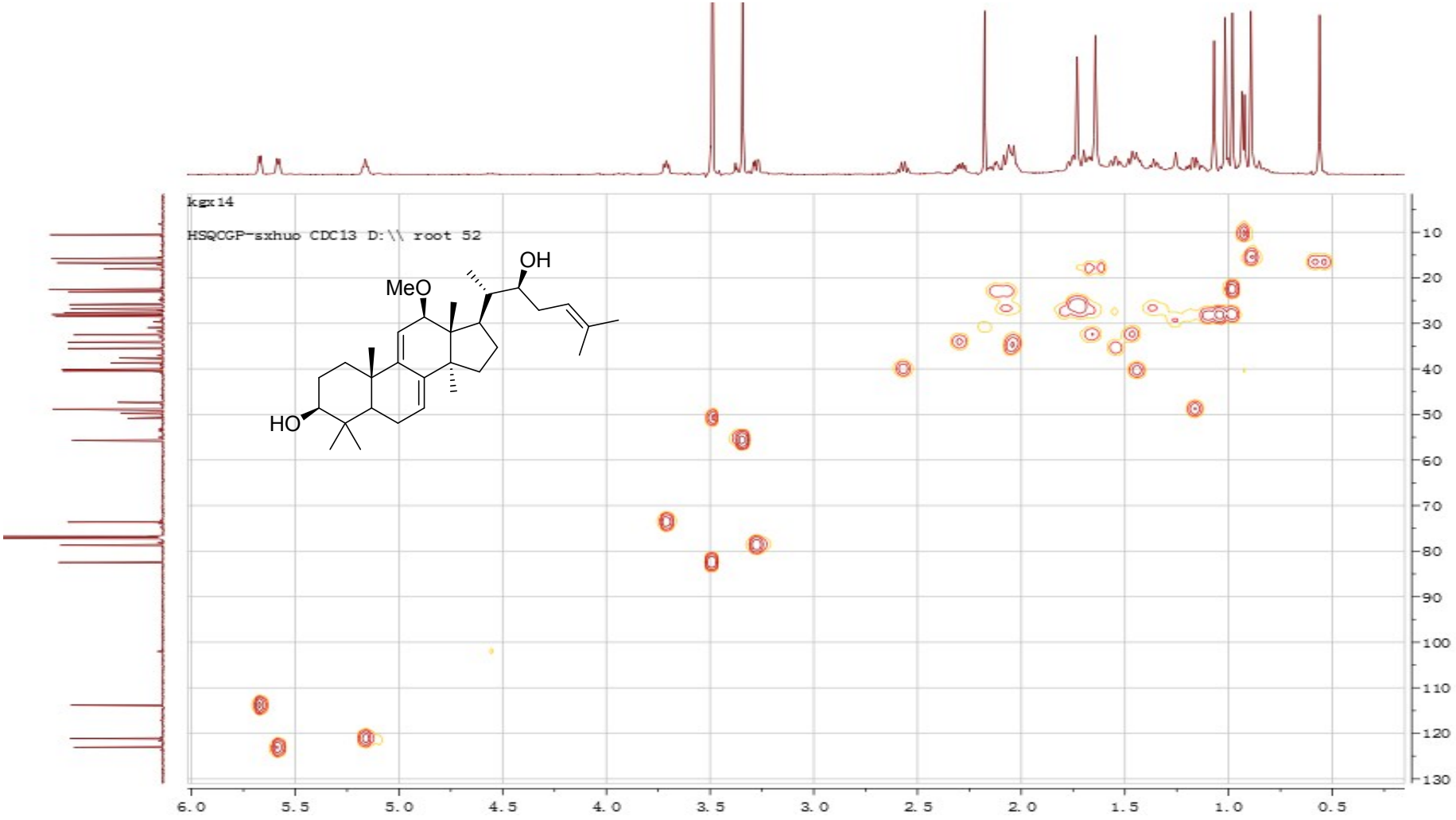

Figure S46. The HMBC spectrum of ganodercochlearin G (8).

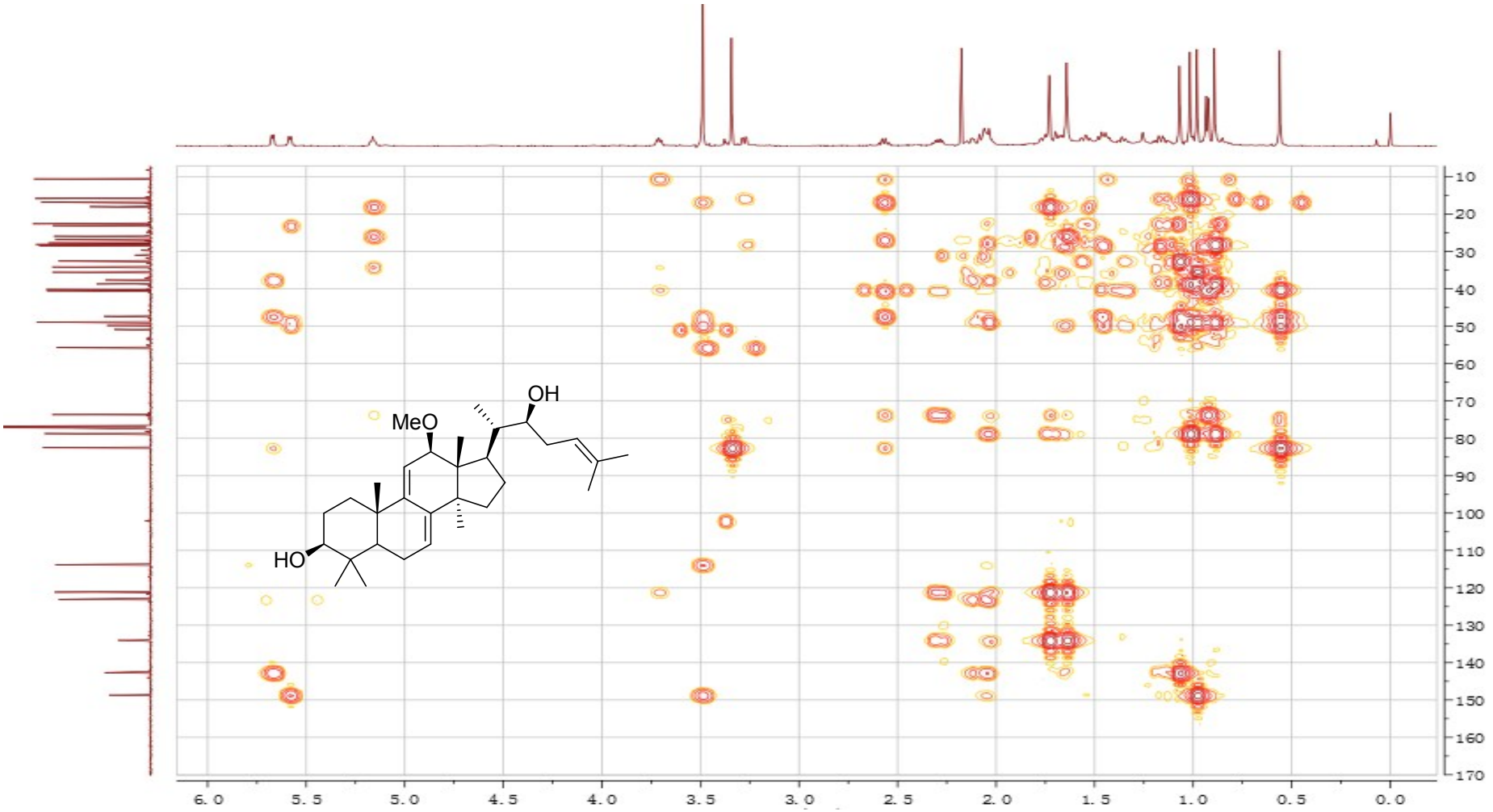

Figure S47. The ^{1}H-^{1}H COSY spectrum of ganodercochlearin G (8).

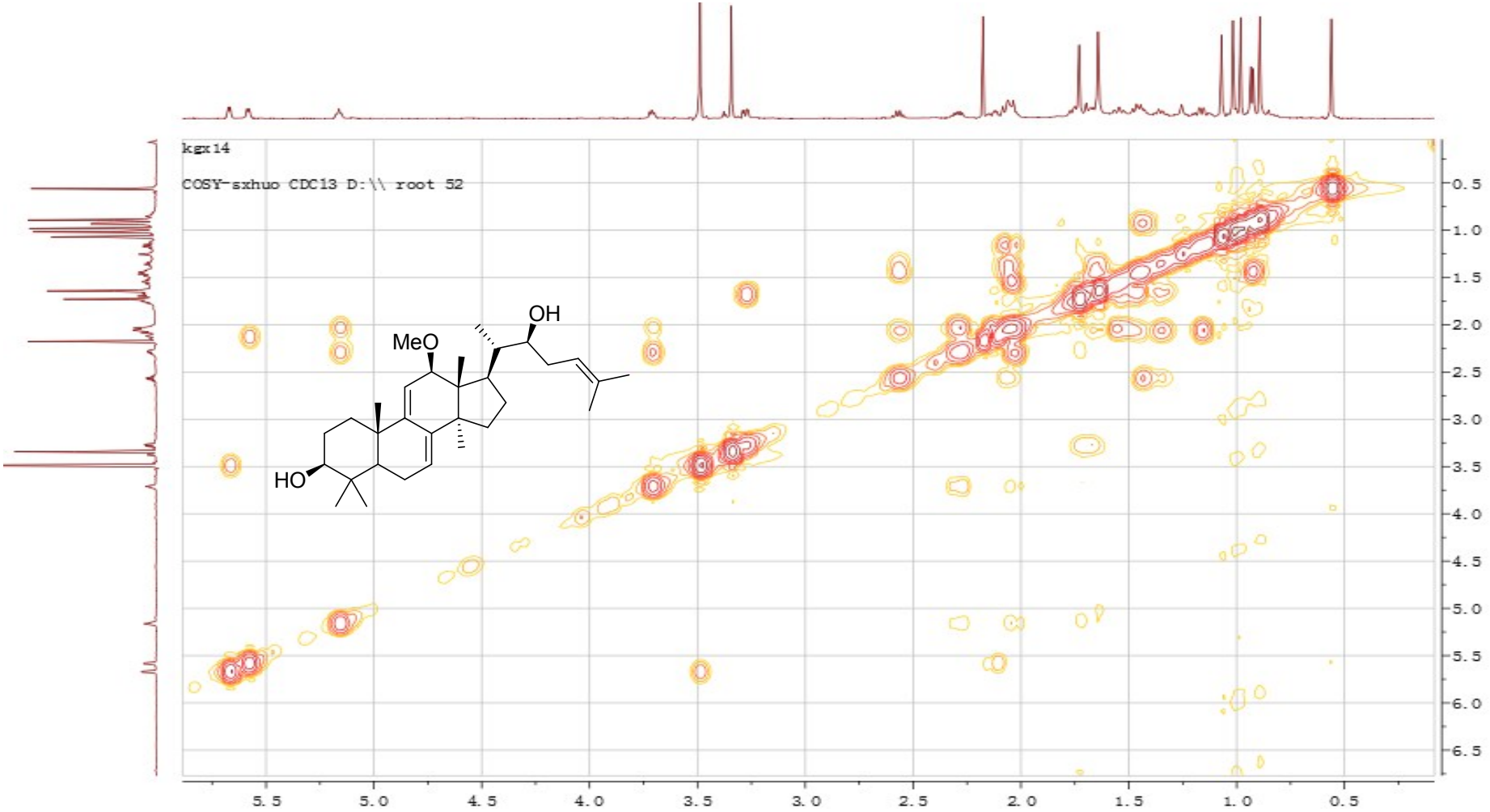

Figure S48. The ROESY spectrum of ganodercochlearin G (8).

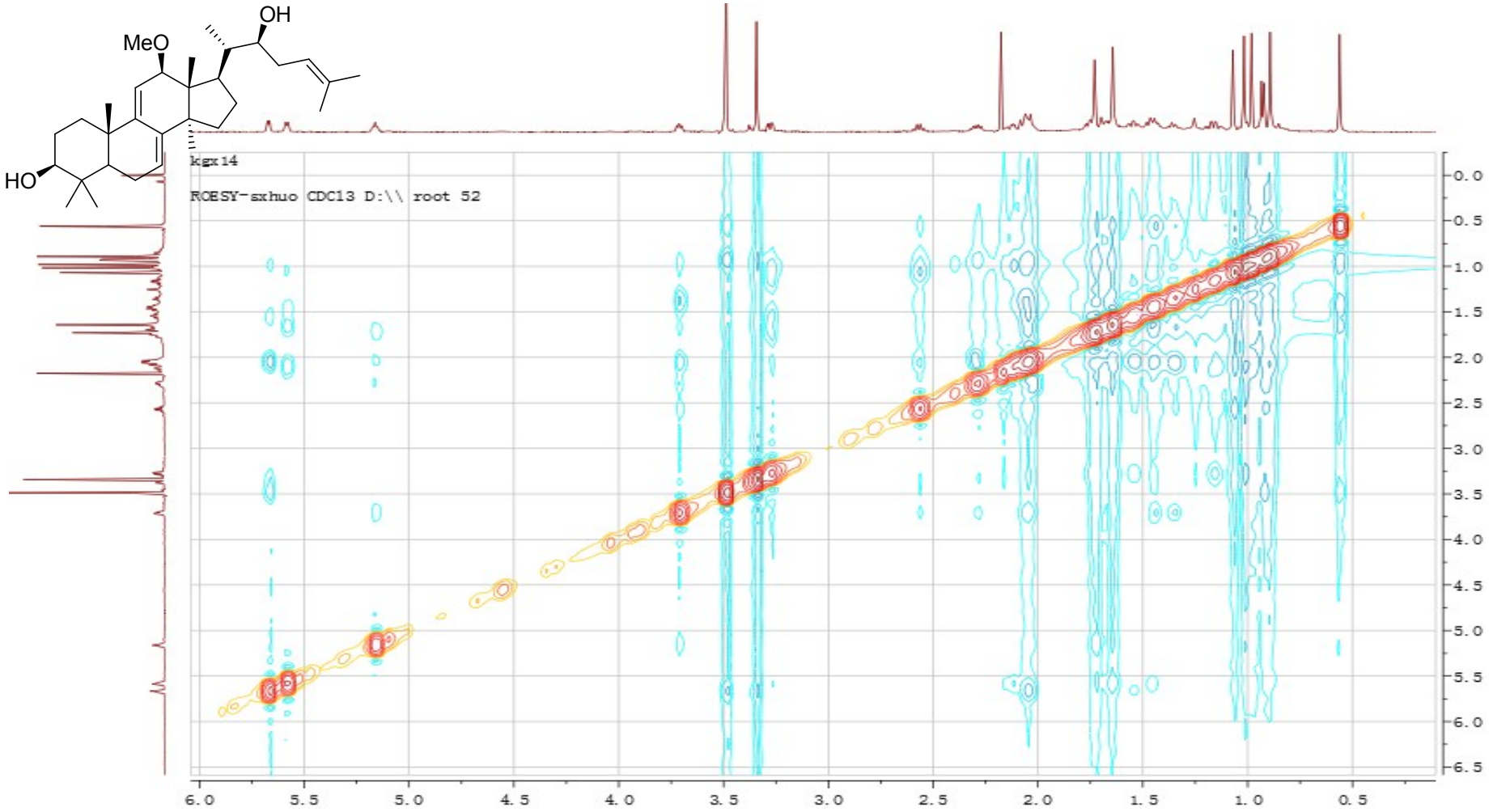

Figure S49. The ^{1}H NMR (600 MHz, $CDCl_3$) spectrum of ganodercochlearin H (9).

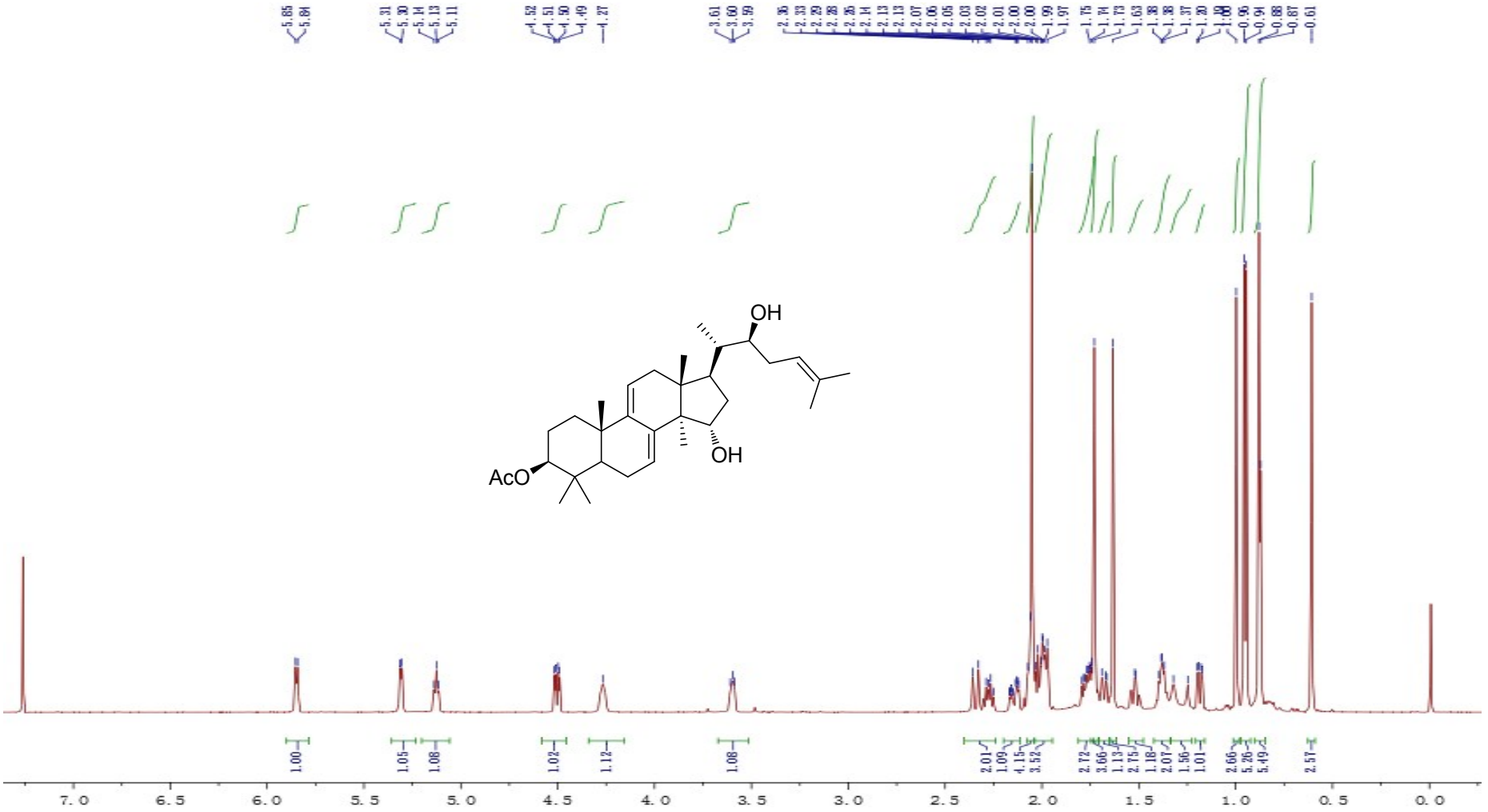

Figure S50. The ^{13}C NMR (150 MHz, $CDCl_3$) spectrum of ganodercochlearin H (9).

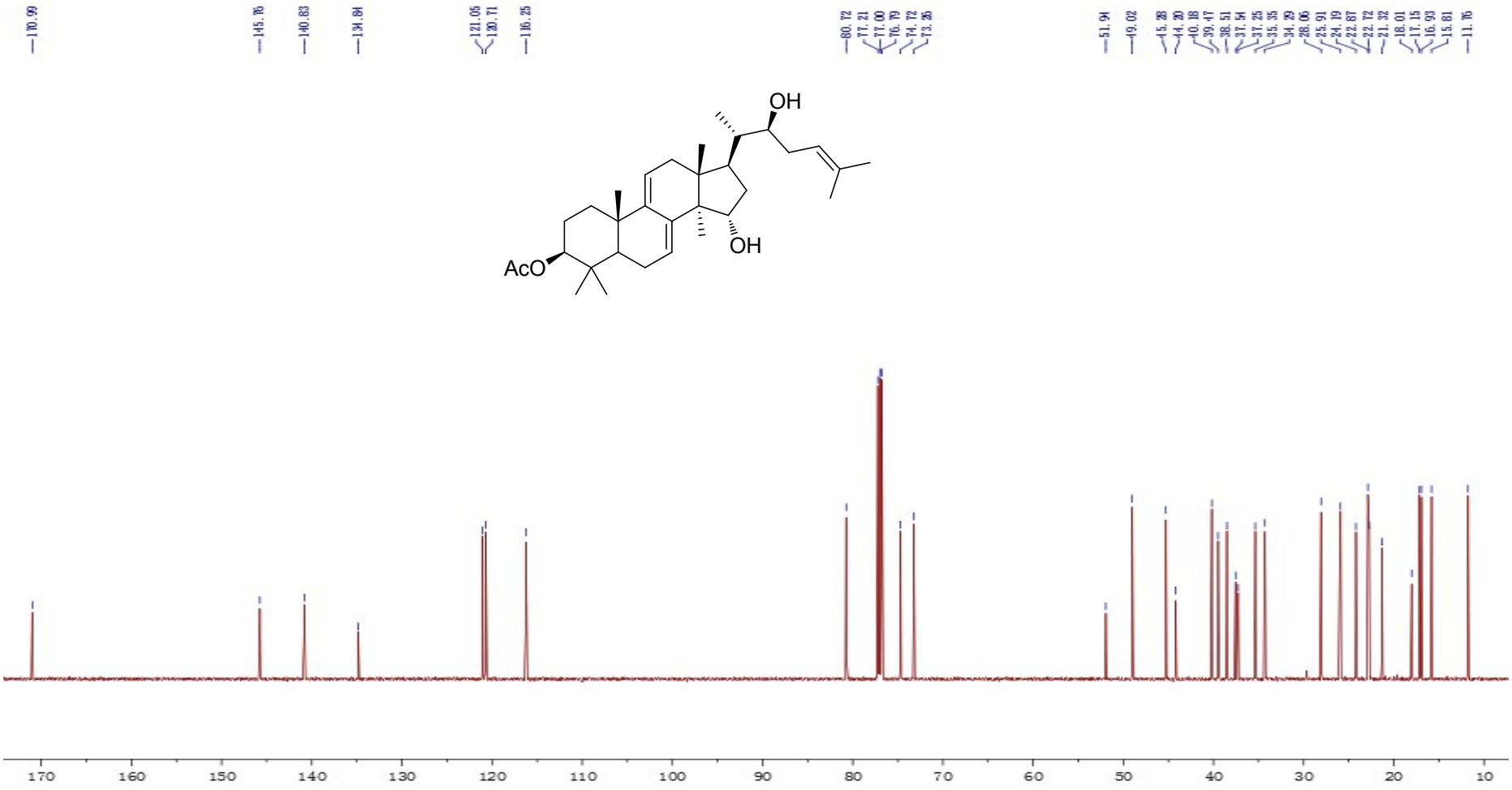

Figure S51. The HSQC spectrum of ganodercochlearin H (9).

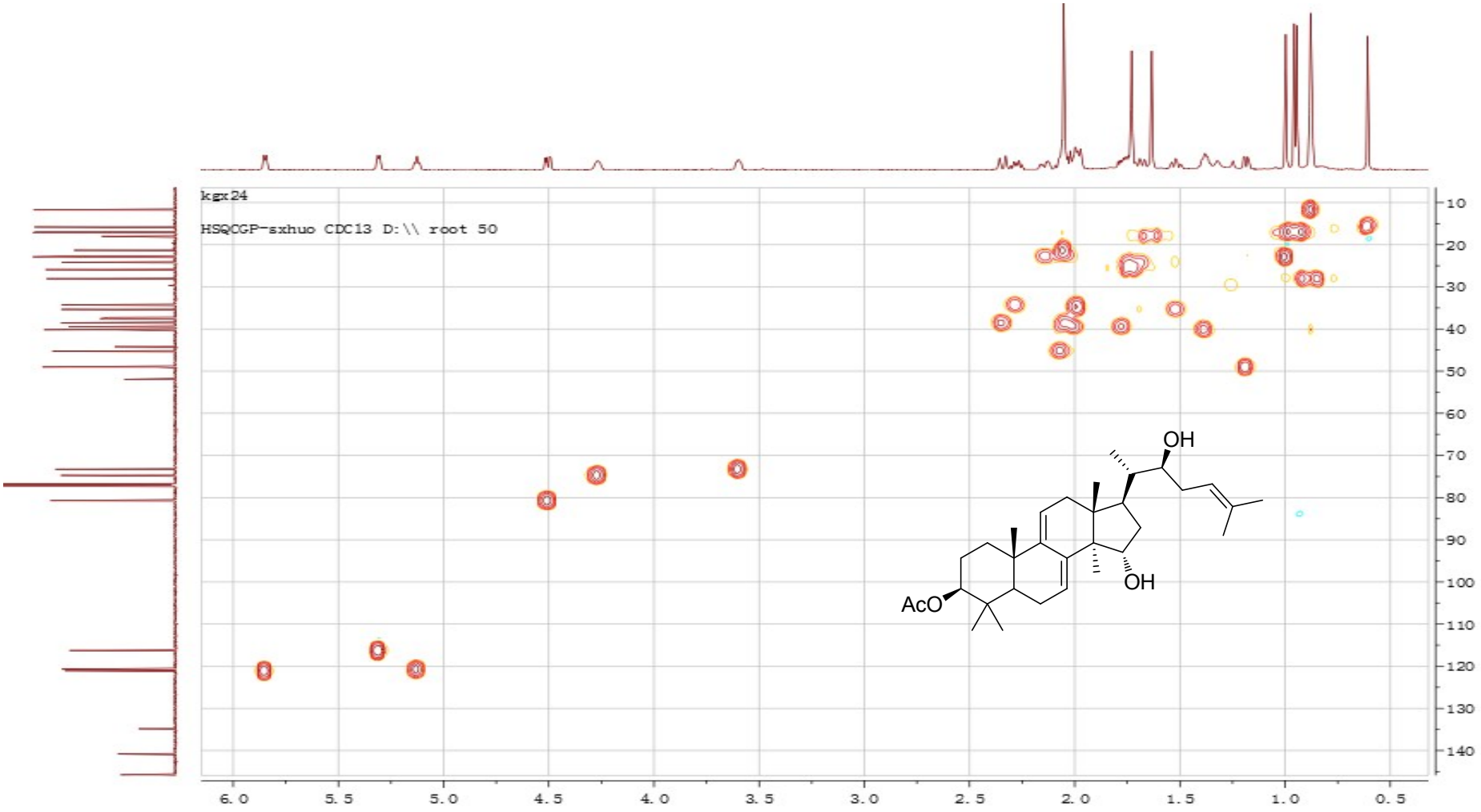

Figure S52. The HMBC spectrum of ganodercochlearin H (9).

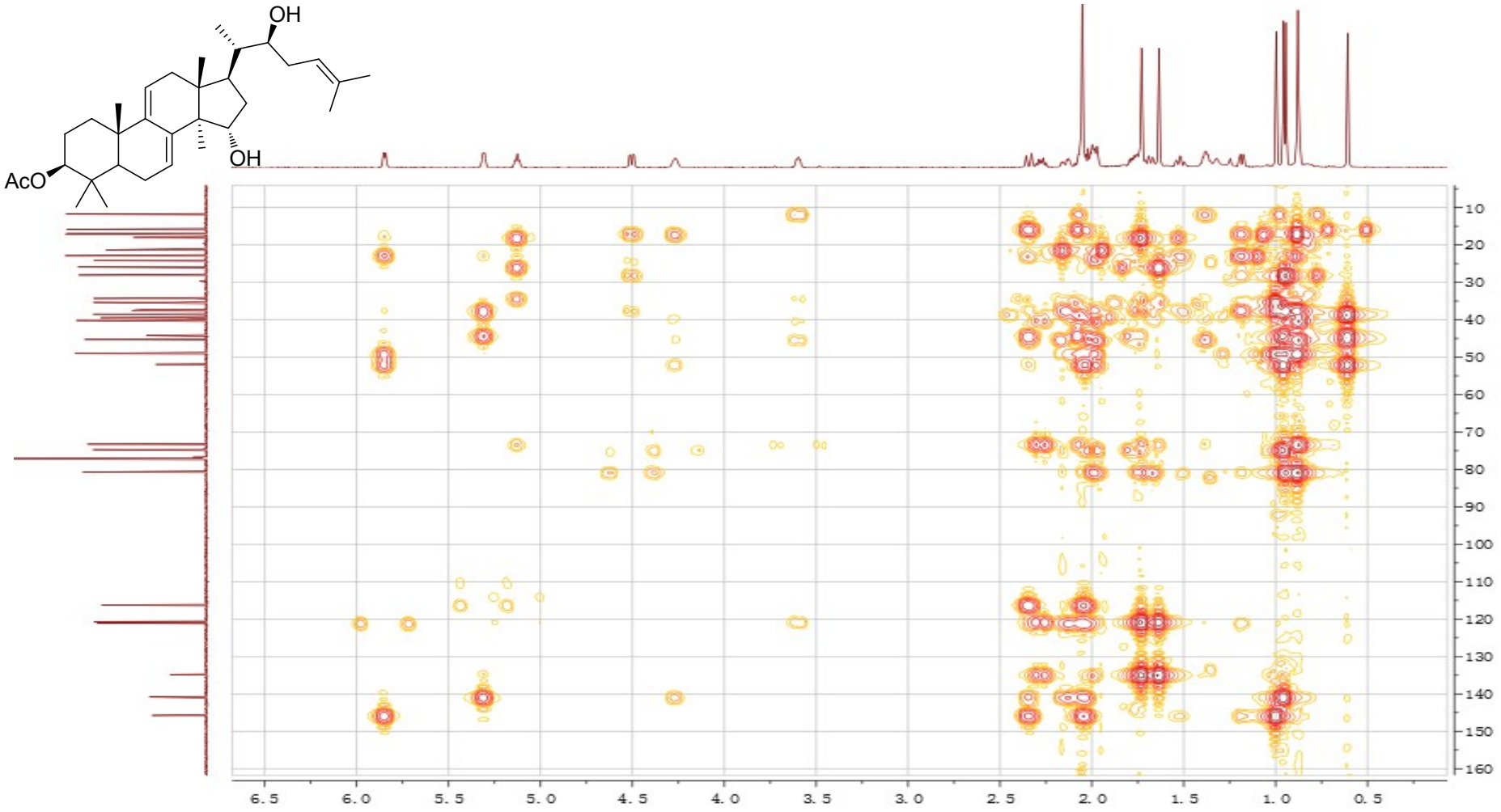

Figure S53. The ^{1}H-^{1}H COSY spectrum of ganodercochlearin H (9).

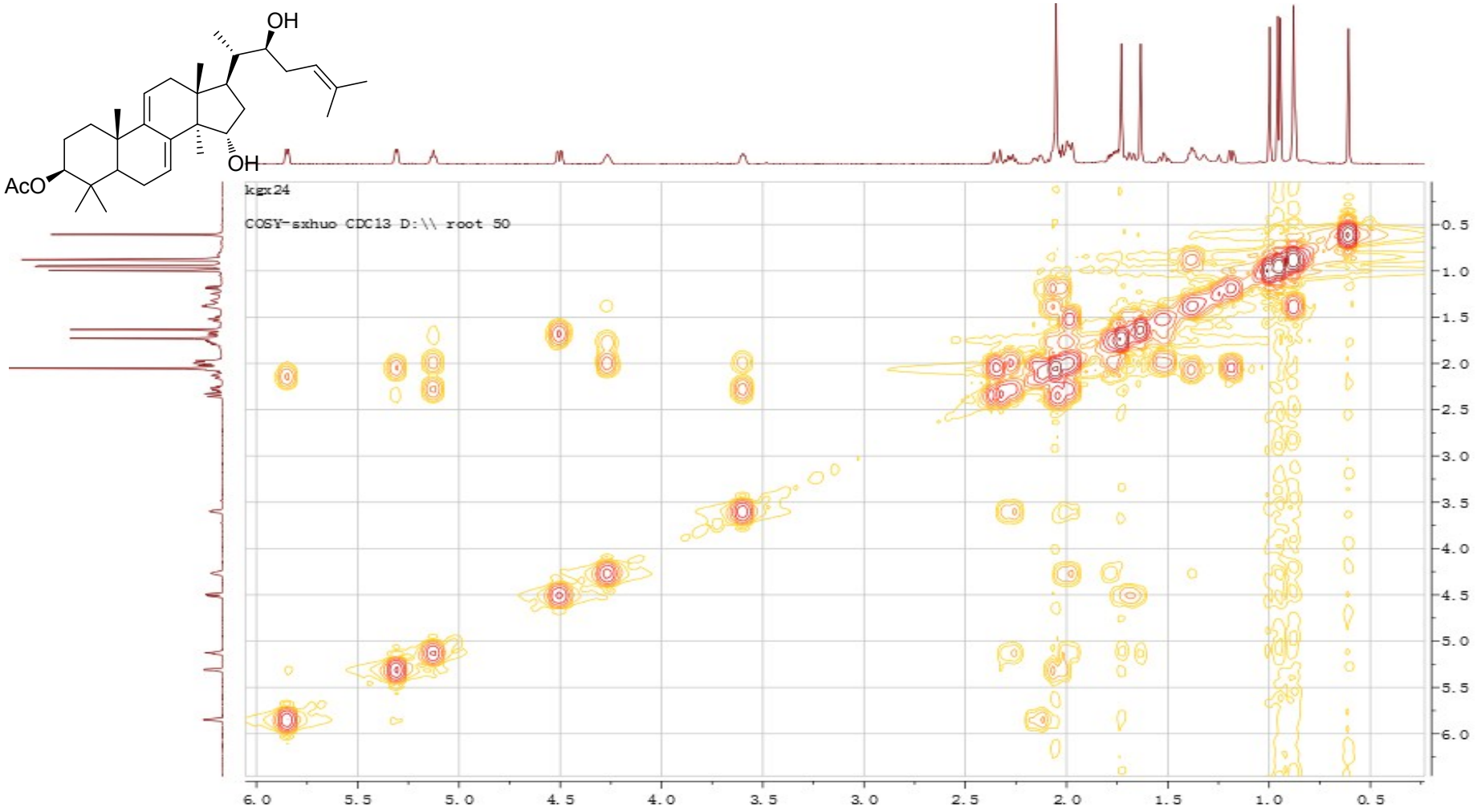

Figure S54. The ROESY spectrum of ganodercochlearin H (9).

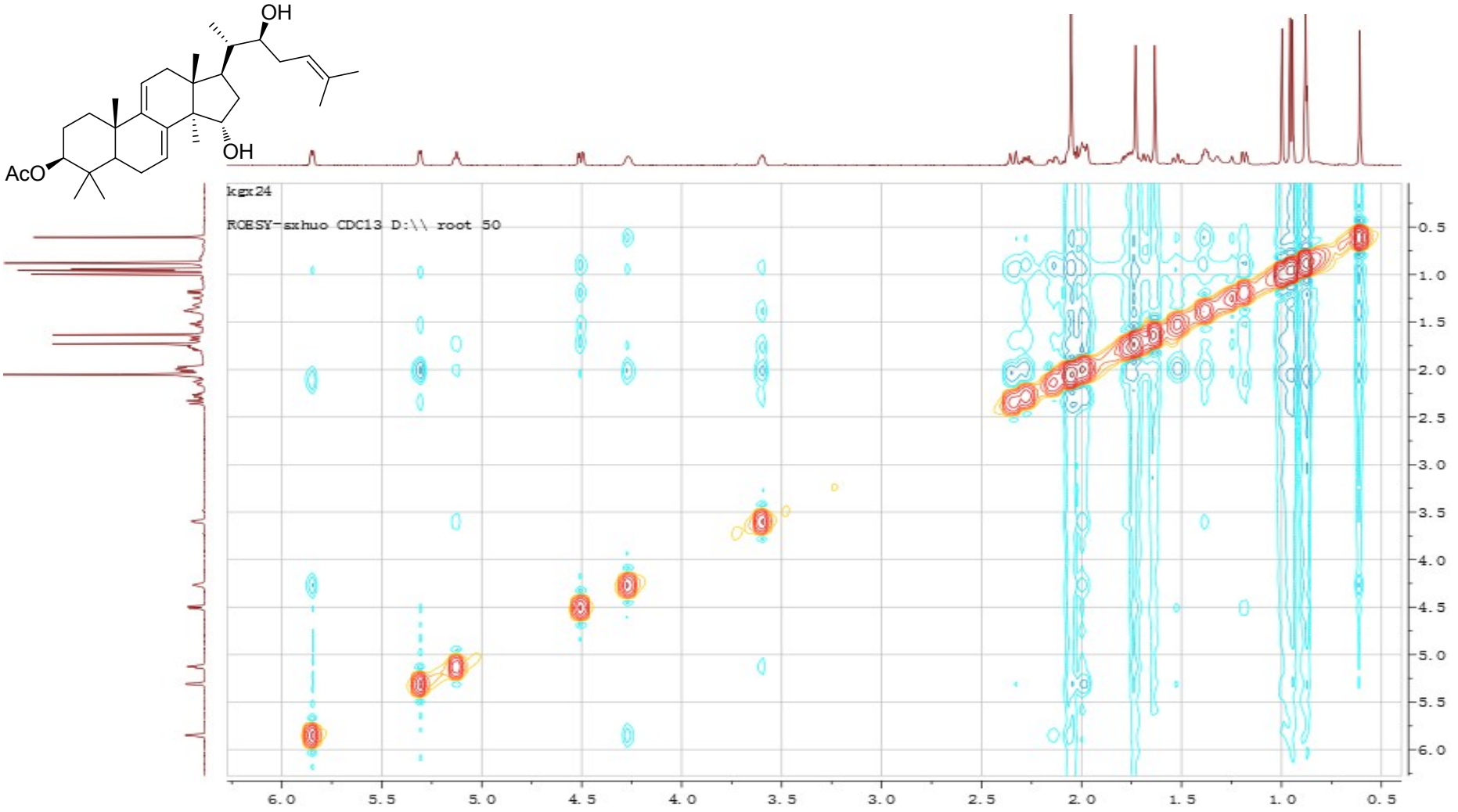

Figure S55. The ^{1}H NMR (600 MHz, $CDCl_3$) spectrum of ganodercochlearin I (10).

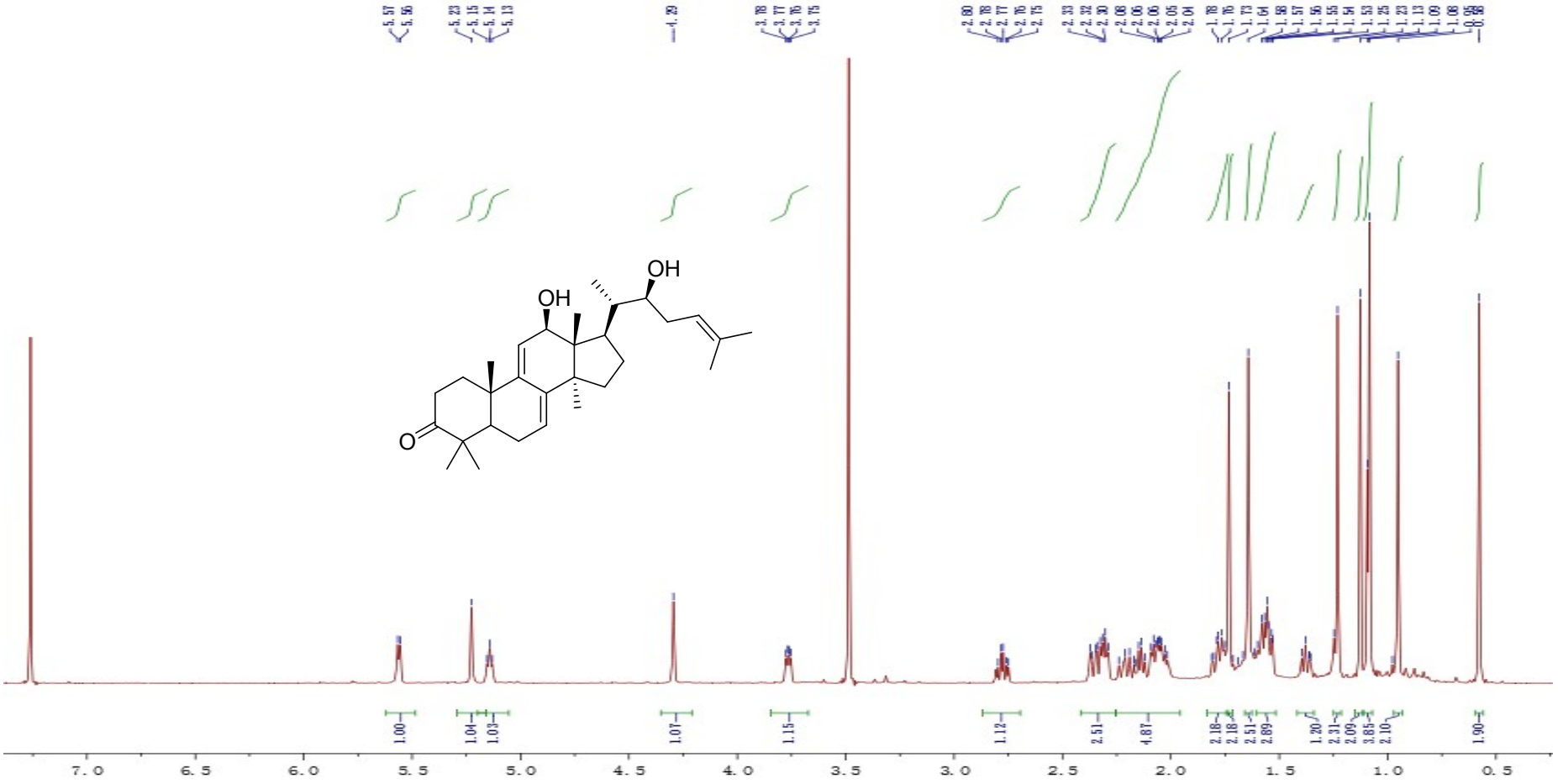

Figure S56. The ^{13}C NMR (150 MHz, $CDCl_3$) spectrum of ganodercochlearin I (10).

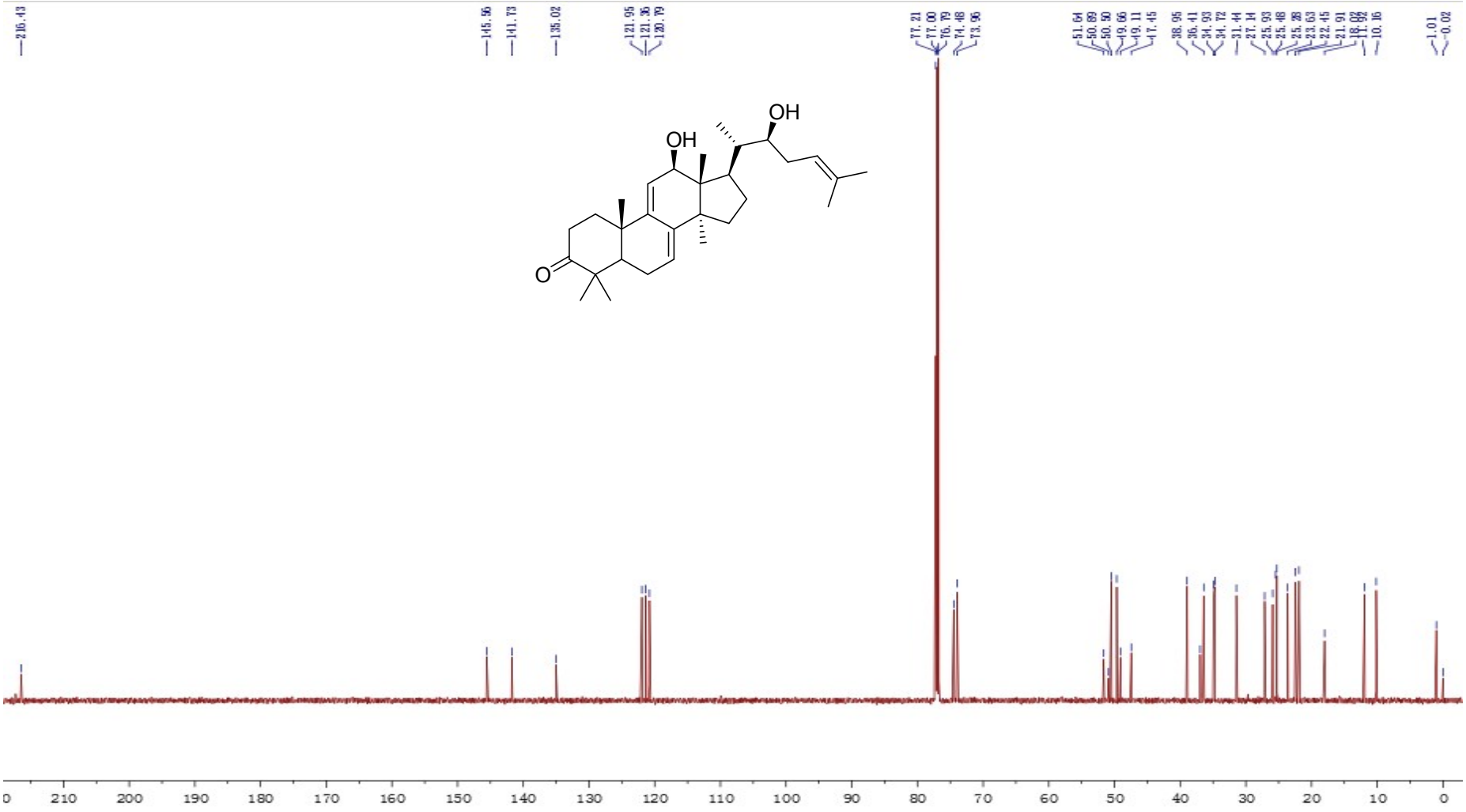

Figure S57. The HSQC spectrum of ganodercochlearin I (10).

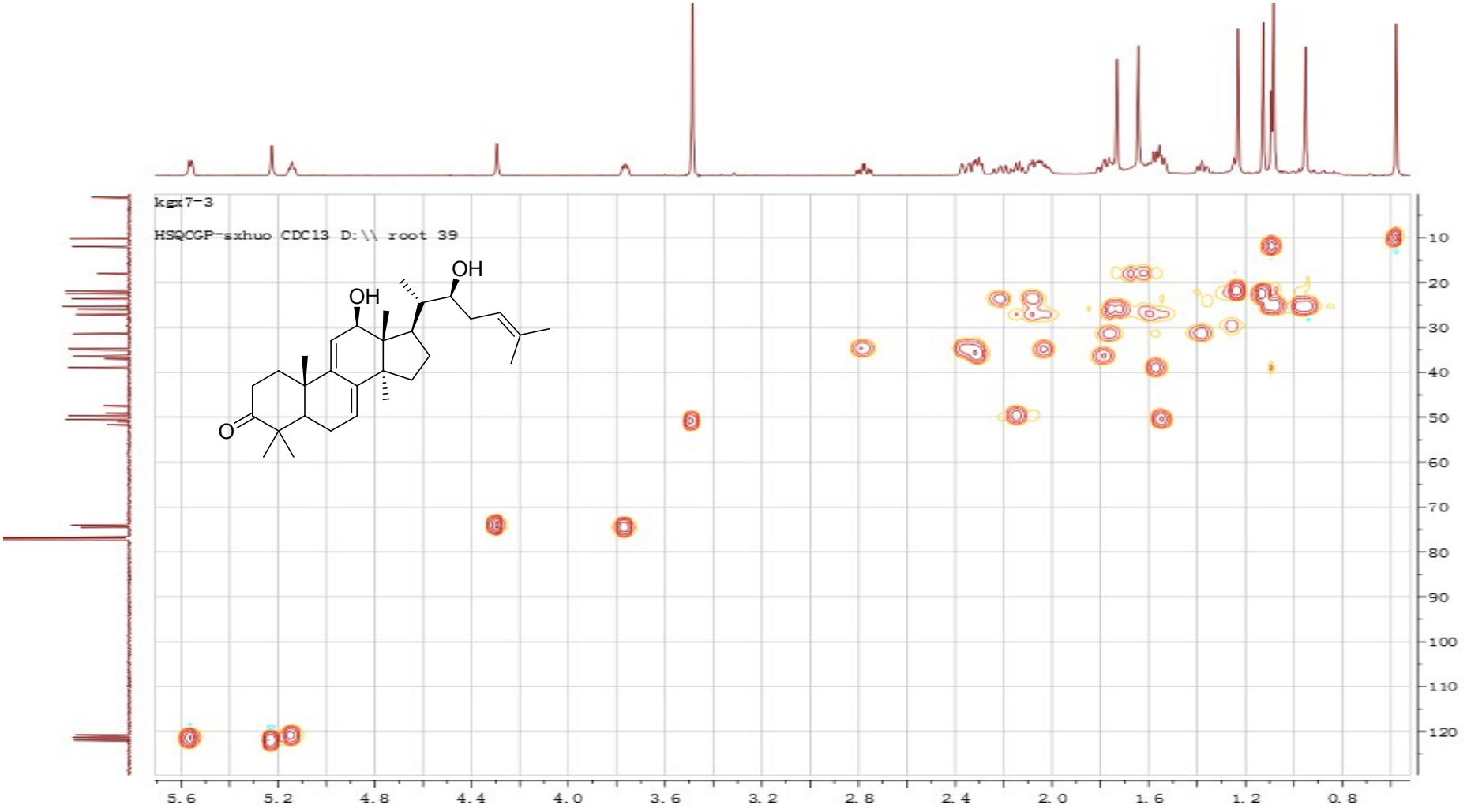

Figure S58. The HMBC spectrum of ganodercochlearin I (10).

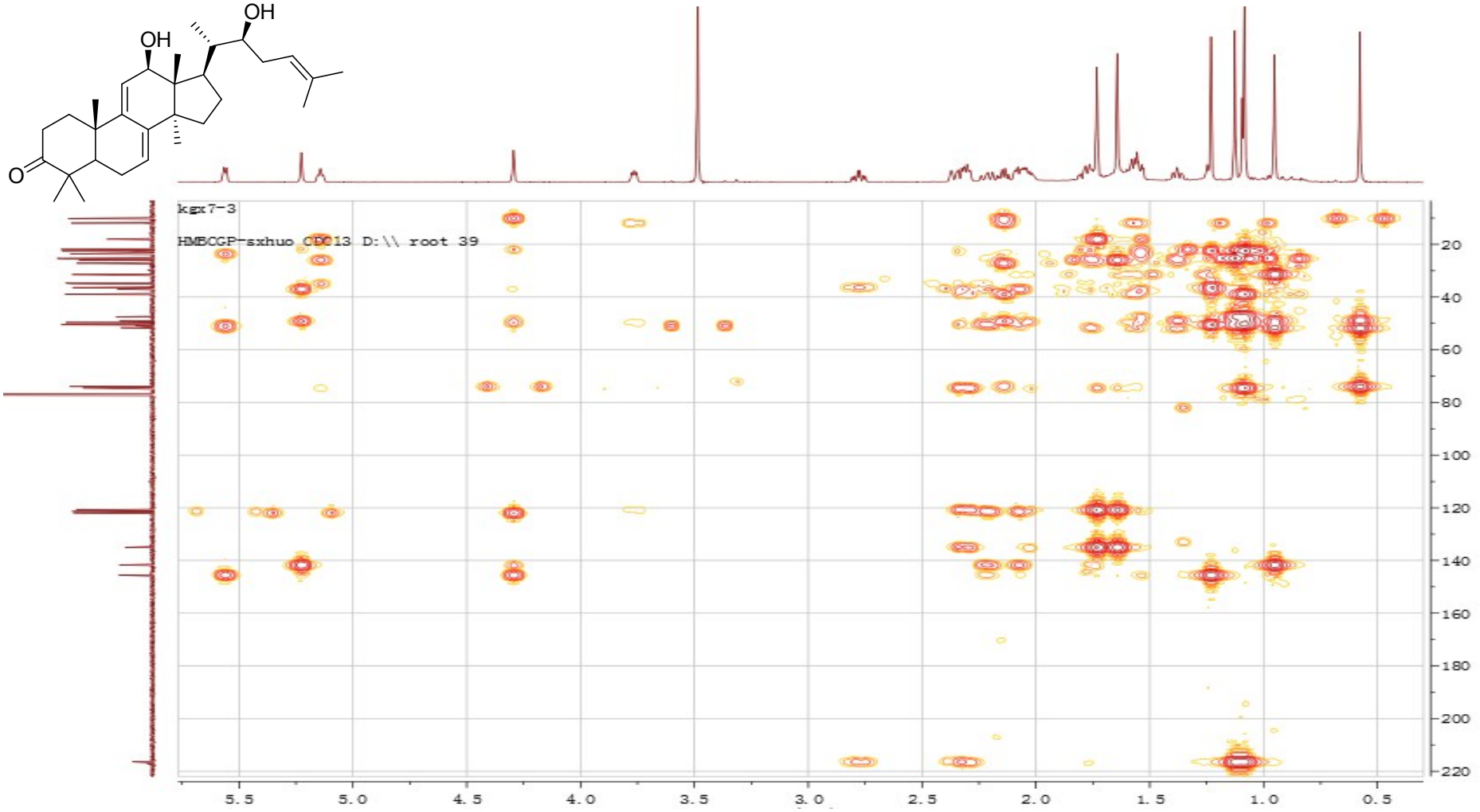

Figure S59. The ^{1}H-^{1}H COSY spectrum of ganodercochlearin I (10).

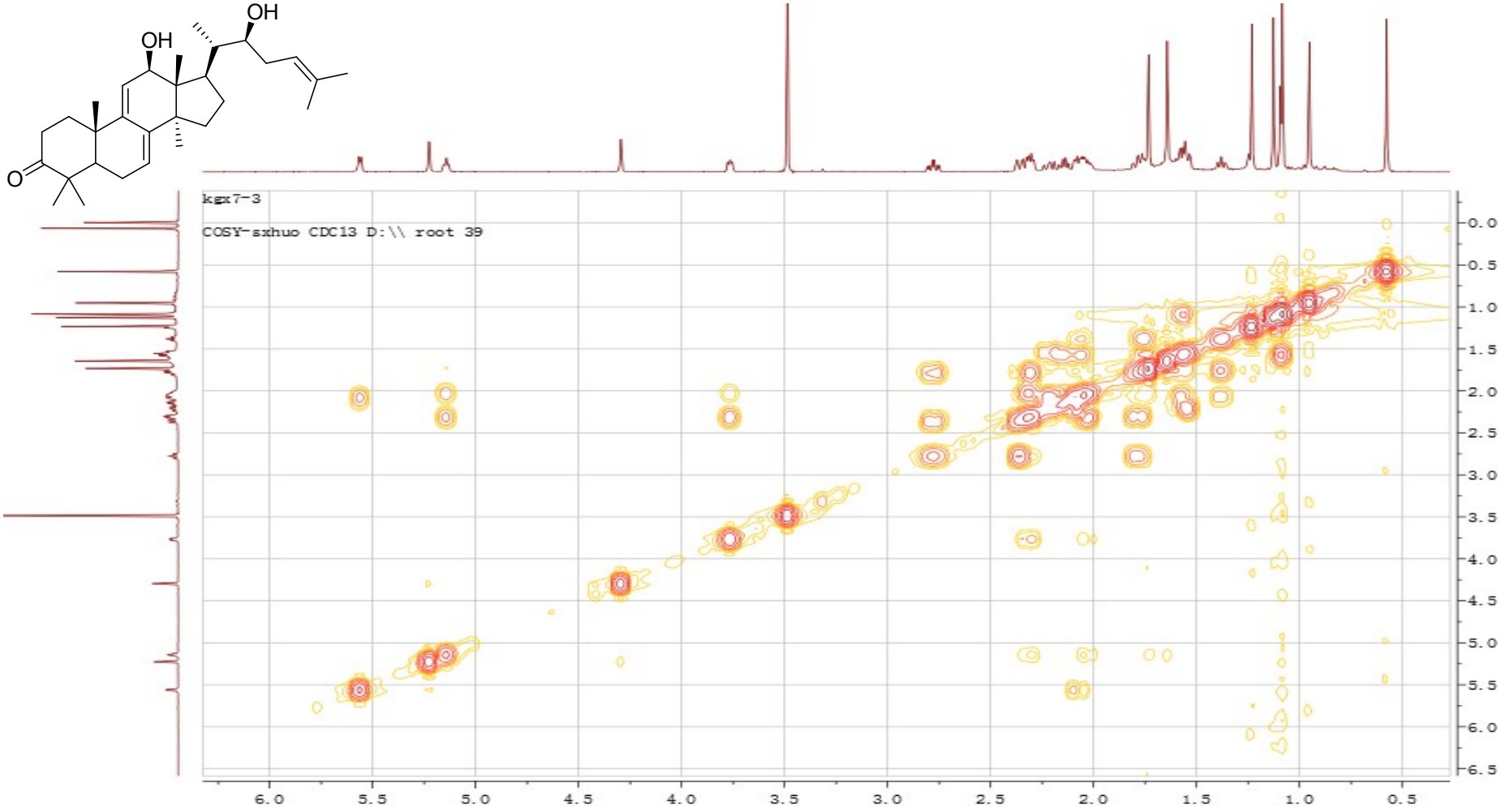

Figure S60. The ROESY spectrum of ganodercochlearin I (10).

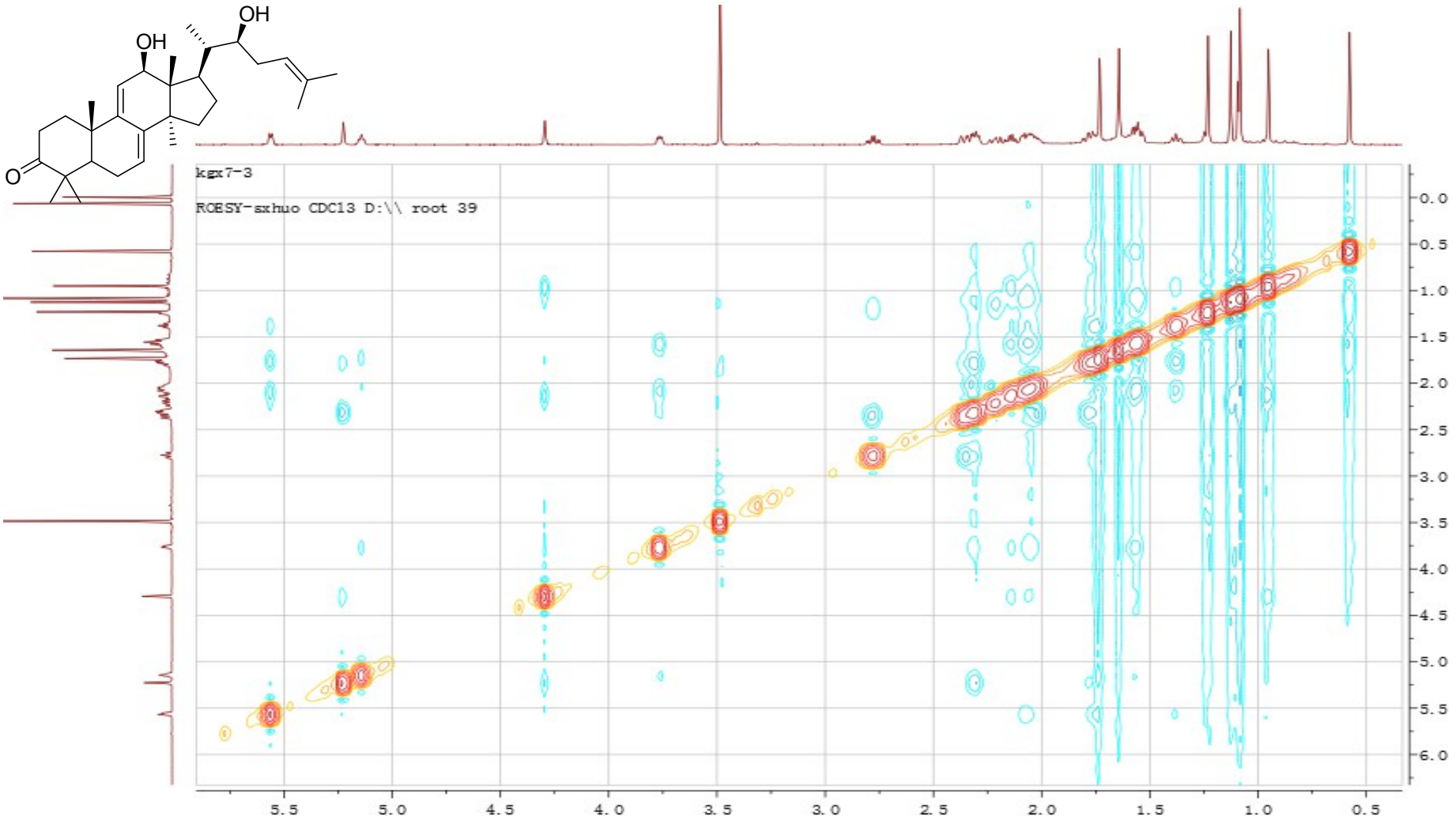

Figure S61. The ^{1}H NMR (600 MHz, $CDCl_3$) spectrum of ganodercochlearin J (11).

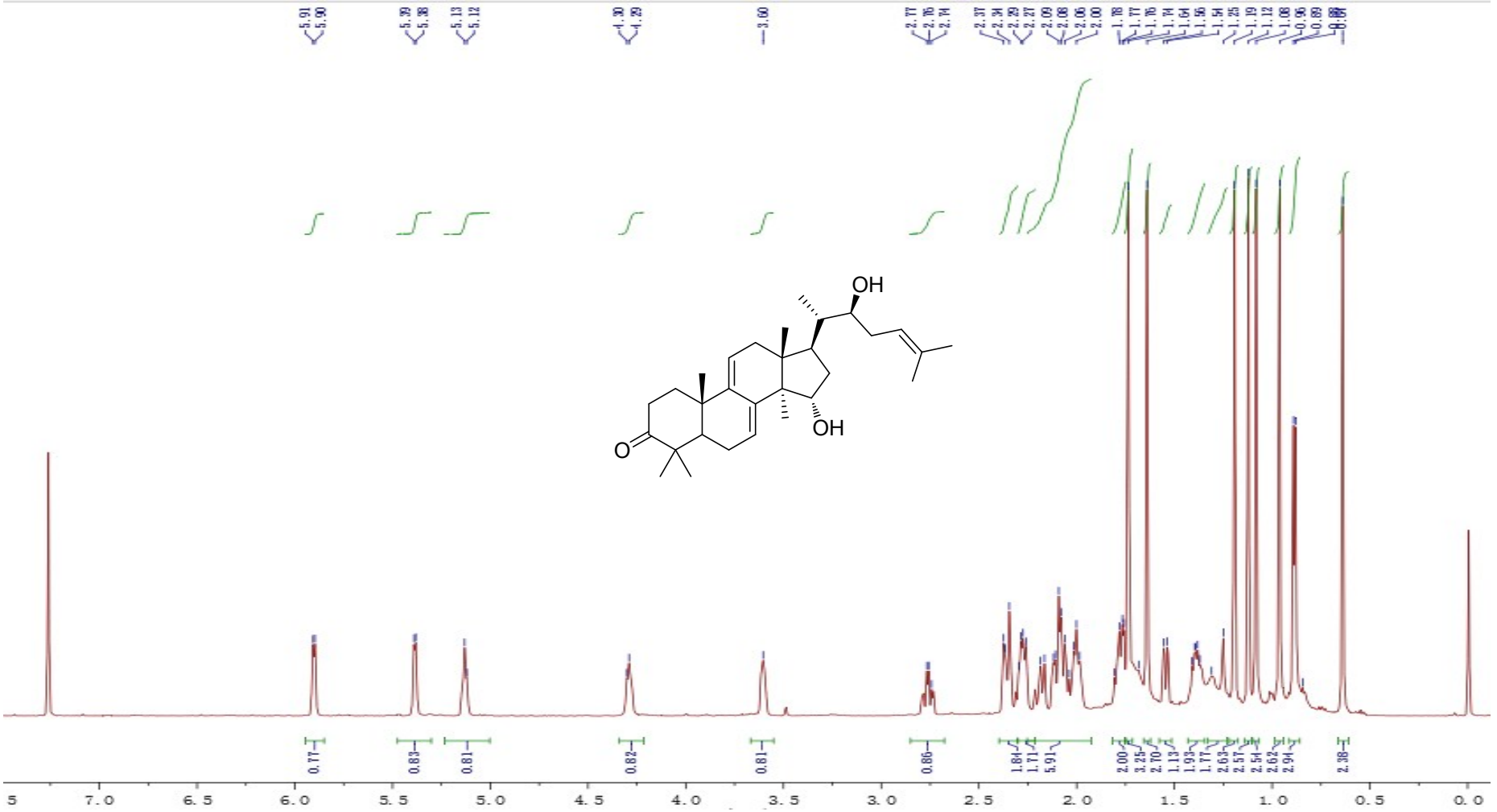

Figure S62. The ^{13}C NMR (150 MHz, $CDCl_3$) spectrum of ganodercochlearin J (11).

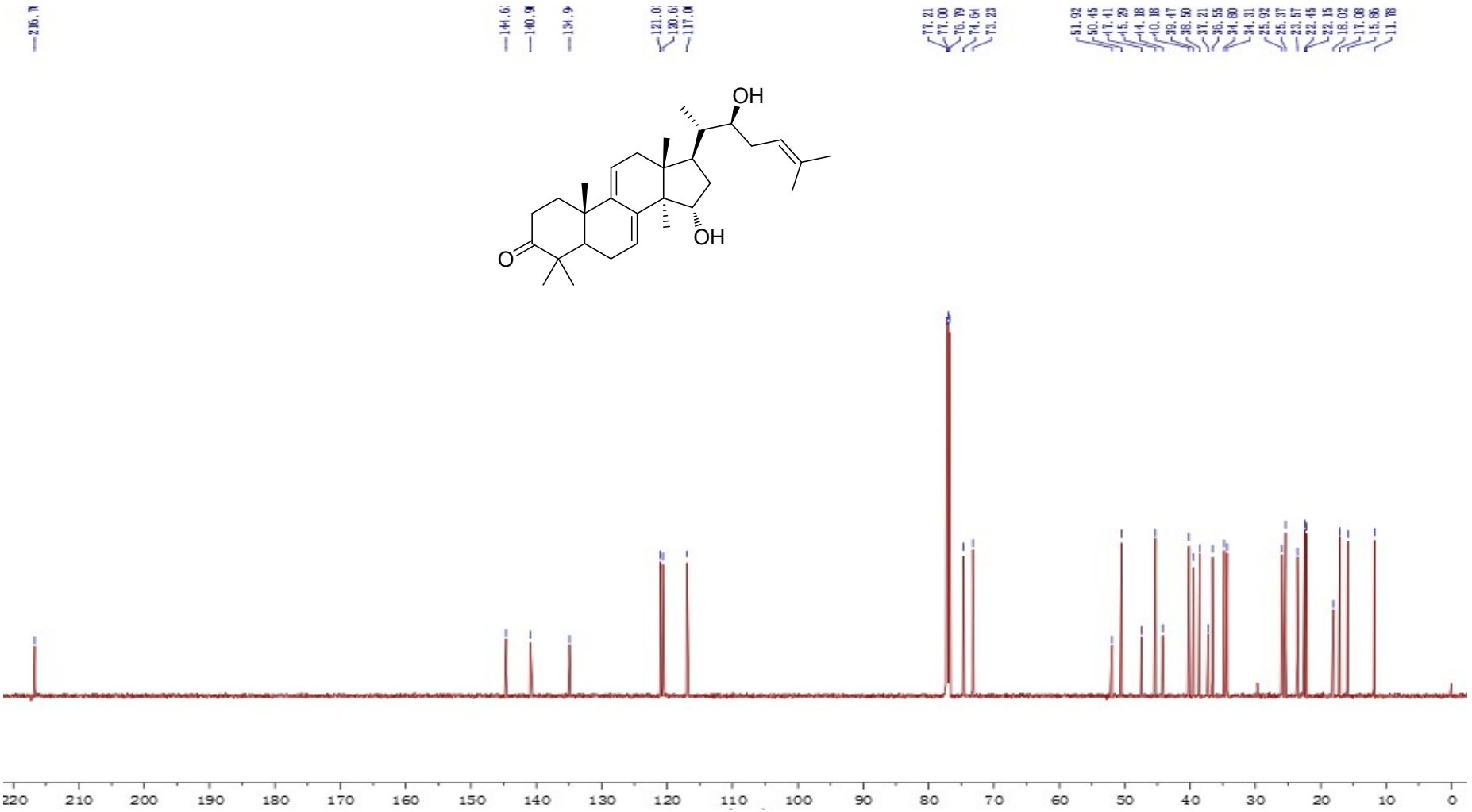

Figure S63. The HSQC spectrum of ganodercochlearin J (11).

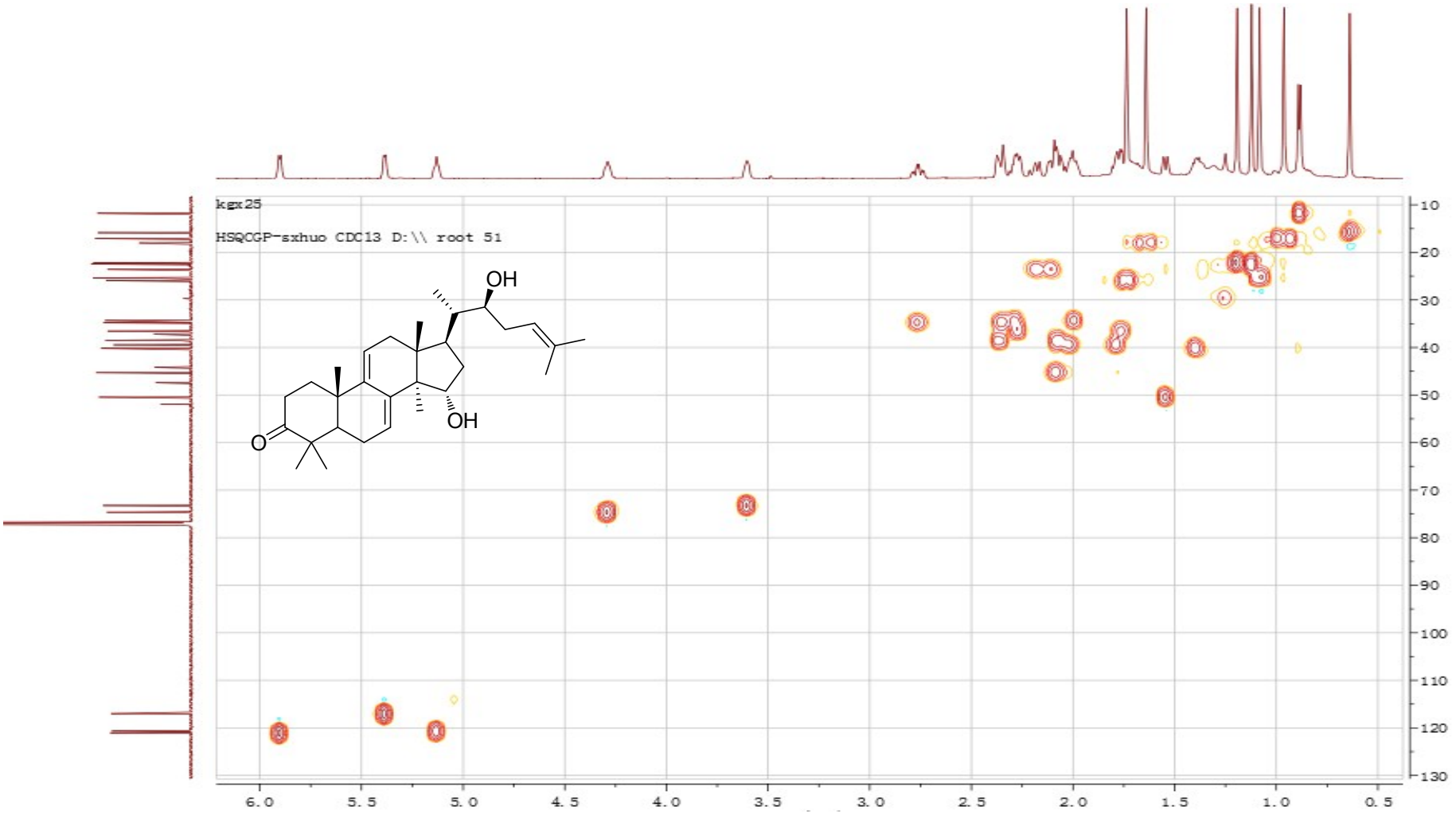

Figure S64. The HMBC spectrum of ganodercochlearin J (11).

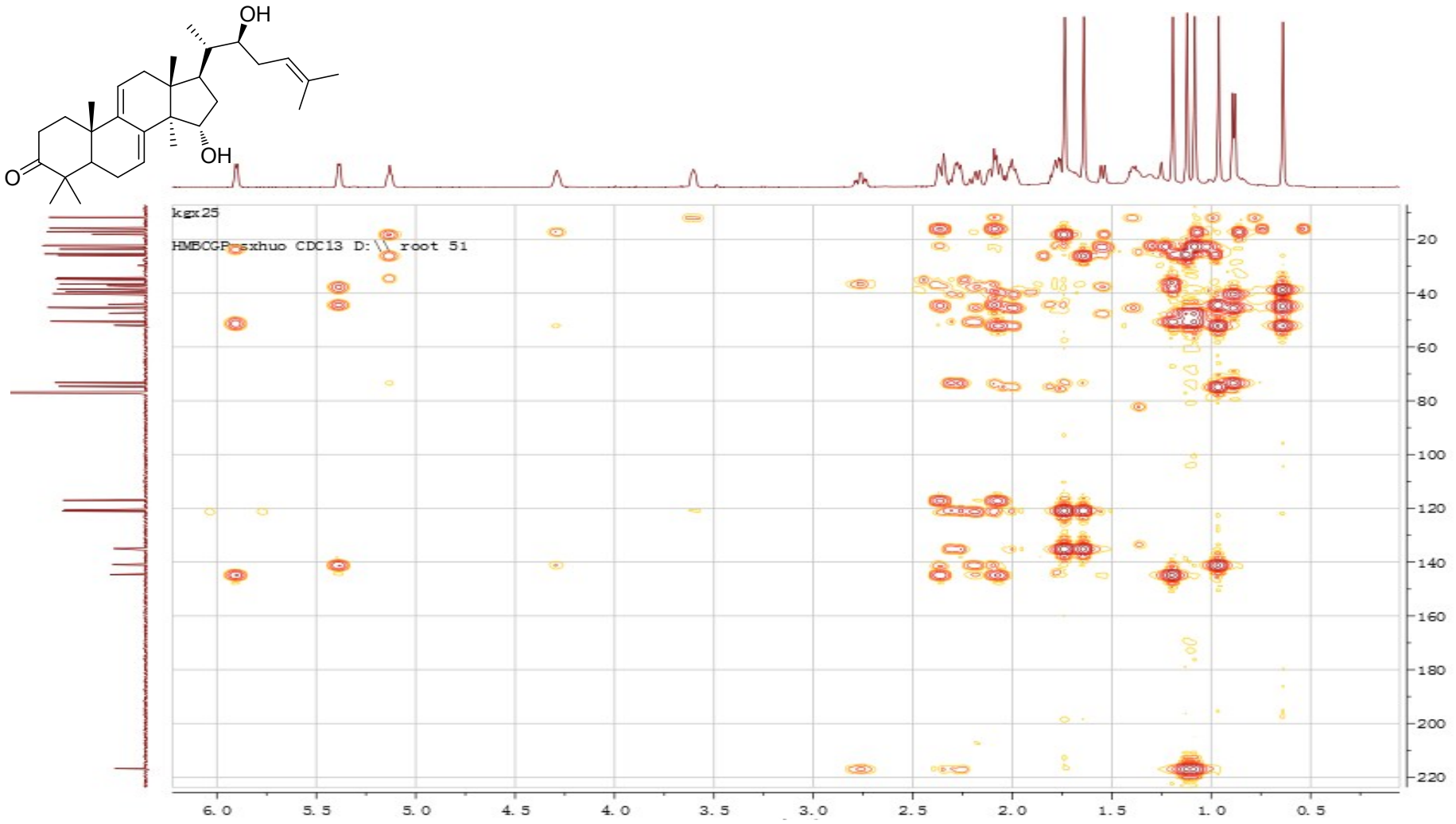

Figure S65. The ^{1}H-^{1}H COSY spectrum of ganodercochlearin J (11).

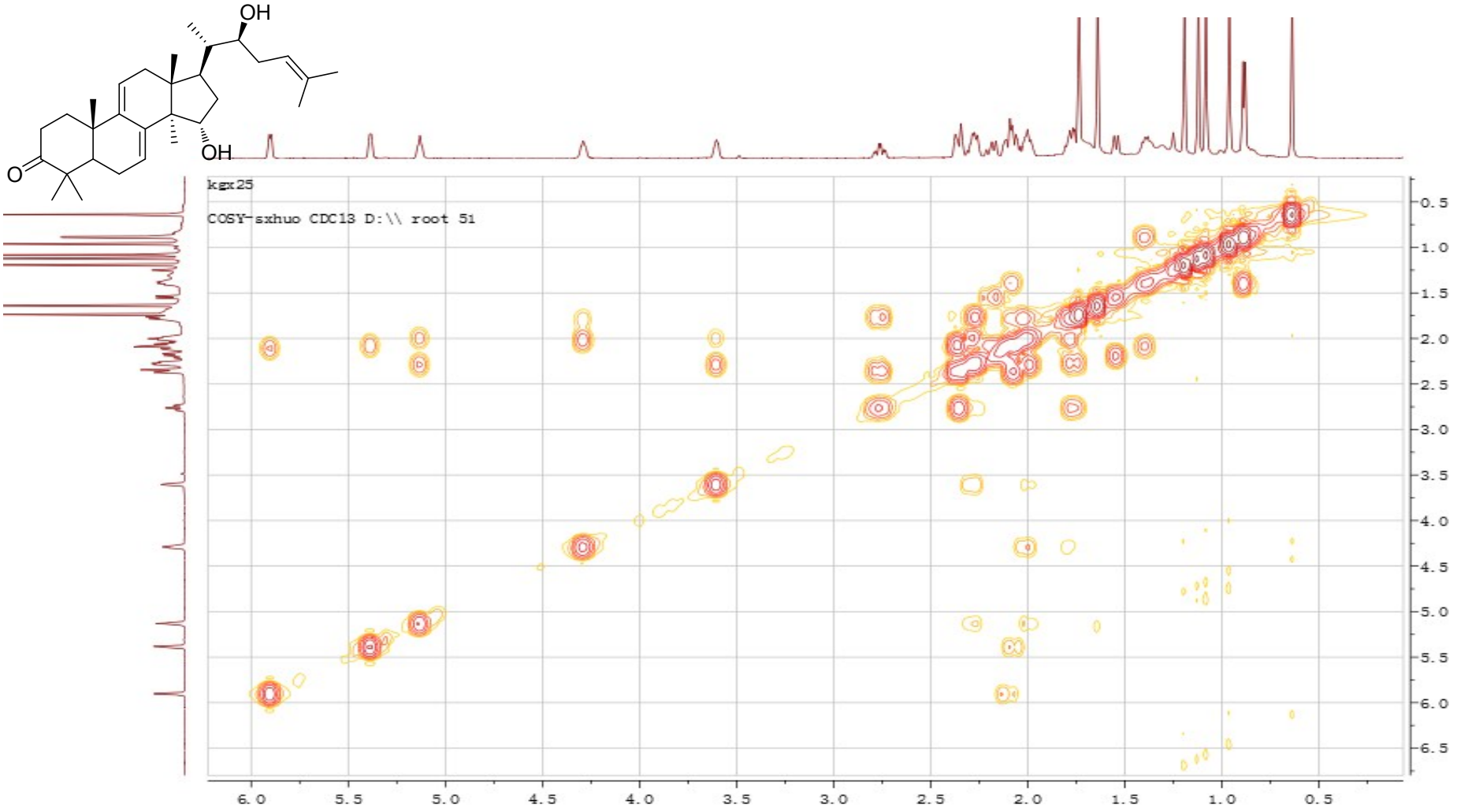

Figure S66. The ROESY spectrum of ganodercochlearin J (11).

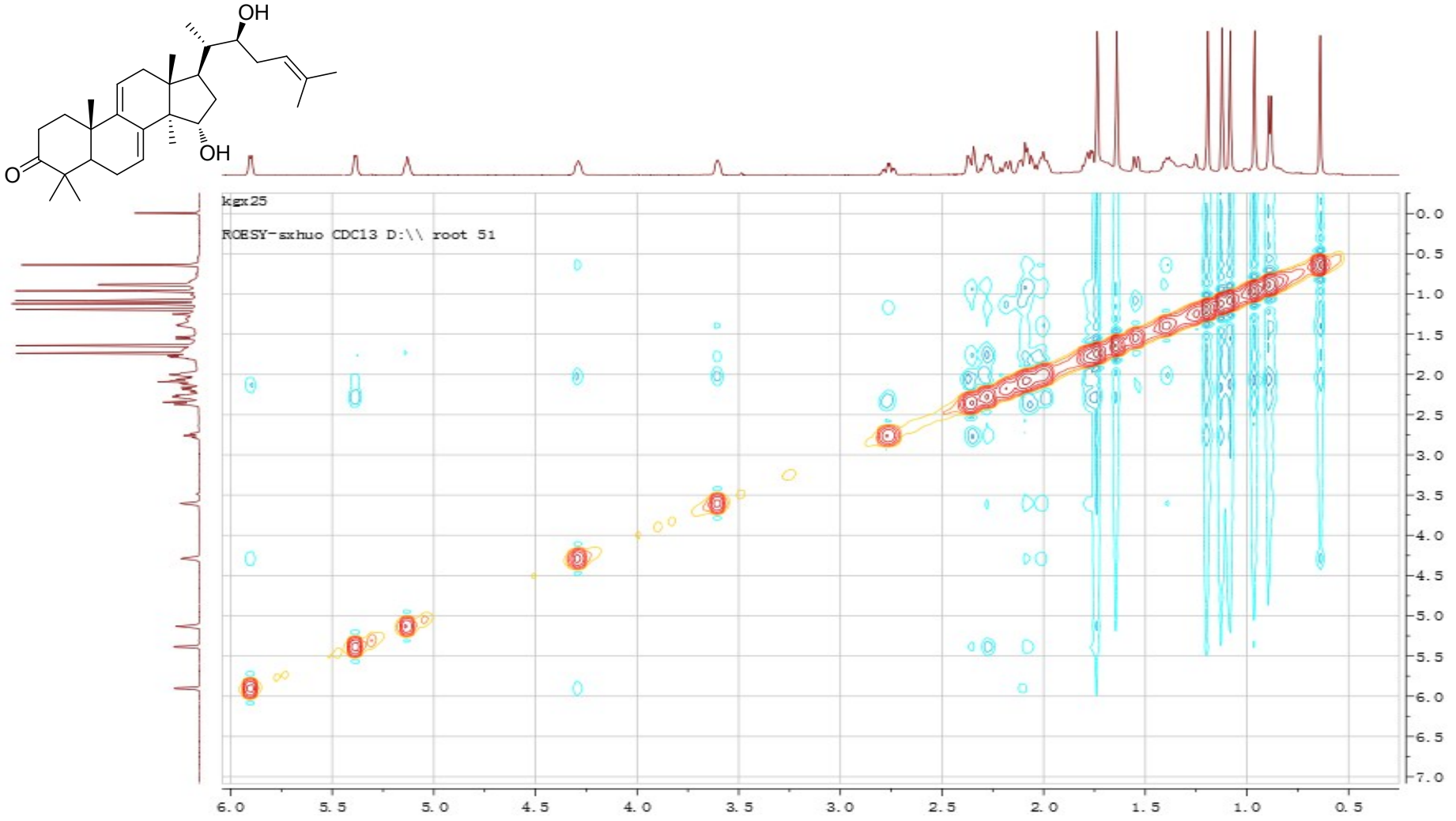

Figure S67. The ^{1}H NMR (600 MHz, $CDCl_3$) spectrum of ganodercochlearin K (12).

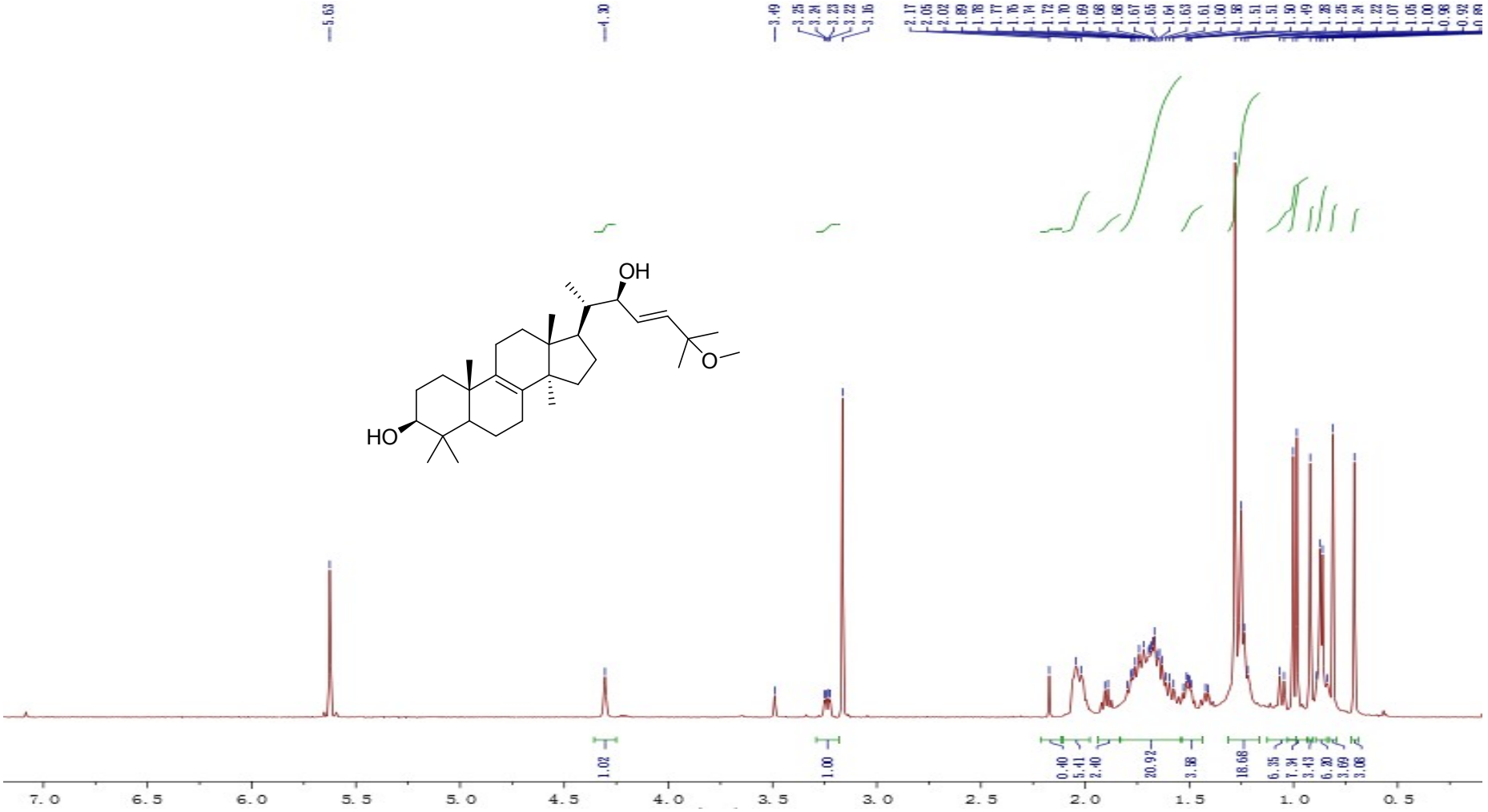

Figure S68. The ^{13}C NMR (150 MHz, $CDCl_3$) spectrum of ganodercochlearin K (12).

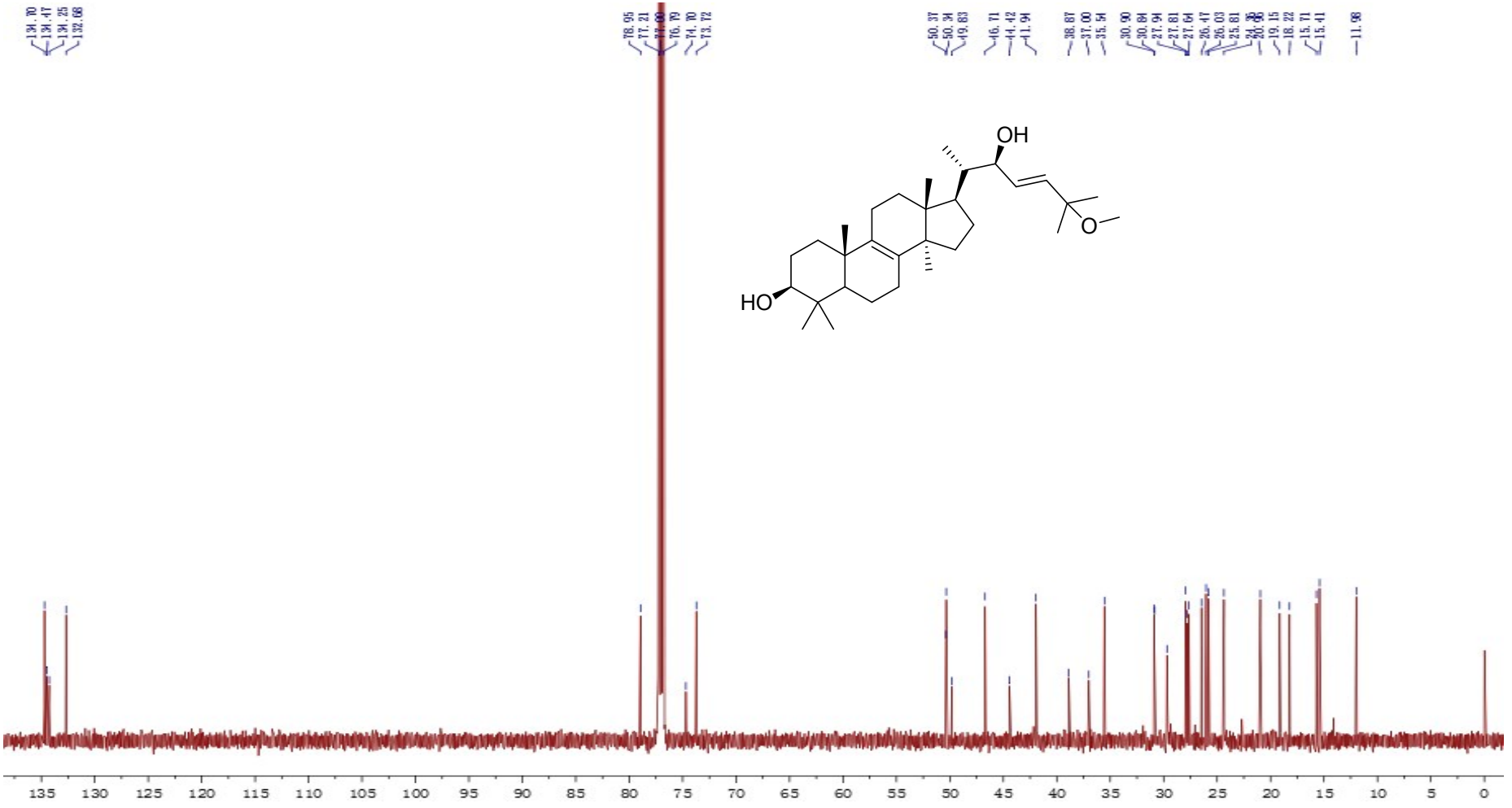

Figure S69. The HSQC spectrum of ganodercochlearin K (12).

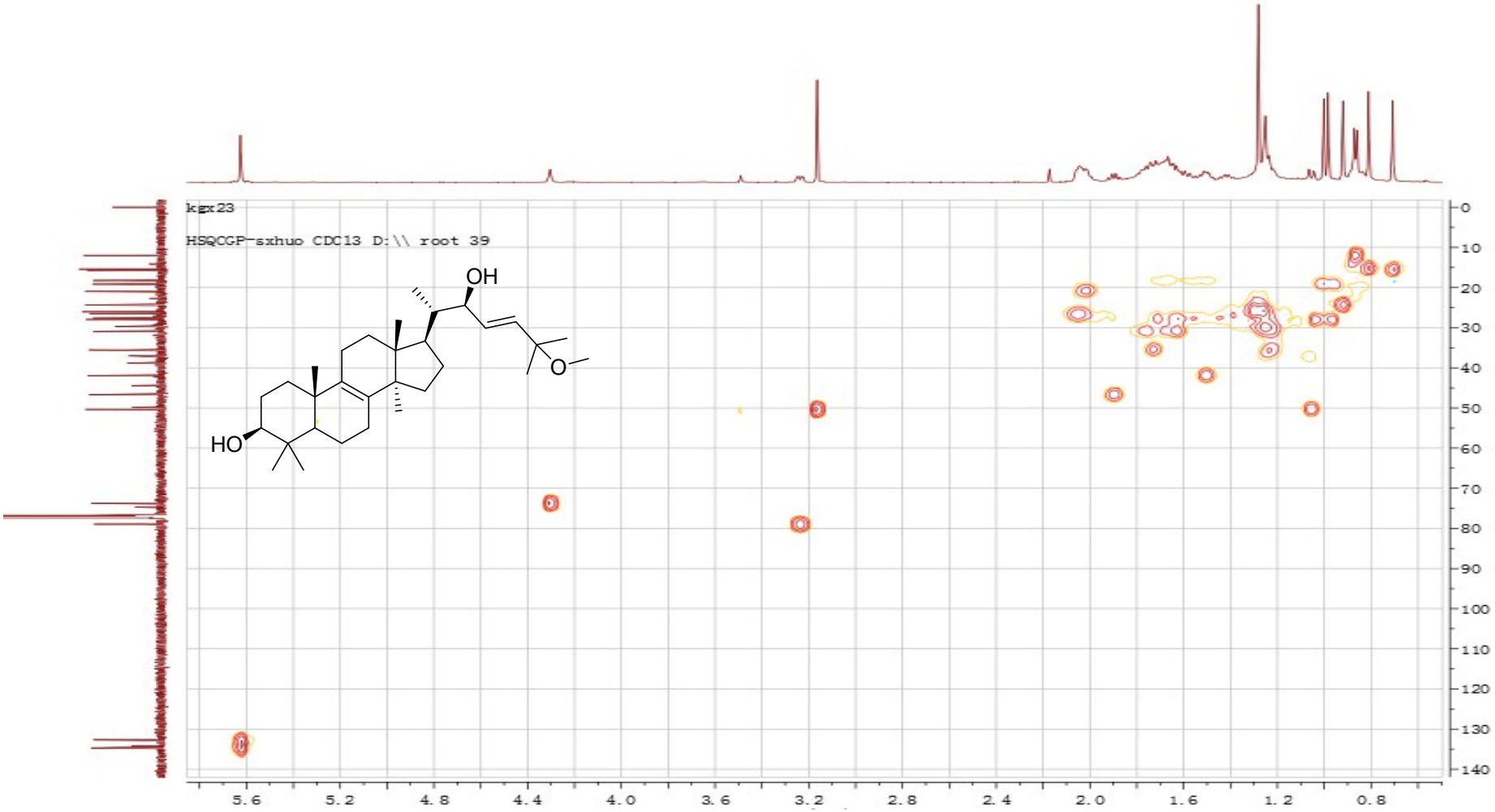

Figure S70. The HMBC spectrum of ganodercochlearin K (12).

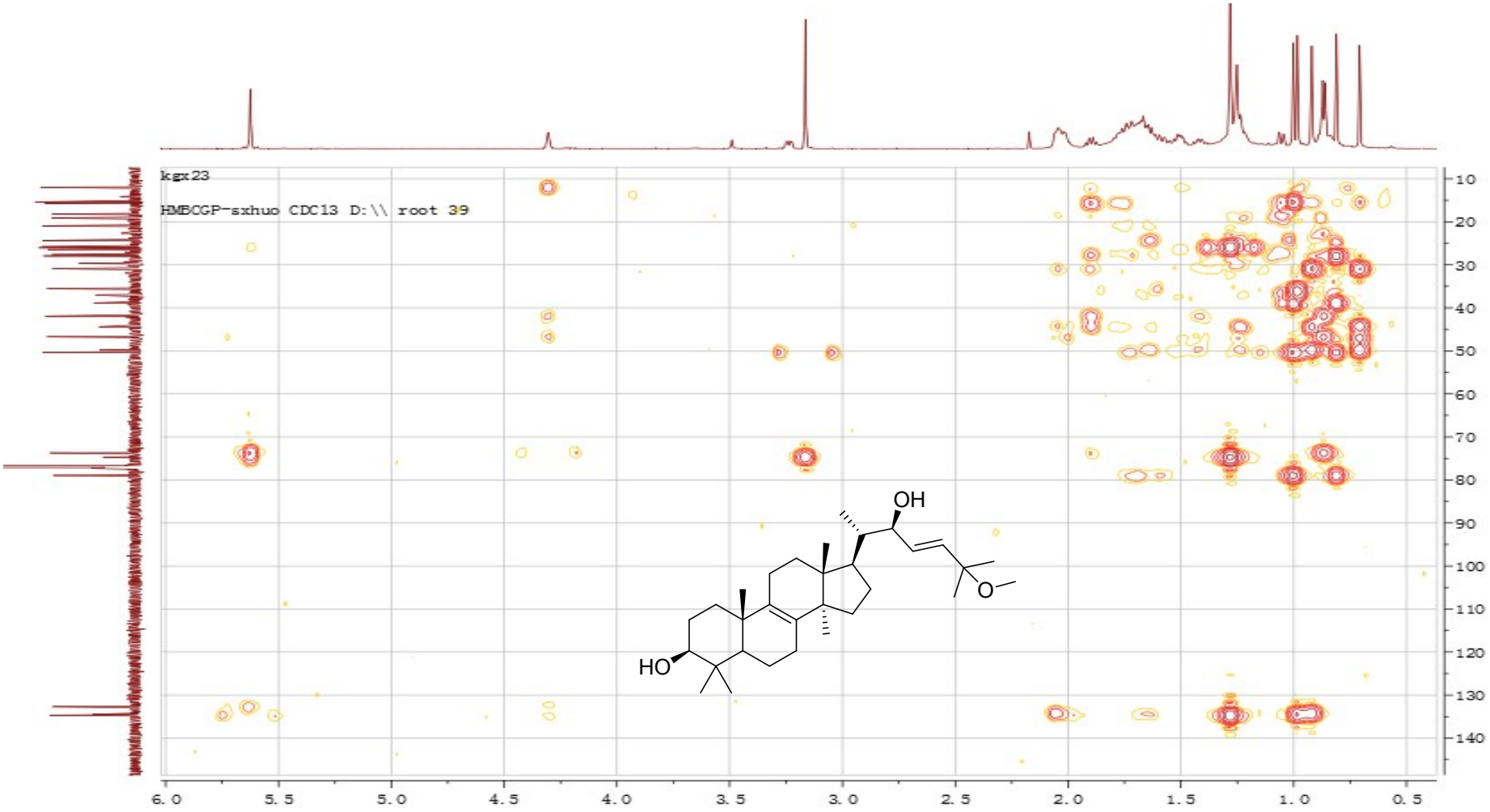

Figure S71. The ^{1}H-^{1}H COSY spectrum of ganodercochlearin K (12).

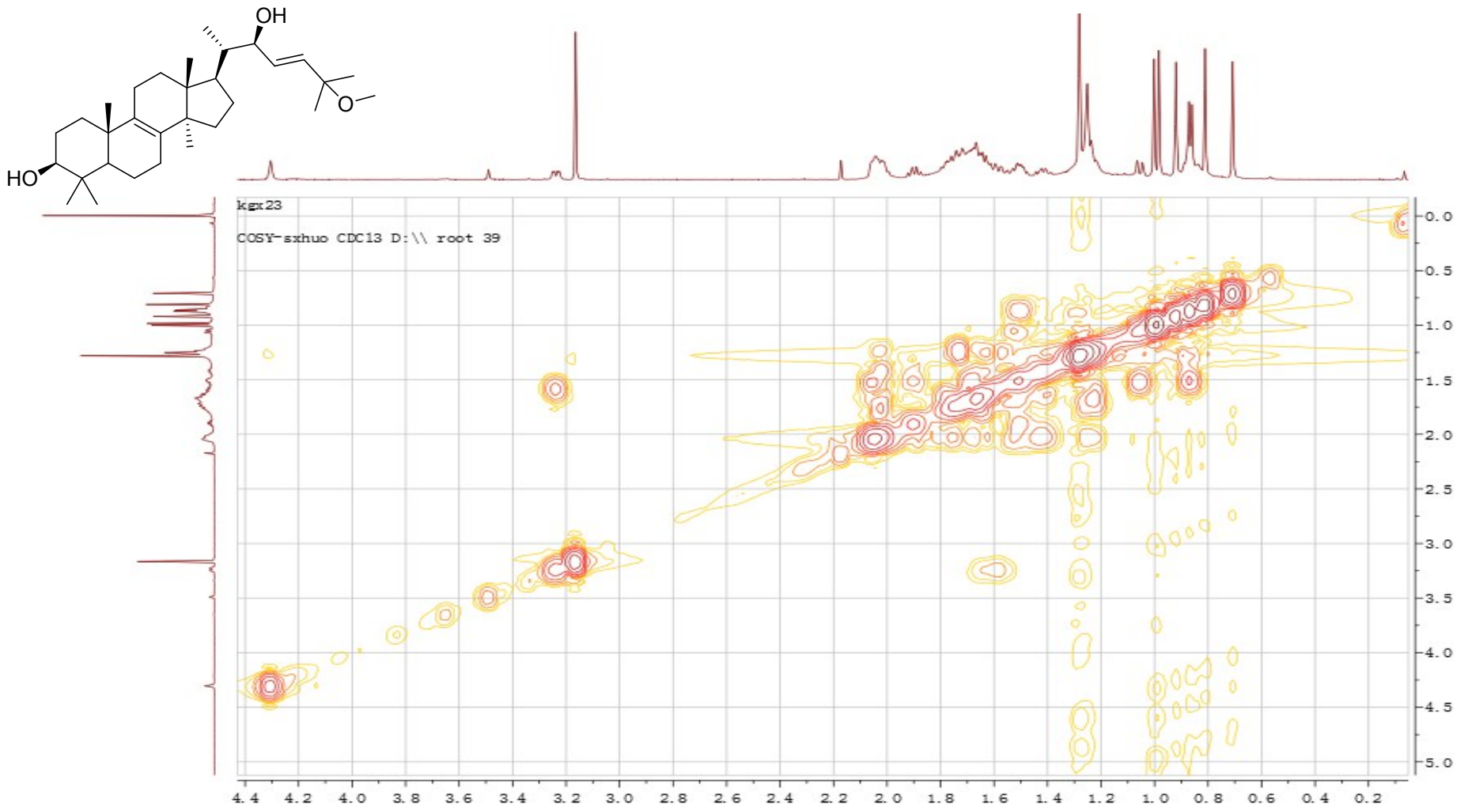

Figure S72. The ROESY spectrum of ganodercochlearin K (12).

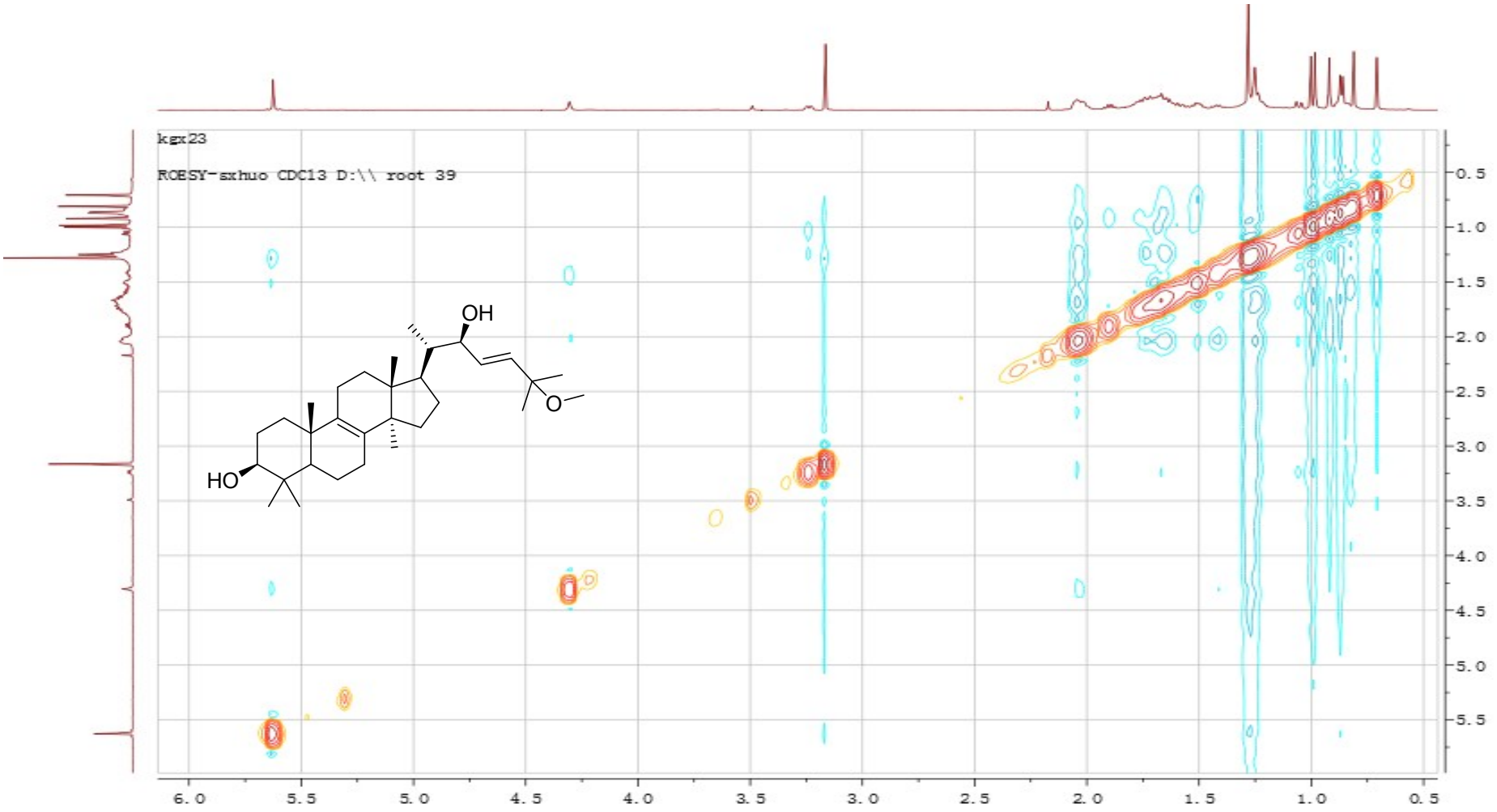

The CD and UV spectra of 1.

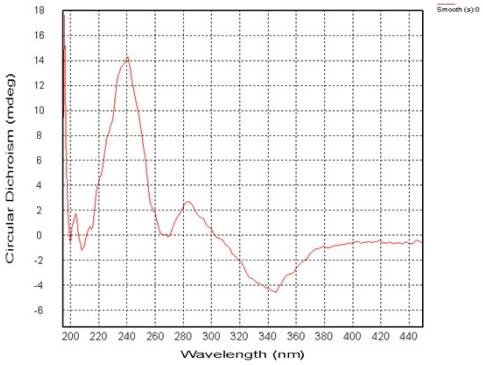

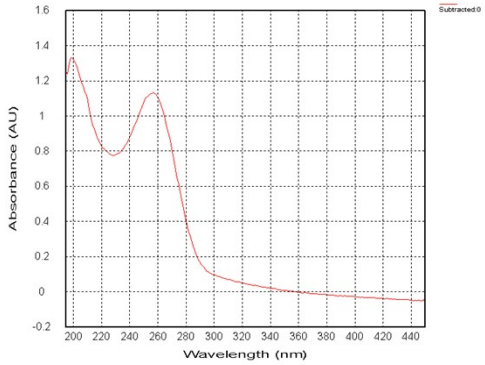

File: CD KFBB10-1mm(195-600)15042509.dsx
ProBinaryX
Attributes :
- Time Stamp :Sat Apr 25 14:27:25 2015

- File ID : {8C996B86-D229-4409-A2DE-BF4DCD8FE6CD}
- Is CFR Compliant : false
- Original unaltered data
Remarks:
  - HV (CDDC channel): 0 v
  - Time per point: 1 s
  - Description: Sample 1
  - Concentration: 0.8000mg/mL MeOH
  - Pathlength: 1 mm

Settings:
  - Time-per-point: 1s (25us x 40000)
  - Wavelength: 195nm - 600nm
  - Step Size: 1nm
  - Bandwidth: 1nm

ECD computational details of 1

Quantum chemical method was used to assign the absolute configuration of compound **1** by comparing the experimental and calculated electronic circular dichroism (ECD) spectra at time-dependent density functional theory (TDDFT). Conformational analysis was initially carried out by using Discovery Studio 4.1 Client conformational searching and molecular mechanics methods (MMFF94). The selected conformers were then optimized at the B3LYP/6-31+G(d,p) level in the gas phase by using the Gaussian09.[1] Further ECD calculations were performed at the PCM-B3LYP/6-31+G(d,p) level in MeOH solution. The results suggested the calculated weighted ECD spectra of **1** with *S* configurations, which is accordance with the experimental spectra. Consequently, the absolute configuration of compound **1** was unambiguously assigned.

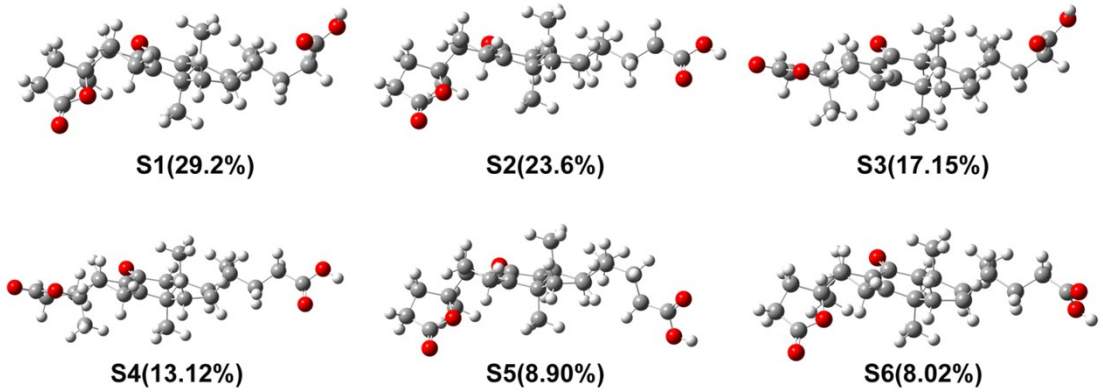

Energy-minmized conformers of **1** in the gas phase using DFT at the B3LYP/6-31+G(d,p) level.

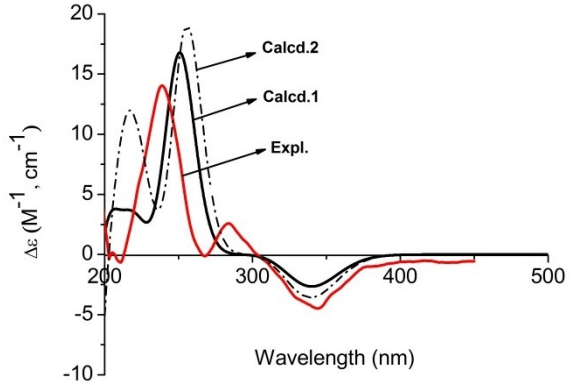

Comparison of experimental (Expl.) and cacluated ECD spectra of **1** and the

stereoisomers (Calcd. 1 for 5*S*,10*S*; Calcd. 2 for 5*R*,10*S*).

1. Frisch, M. J.; Trucks, G. W.; Schlegel, H. B.; Scuseria, G. E.; Robb, M. A.; Cheeseman, J. R.; Scalmani, G.; Barone, V.; Mennucci, B.; Petersson, G. A.; Nakatsuji, H.; Caricato, M.; Li, X.; Hratchian, H. P.; Izmaylov, A. F.; Bloino, J.; Zheng, G.; Sonnenberg, J. L.; Hada, M.; Ehara, M.; Toyota, K.; Fukuda, R.; Hasegawa, J.; Ishida, M.; Nakajima, T.; Honda, Y.; Kitao, O.; Nakai, H.; Vreven, T.; Montgomery, J. A., Jr.; Peralta, J. E.; Ogliaro, F.; Bearpark, M.; Heyd, J. J.; Brothers, E.; Kudin, K. N.; Staroverov, V. N.; Keith, T.; Kobayashi, R.; Normand, J.; Raghavachari, K.; Rendell, A.; Burant, J. C.; Iyengar, S. S.; Tomasi, J.; Cossi, M.; Rega, N.; Millam, J. M.; Klene, M.; Knox, J. E.; Cross, J. B.; Bakken, V.; Adamo, C.; Jaramillo, J.; Gomperts, R.; Stratmann, R. E.; Yazyev, O.; Austin, A. J.; Cammi, R.; Pomelli, C.; Ochterski, J. W.; Martin, R. L.; Morokuma, K.; Zakrzewski, V. G.; Voth, G. A.; Salvador, P.; Dannenberg, J. J.; Dapprich, S.; Daniels, A. D.; Farkas, O.; Foresman, J. B.; Ortiz, J. V.; Cioslowski, J.; Fox, D. J. Gaussian 09, Revision C.01; Gaussian, Inc., Wallingford, CT, 2010.

X-ray crystallographic data of 3

Crystal data for 3: $C_{27}H_{38}O_6 \bullet H_2O$, M = 476.59, triclinic, a = 8.1696(8) Å, b = 11.5686(9) Å, c = 13.0762(8) Å, α = 89.962(4)°, β = 89.807(2)°, γ = 87.127(4)°, V = 1234.28(17) Å^3, T = 100(2) K, space group $P1$, Z = 2, μ(CuKα) = 0.742 mm^{-1}, 9504 reflections measured, 4501 independent reflections (R_{int} = 0.0409). The final R_1 values were 0.0697 ($I > 2\sigma(I)$). The final $wR(F^2)$ values were 0.1913 ($I > 2\sigma(I)$). The final R_1 values were 0.0736 (all data). The final $wR(F^2)$ values were 0.1976 (all data). The goodness of fit on F^2 was 1.087. Flack parameter = -0.2(3).

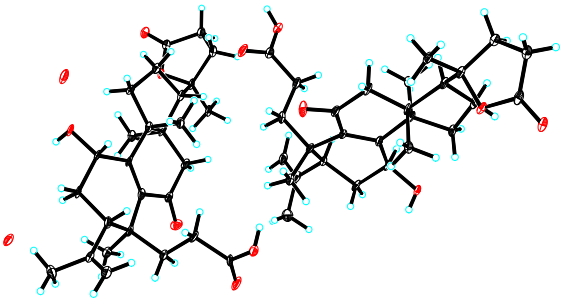

View of the molecules in an asymmetric unit.
Displacement ellipsoids are drawn at the 30% probability level.

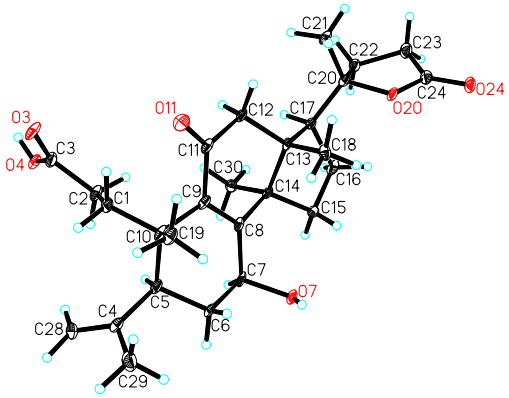

View of a molecule of **3** with the atom-labelling scheme.
Displacement ellipsoids are drawn at the 30% probability level.

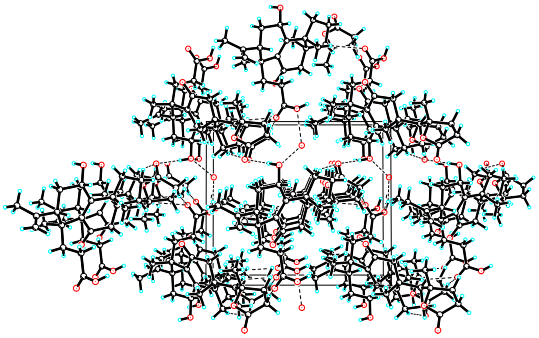

View of the hydrogen-bonded motif of 3. Hydrogen-bonds are shown as dashed lines.

X-ray crystallographic data of 4

Crystal data for 4: $C_{30}H_{48}O_3 \bullet CH_4O$, M = 488.73, monoclinic, a = 6.2648(3) Å, b = 33.5254(16) Å, c = 6.9559(3) Å, α = 90.00°, β = 107.704(2)°, γ = 90.00°, V = 1391.76(11) Å^3, T = 100(2) K, space group $P21$, Z = 2, μ(CuKα) = 0.580 mm^{-1}, 11475 reflections measured, 4453 independent reflections (R_{int} = 0.0469). The final R_1 values were 0.0597 ($I > 2\sigma(I)$). The final $wR(F^2)$ values were 0.1645 ($I > 2\sigma(I)$). The final R_1 values were 0.0598 (all data). The final $wR(F^2)$ values were 0.1646 (all data). The goodness of fit on F^2 was 1.089. Flack parameter = 0.0(3). The Hooft parameter is -0.04(7) for 2035 Bijvoet pairs.

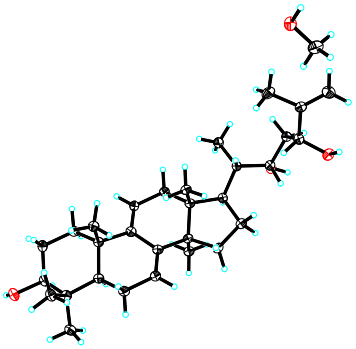

View of the molecules in an asymmetric unit.
Displacement ellipsoids are drawn at the 30% probability level.

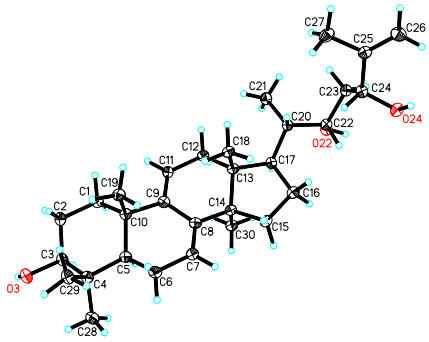

View of a molecule of **4** with the atom-labelling scheme.
Displacement ellipsoids are drawn at the 30% probability level.

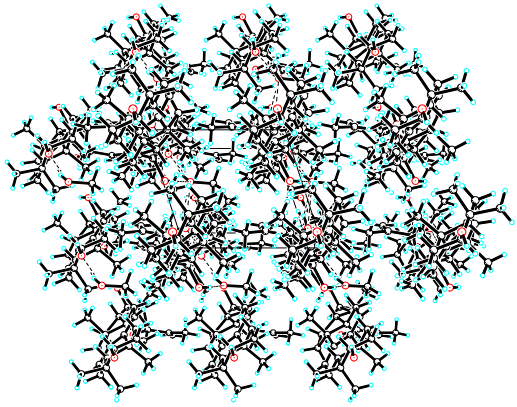

View of the hydrogen-bonded motif of **4**. Hydrogen-bonds are shown as dashed lines.